Progress in Energy and Combustion Science 105 (2024) 101176

Contents lists available at ScienceDirect

Progress in Energy and Combustion Science

journal homepage: www.elsevier.com/locate/pecs

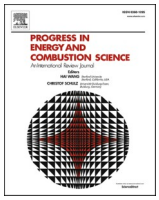

Multifunctional fluidized bed reactors for process intensification

D. Zapater [a], S.R. Kulkarni [a], F. Wery [c], M. Cui [a], J. Herguido [b], M. Menendez [b], G.J. Heynderickx [c], K.M. Van Geem [c], J. Gascon [a], P. Castaño [a,*]

[a] KAUST Catalysis Center (KCC), King Abdullah University of Science and Technology (KAUST), Thuwal, 23955-6900, Saudi Arabia
[b] Catalysis and Reactor Engineering Group (CREG), Department of Chemical and Environmental Engineering, Aragon Institute of Engineering Research (I3A), Universidad Zaragoza, 50018, Zaragoza, Spain
[c] Laboratory for Chemical Technology, Ghent University, Zwijnaarde, Ghent, 9052, Belgium

ARTICLE INFO

Handling Editor: Christof Schultz

Keywords:
Fluidized reactors
Multifunctional
Process intensification
TZFBR
Vortex
ICFBR

ABSTRACT

Fluidized bed reactors (FBRs) are crucial in the chemical industry, serving essential roles in gasoline production, manufacturing materials, and waste treatment. However, traditional up-flow FBRs have limitations in applications where rapid kinetics, catalyst deactivation, sluggish mass/heat transfer processes, particle erosion or agglomeration (clustering) occur. This review investigates multifunctional FBRs that can function in multiple ways and intensify processes. These reactors can reduce reaction steps and costs, enhance heat and mass transfer, make processes more compact, couple different phenomena, improve energy efficiency, operate in extreme fluidized regimes, have augmented throughput, or solve problems inherited by traditional reactor configurations. They address constraints associated with conventional counterparts and contribute to favorable energy, fuels, and environmental footprints. These reactors can be classified as two-zone, vortex, and internal circulating FBRs, with each concept summarized, including their advantages, disadvantages, process applicability, intensification, visualization, and simulation work. This discussion also includes shared considerations for these reactor types, along with perspectives on future advancements and opportunities for enhancing their performance.

Contents

* Corresponding author.
E-mail address: pedro.castano@kaust.edu.sa (P. Castaño).

https://doi.org/10.1016/j.pecs.2024.101176
Received 20 February 2024; Received in revised form 15 May 2024; Accepted 9 July 2024
Available online 26 July 2024

1. Introduction

Since the emergence of the chemical industry, various reactor technologies have significantly influenced its expansion [1]. Reactor configurations provide an environment to carry out chemical reactions [2], including catalytic and non-catalytic processes, influencing the development of the industry. In this review, we focus on catalytic processes, which allow a wider variety of strategies for process intensification due to the persistent pursuit of enhanced process efficiency and the transformation towards a more sustainable chemical industry. However, the applied reactor technology significantly impacts the performance of the catalyst. Packed bed reactors with a simple design and straightforward construction suffer from pressure drop, hot or cold spots, catalyst deactivation, and low stability. In contrast, fluidized bed reactors (FBRs) allow the catalyst to behave as a fluid, solving most of these problems, but are less commonly used on a laboratory scale because of their more complex flow behavior. Packed bed reactors approach plug-flow behavior more than other reactor types, making them more attractive for catalytic kinetic studies. The development of fluidized bed technology marked a milestone in industry development, such as the first fluid catalytic cracking (FCC) unit, which went into operation in 1942 and eventually became the industry standard for gasoline production [3]. This example and its application to ethylene polymerization demonstrate the importance of FBRs in the current chemical industry. Other examples include gasification, Fischer-Tropsch synthesis, chemical recycling [4], and numerous physical processes, such as particulate material drying and coating [5].

In traditional up-flow FBRs, gas bubble properties—such as size, shape, formation, upward velocity, and coalescence—are quantitatively comparable to liquid ones. However, the fluid behavior of the bed allows for continuous feed, removal of solids, and rigorous mixing, resulting in a uniform temperature, even for highly exothermic or endothermic reactions. This also improves solid and fluid contact, enhancing heat and mass transfer. Unfortunately, FBRs encounter design and operational problems despite their versatility and operation in several fluidization regimes [6,7]. Working at an industrial scale means FBRs often operate in the bubbling or turbulent fluidization regime, which leads to gas-bypass and particle entrainment issues for conventional FBRs.

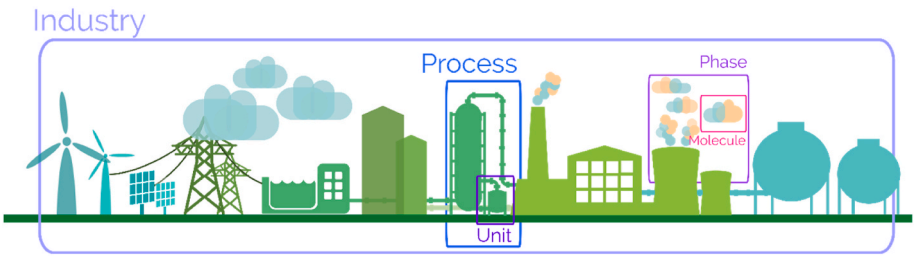

Fig. 1. Schematic representation of the multi-scale opportunities for process intensification in a generic industrial plant.

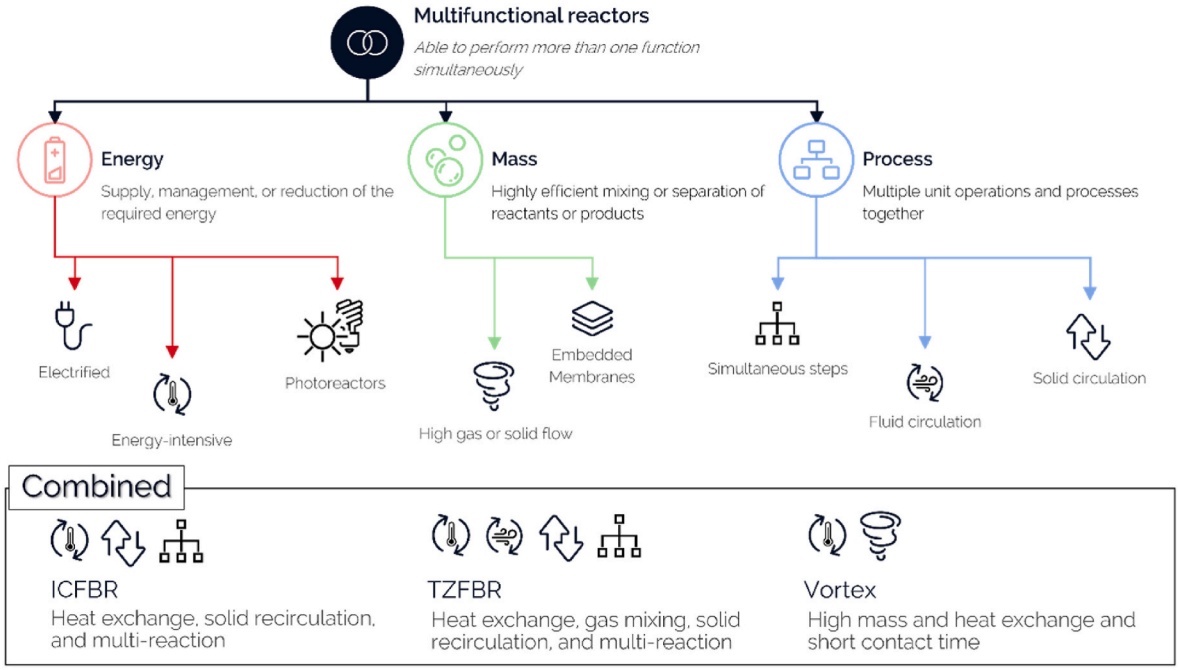

Fig. 2. Classification of multifunctional reactors based on their main objectives.

Additionally, continued solid mixing produces fines through attrition [8,9], and operating at high fluidization velocities causes fines elutriation and entrainment [10–12]. Moreover, because of the rigorous mixing in the bed, an FBR can be seen as a continuously stirred tank reactor with a varying solid residence time distribution (RTD). For up-flow FBRs that operate at high gas velocity and a diluted phase of solids (*e.g.*, riser), the most concerning limitations relate to particle erosion and cluster formation, both causing an uneven contact time between the gas and the solid, and less control of the reaction [13,14]. All these phenomena limit the application of conventional FBRs for certain processes. For example, traditional FBRs cannot operate for a long time on stream in processes with fast catalyst deactivation, such as MTO or FCC processes [15–20]. Furthermore, if substantial mass or heat transfer restrictions exist, such reactors provide low conversion and poor performance, such as in biomass fast pyrolysis [21–24].

To address these challenges, numerous adjustments to conventional processes have been implemented. The prevalent options involve incorporating extra reactors either in a serial or parallel arrangement, as seen in the FCC process or transferring the catalyst between diverse reactors and fluidization regimes [25–27]. Alternatively, some strategies, such as the MTG process, utilize the same reactor but shift between reaction-regeneration cycles by altering the fluidization gas composition from the process gas to an oxygen flow, facilitating the combustion of coke deposited on the catalyst [28,29]. Recent alternatives focus on changing reactor design to meet specific needs, such as reaction-separation systems like embedded cyclones or membranes [30–32]. Other methods include the addition of internals such as membranes, baffles, or mechanical agitators to disrupt bubble formation and improve gas-solid contact and gas flow development inside the bed [6,33,34]. For highly endothermic or exothermic reactive systems, heat transfer tubes can be suspended in the bed to additionally supply or withdraw energy to or from the bed [5]. Recent trends driven by electrification [35] aim to control the heating of the bed using induction heating [36,37] and induce more uniform fluidization of the solid through vibration [38,39] or electromagnetic fields [40–42]. These methods trade off an increase in capital or operating expenses, energy consumption, or specific catalyst properties for an increase in process efficiency. However, they open up a new way to understand FBRs and the insights and methods gained from these modifications contribute to process intensification (PI). Process intensification principles can also be used to design novel FBRs that allow for multifunctional and intensified operation. For example, operating in the centrifugal field instead of the gravitational field would be an example of intensified operation. Process intensification aims to minimize the number of units in the plant design, reduce costs, or simplify the overall process. Reactive distillation is one of the most common examples of process intensification, as it integrates a reactor and a distillation column in the same unit. PI can be implemented at different scales (Fig. 1). An arbitrary classification based on Van Gerven and Stankiewicz [43] could include industry, process, unit, phase, and molecule. The industry scale considers the complete plant, from the energy source to product storage. The process scale accounts for each step, such as reaction or separation. The unit scale focuses on

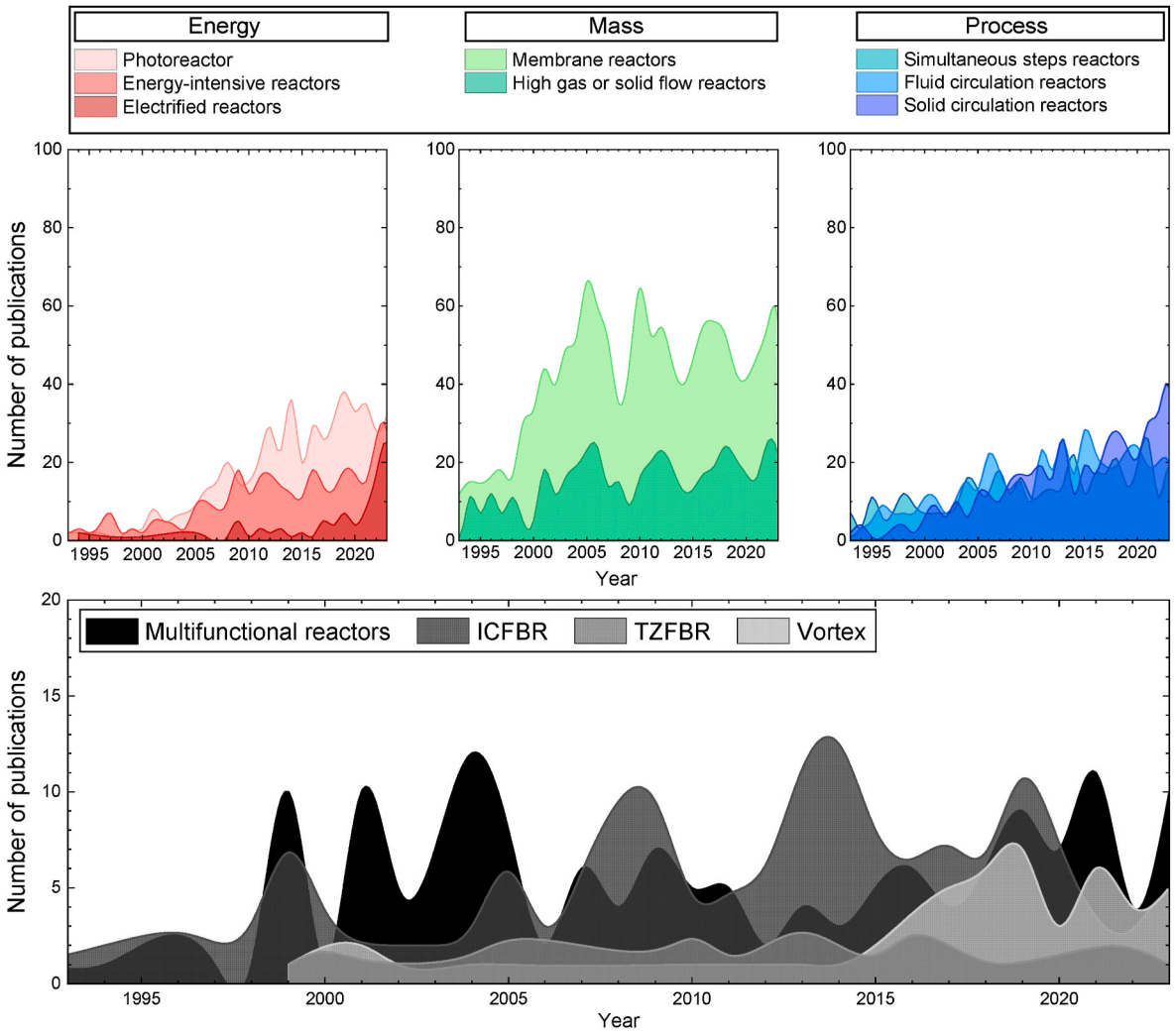

Fig. 3. Statistics on the number of publications by keyword collected from the previous classification of multifunctional reactors (Source: Scopus© database by Elsevier B.V.).

the equipment comprising each process, such as a condenser, boiler, reflux drum, or plate tower in a distillation column. The phase scale considers the building blocks that make a unit work, while the molecular scale accounts for the molecular behavior, mainly in reactive systems.

A common way to apply PI at every scale is by using multifunctional systems. Among the wide variety of these systems, multifunctional reactors are of interest because they usually improve the most critical step in the chemical industry. These reactors can function in more than one way, and their design is strongly oriented to process intensification as they can reduce reaction steps and cost, enhance heat and mass transfer, make processes more compact, couple different phenomena, enhance energy efficiency, operate in highly fluidized regimes, have augmented throughput, or solve problems inherited by traditional reactor configurations. These systems can be classified based on their objective (Fig. 2): energy (heat supply or management), matter (mixing or separation), process (reaction-regeneration), or a combination of them (*e.g.*, Vortex or multi-zone fluidized reactors).

Multifunctional reactors have been a topic of interest for over 30 years. However, since 2005, their attention has steadily increased. This rise in attention could be attributed to the growing interest in process intensification for chemical industry processes, which may arise from the profitability of the processes, market trends, or environmental concerns. Despite the broad definition of multifunctional reactors, it is possible to use the previous classification to analyze statistics about publications on this topic. Fig. 3 presents the number of publications in the last three decades using Fig. 2 keywords.

Before the 2000s, there were only a small number of publications related to reactor energy supply, management, or use. Although photoreactors and energy-intensive systems have grown consistently in the past 20 years, the attention to electrified reactors remained small until 2020. Research on multifunctional reactors that focus on mass transfer or separation was conducted before the 90s, with approximately 30 publications per year. The interest in these systems increased rapidly in the following years. Even though they have experienced fluctuations, they have had an average of 70 publications per year since 2005. This could be attributed to the interest in membrane reactors, which account for more than 70 % of the total publications in this category. Reactors focusing on a specific process are generally studied less than others, probably because their operation is more complex and/or unique. Few publications related to them were released until 2003, when they experienced a small growth that eventually stabilized until 2020. Since then, the attention to reactors capable of simultaneously carrying out more than one process has sharply increased.

This article reviews three intensified, multifunctional FBR geometries: the two-zone (TZFBR), vortex, and internal circulating FBR (ICFBR) reactors. Each reactor is explained in terms of its concept, weak and robust features, applicability, and simulation works. Additionally, common considerations about these FBRs are summarized, and a perspective of upcoming enhancements is presented. This review aims to provide a comprehensive overview of these versatile systems across

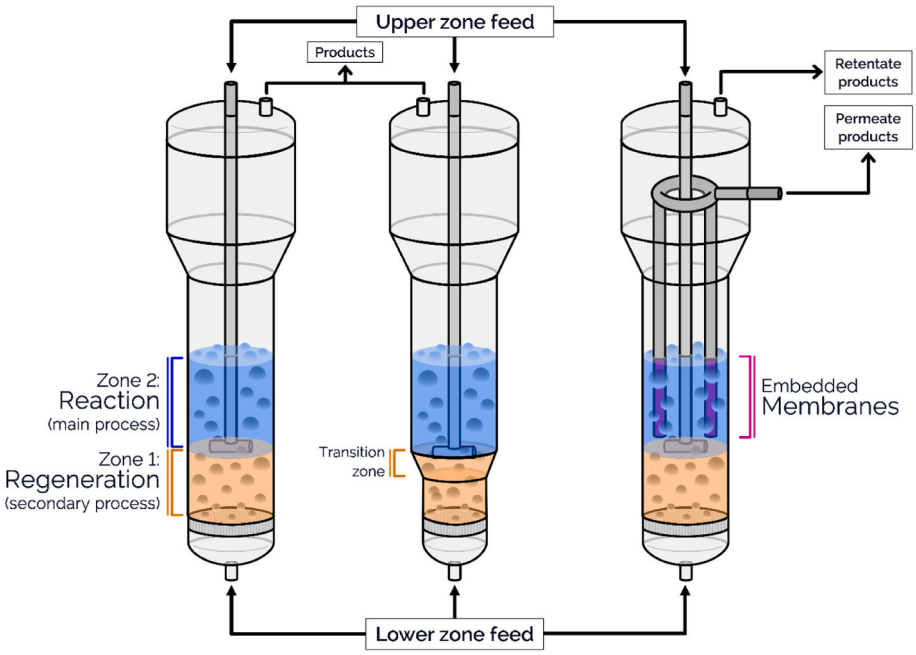

Fig. 4. Schematic representation of TZFBR (left), TS-TZFBR (center), and TZFBR + MB (right).

various applications.

2. TZFBR

Although an earlier version of this reactor was proposed [44,45], it was first tested on a laboratory scale at the University of Zaragoza [46]. The main advantage of this reactor is its capacity to carry out two reactions continuously at the same time, one in the upper zone and the other in the lower zone [47–49] while maintaining a constant flow of solid particles between them. The following sections describe its concept and operation, its strong and weak points, how this technology can be applied to some processes, several modifications to achieve new functions or enhancements, and some visualization and simulation research.

2.1. Concept and functionality

As mentioned, the TZFBR can generate two distinct reaction environments in a single vessel by feeding two streams with different compositions individually. This is an example of process intensification, as it reduces equipment cost and required space [50]. The two zones are formed by feeding one of the streams to the bottom part of the FBR and the other to a point inside it. The gas bubbles formed in FBRs transport the solid between zones, allowing it to reside in each zone for a while [48,51,52]. A schematic representation of the conventional TZFBR is shown in Fig. 4 (left). The TS-TZFBR (center) and TZFBR + MB (right) are two modified versions of the conventional TZFBR.

Because the boundary between the two zones is not physical, the optimal control of the reaction atmosphere in both zones depends on managing the feeding, lower and upper reaction rates, and catalyst flow. Sometimes, if the gas fed to the lower zone (typically an oxidation one) is fully converted before reaching the interzone, an additional zone is created where the oxidizing gas concentration is zero, resulting in no reaction [47,49,53]. A similar situation can occur in the upper zone. In such cases, the reactor can be called a multi-zone FBR (MZFBR).

The movement of particles from one zone to another is determined by the fluidized behavior of the solid bed. Specifically, the best results can be achieved if the fluidization regime is smooth or bubbling because bubble formation and development allow for better control of the solid upward-downward flow. To manage fluidization in each zone, it is crucial to note that gases from the lower zone mix with those fed to the upper zone. Therefore, the gas velocity in the upper zone is higher than in the lower zone. To ensure good movement of solids through and between both zones, it is recommended to operate slightly above the minimum fluidization velocity in the lower zone with solids of type B in Geldart's classification. This is typically accompanied by a reduced velocity ($u_r = u_{sg}/u_{mf}$) greater than 1.5 and, ideally, a reduced velocity of at least 1–2 greater in the upper zone [54–60]. However, u_r must be limited; high reduced velocities are not recommended because they can result in undesired gas back-mixing between zones [48,61].

Gas distributors also play a crucial role in the reactor's functionality and can either improve or worsen the solid movement by altering the gas flow through the bed. The most used distributor is a porous plate with a smaller pore size than the solid particle's diameter. However, the pores of the gas distributor plate could be affected by temperature or coke deposition, especially since the lower zone is often used to burn coke on the catalyst at high temperatures. Controlling both parameters is essential to prevent pore blockage and uneven gas distribution in the lower zone. The gases are typically fed to the upper zone through a rod inserted through the top plate of the reactor. Usually, the most suitable shape for this gas injector is a rod with a T-shaped end (Fig. 4) or, in some cases, one with more than two horizontal branches. The height at which it is placed above the bed's bottom is one of the most relevant aspects, as it determines the division and height of both zones [46,62,63]. To correctly set the upper feeding point, two aspects must be considered. First, in processes with coke deactivation of the catalyst in the upper reaction zone and regeneration through an oxygen flow in the bottom zone, it is crucial to know about coke formation and combustion rate per gram of catalyst. These factors could depend on experimental conditions or catalytic behavior. However, it is essential to understand that if the catalyst strongly tends to form coke, the system requires more catalyst in the regeneration zone than in the reaction zone [54,64–66]. Second, it is necessary to ensure that the residence time of oxygen in the lower zone is sufficient to achieve complete conversion and prevent a decline in selectivity in the upper reaction zone, leading to an increase in unwanted oxidation products and eliminating the risk of an explosion [48,49,67].

2.2. Advantages and shortcomings

Using a TZFBR can offer several advantages over conventional FBRs.

Table 1
Summary of TZFBR applications (A: article; P: patent; E: experimental; M: reaction modeling; C: computational fluid dynamics).

Authors	Application	Type	Highlights	Comments
A. Roshanaei et al. [84]	Propane aromatization	TZFBR (A, E)	Increased aromatics (BTX) yield and stability	
D. Zapater et al. [15]	Methanol to olefins	TZFBR (A, E)	Increased yield of olefins (ethylene and propylene) and stability. Unconverted O_2 burns the olefins at low coke concentration	
D. Zapater et al. [16]	Methanol to olefins	TZFBR (A, E)	Slower catalyst deactivation corroborates the olefin yield evolution proposed by the dual-cycle mechanism	Comparison between conventional FBR and TZFBR
B. Katryniok et al. [83]	Dehydration of glycerol to acrolein	TZFBR (A, E)	Unconverted O_2 could react with glycerol depending on the height of the regeneration zone	
L. Pérez-Moreno et al. [81]	Ethanol steam reforming	TZFBR (A, E)	Lower coke concentration for the same TOS, more stable operation, H_2 yield of 0.6–0.9, and greater performance than other works from literature	
M. Yus et al. [64]	Glycerol steam reforming	TZFBR (A, E)	Tested CO_2 and H_2O instead of O_2 as regenerating stream components to avoid oxidation of the catalyst metal phase	
M. P. Lobera et al. [80]	Preferential oxidation of CO	TZFBR (A, E)	Tunable catalyst oxidation based on the feeding point or co-feeding	Several modes of feed, bed, and operation
A. Sanz-Martínez et al. [57]	Methanol to hydrocarbons	TZFBR (A, E)	Increased stability and higher olefins yield	Comparison between conventional FBR and TZFBR
A. Talebizadeh et al. [77]	Oxidative coupling of methane	TZFBR (A, E)	Higher C_2 selectivity and enhanced operational stability	
J. Soler et al. [78]	Oxydehydrogenation of n-butane	TZFBR (A, E)	Axial O_2 and C_4H_{10} concentration profiles in the catalyst bed	
G. García et al. [85]	Catalytic upgrading of gasification gas obtained from sewage sludge, bituminous coal, and lignite with *in situ* desulfuration	TS-TZFBR (A, E)	Increased H_2 and CO contents with improved operational stability	TZFBR is included in a larger process with other units working simultaneously
J. A. Medrano et al. [82]	Propane dehydrogenation	TS-TZFBR (A, E) and TS-TZFBR + MB (A, E)	Higher stability and propylene yield due to membranes	
M. P. Gimeno et al. [68]	Methane aromatization	TZFBR (A, E) and TS-TZFBR (A, E)	Enhanced stability and positive fluid dynamic effects associated with changes in reactor section section	
I. Julián et al. [52]	Fluid dynamics by PIV/DIA	2D TS-TZFBR (A, C)	Channeling and slugging phenomenon, the effect of reactor design, and fluid dynamics modeling	
I. Julián et al. [86]	Fluid dynamics by PIV/DIA	2D TS-TZFBR (A, C)	Non-parametric correlation for bubble size modeling and effect of reactor design	
I. Julián et al. [87]	Fluid dynamics by CFD simulations	2D TS-TZFBR (A, C)	Effect of reactor design, feeding point, and shape on bubble size and distribution with axial position in the bed	
I. Julián et al. [51]	Fluid dynamics by PIV/DIA	2D TS-TZFBR with an immersed tube bank (A, C)	Modeling the effect of tube number, disposition, and location over bubble size and distribution and solid flow	
I. Julián et al. [88]	Fluid dynamics by CFD simulations	2D TS-TZFBR + MB (A, C)	Effect of reactor design and membranes on bubble size and distribution with axial position in the bed	
M. Alabdullah et al. [74]	One-step conversion of crude oil to light olefins	TS-TZFBR (A, E, C)	Proof of concept, higher olefins yield, and greater stability	
J. Gascon et al. [65]	Propane dehydrogenation	TZFBR (A, E) (+ICFBR (A, E))	Higher propylene yield and better stability operation	Includes an additional reactor configuration based on TZFBR + ICFBR technology
J. Gascon et al. [75]	Propane dehydrogenation and partial oxidation of butene	TZFBR (A, M, C) (+ICFBR (A, M, C))	Mathematical models to describe fluid dynamics and kinetics	Includes an additional reactor configuration based on TZFBR + ICFBR technology
D. Zambrano et al. [70]	Dry reforming of methane	TZFBR (A, M, C) and TZFBR + MB (A, M, C)	Mathematical models to describe fluid dynamics (three-phase) and kinetics	
P. Ugarte et al. [55]	Dry reforming of methane	TZFBR + MB (A, E)	Presence of an initial activation period, unconverted O_2 that can oxidize the catalyst and facilitate CH_4 combustion, and higher conversion and stability	Additional comparison with conventional FBR and TZFBR without membranes
P. Duran et al. [56]	Dry reforming of biogas	TZFBR + MB (A, E)	Higher stability, conversion, and H_2 selectivity (70–85 % with a purity >99 %)	Several feeds, membranes, bed, and operation configurations tested.
J. Lachen et al. [50]	Dry reforming of biogas	TZFBR + MB (A, M, C)	Lower operating costs than a similar conventional process	Techno-economic assessment of the process
M. P. Gimeno et al. [89]	Alkane dehydrogenation	TZFBR + MB (A, E) and TS-TZFBR + MB (A, E)	Better stable operation, higher conversion due to membranes, troubleshooting with membranes in FBR operations	

The most obvious advantage is its ability to regenerate the catalyst in the lower zone while being deactivated in the upper zone. If the operating parameters are well controlled, this feature can help reach a steady state where coke formation and combustion rates are in equilibrium (net deactivation rate close to zero), allowing the process to run for longer times than those achievable in a conventional FBR [48,54,64,65,68]. However, achieving this goal may be challenging because some of the parameters selected for the lower zone also influence the upper zone.

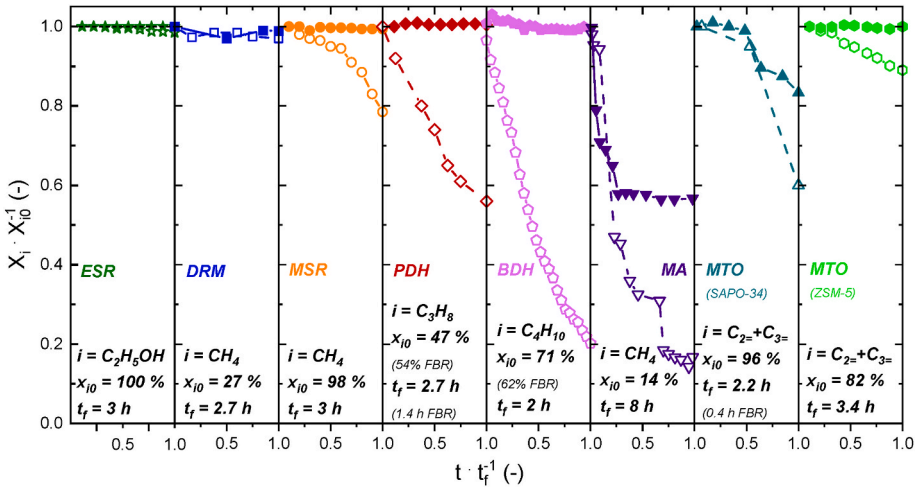

Fig. 5. TZFBR *vs*. FBR performance for several processes. $x_i \cdot x_{i0}^{-1}$ represents the ratio between conversion at a given time and time zero for the species *i* while $t \cdot t_f^{-1}$ is the ratio between a given time and the final time on stream. ESR denotes ethanol steam reforming, DRM denotes dry reforming of methane, MSR denotes methane steam reforming, PDH denotes propane dehydrogenation, BDH denotes butane dehydrogenation, MA denotes the methane aromatization, and MTO denotes methanol-to-olefins. Full markers represent TZFBR, while hollow markers represent conventional FBR experimental data. Reproduced with permission from Ref. [61].

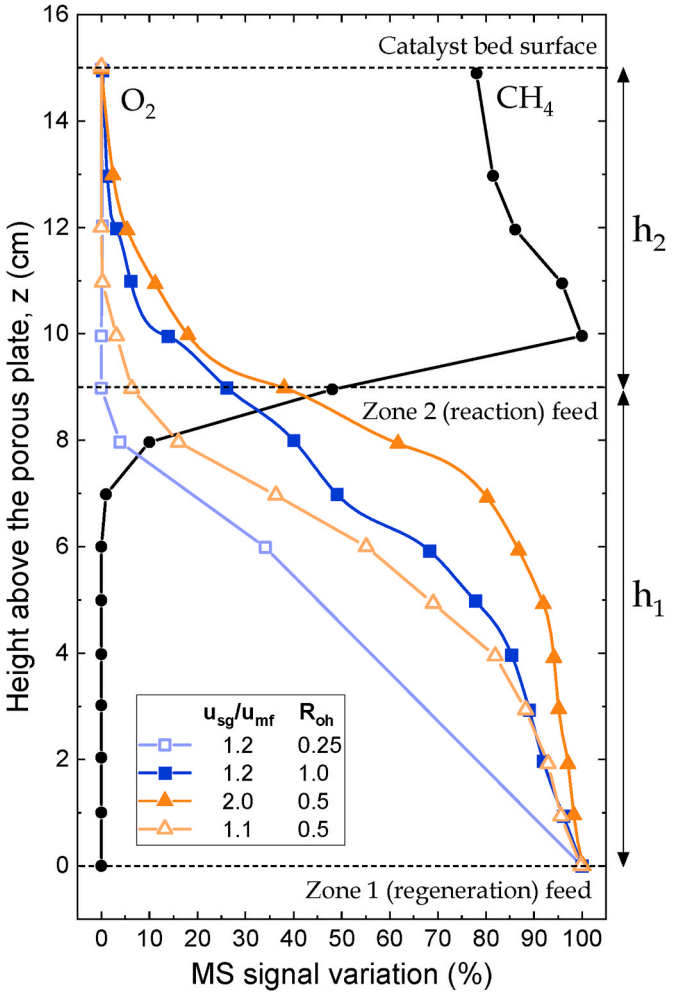

Fig. 6. Axial concentration profiles obtained in a TZFBR for oxidative coupling of methane [48]. h_1 is the regeneration zone, h_2 is the reaction zone, and R_{oh} is the oxygen/hydrocarbon ratio.

For example, a lower zone flow rate change will affect contact time, bubble formation and development, and fluidization behavior. It will also impact the upper zone because there is no physical separation between zones and both flows (the one introduced from the top and the one raised from the bottom) mix in the interzone. This could result in the oxidizing agent mixing with the reactant/product stream, leading to the loss of valuable materials and the formation of dangerous explosive mixtures [46,47,54]. Another relevant issue associated with having two zones in the same catalyst bed is the back-mixing of gases. In an FBR, the solid material dragged upwards by the bubble creates a counterflow of solid moving downwards [52,62,69,70]. If the solid velocity downwards exceeds the minimum fluidization velocity, it drags gas from the upper zone to the lower zone, producing gas back-mixing. This phenomenon is related to the mixing of solids, and it is crucial when reactors operate in turbulent or fast fluidization regimes [71,72].

The isothermal behavior of both the upper and lower fluidized zones is another relevant point, especially in highly exothermal reactions such as catalytic oxidation. The TZFBR reduces the effect of hot spots, sharing the heat generation in a larger mass of catalysts. In the TZFBR, the amount of heat produced or removed is shared with both the reaction and regeneration zones catalyst, contributing to a more efficient energy transfer. Otherwise, if the upper reaction is endothermal (*e.g.*, catalytic dehydrogenation), the heat generation due to the regeneration could make the global process autothermal by the movement of the catalyst, which acts as a heat carrier [73–75]. However, this advantage can also be considered a drawback because the individual temperature control in both zones could be tricky since there is no physical separation between them. Both the gases from the lower zone and the solid that acts as a heat carrier end in the upper zone, exchanging heat through the whole bed. This effect could be even worse, considering that the lower zone is usually used to burn coke and regenerate the catalyst, which is favored at high temperatures and is highly exothermal. However, strategies are based on operating at different temperatures in each zone, such as using two other heating/cooling systems or feeding reactants at different temperatures [74,76].

Another advantage of the TZFBR configuration is that it frequently enhances the targeted product selectivity relative to the traditional FBR [47,57,66,77,78] at the same conversions. Nonetheless, this aspect varies extensively depending on the process and catalyst employed, so evaluating each catalyst and reaction is recommended. It is crucial to remember that upper-zone products are diluted and may even react with those from the lower zone in some instances.

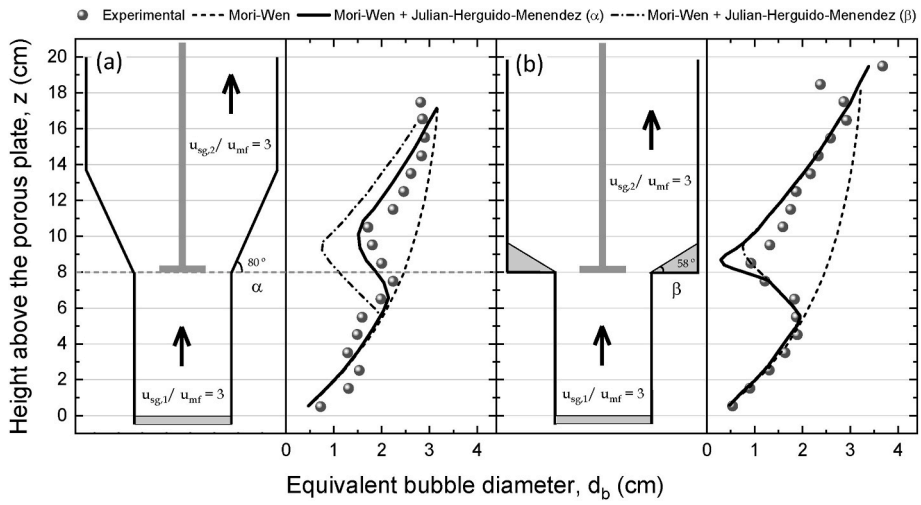

Fig. 7. Experimental $d_b(z)$ prediction using (a) the transition section angle, α, for gradual geometries and high gas velocities and (b) the defluidization angle, β, for sharp transition geometries. Reproduced with permission from Ref. [86].

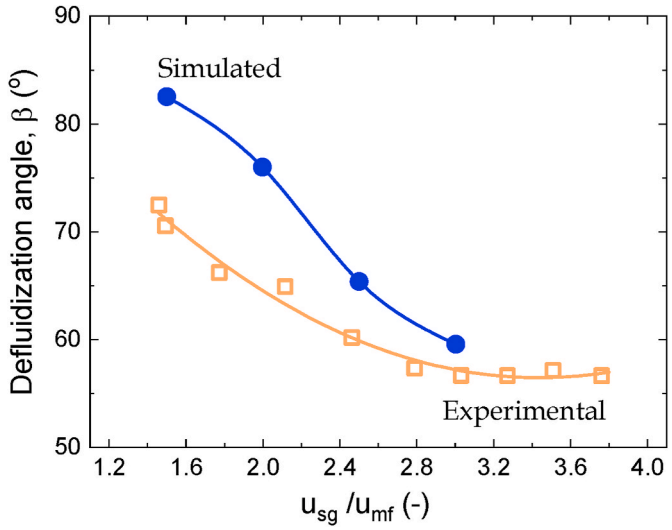

Fig. 8. Comparison between simulated and experimental β values in a sharp transition section TS-TZFBR. Reproduced with permission from Ref. [87].

2.3. Applications of TZFBRs

The TZFBR has been proven to apply to several processes, as summarized in Table 1. These processes can be divided into two categories: (i) processes where the catalyst acts as an oxygen carrier and (ii) processes where the catalyst is deactivated by coke.

2.3.1. Solid as an oxygen carrier

The TZFBR provides two zones where the solid can achieve other oxidation states in these reactions. The desired reaction occurs in one zone. Usually, the upper one and the solid is reduced by releasing oxygen from its lattice. In the other zone, an oxidizing agent is fed to the solid to recover its previous oxidized state and the capacity to perform the upper reaction. In this way, the solid acts as an oxygen carrier, transporting oxygen from the lower zone (oxidation zone) to the upper zone (reduction zone). The difference with a conventional reactor, co-feeding reactants, lies in the absence (or at least lowered concentration) of oxygen in the gas phase in the reaction zone. The solid provides the oxygen required for the oxidation step, and this may change the selectivity concerning the conventional operation with the co-feeding of reactants.

Several reactions where this TZFBR technology has been applied are shown in Fig. 5: the oxidative coupling of methane [46,77], oxidative dehydrogenation of hydrocarbons [47,49,66,67,78], oxidation of butane to maleic anhydride [62], oxidation of benzene to phenol [79], and H_2 purification by preferential oxidation of CO [80].

2.3.2. Solid as a heat carrier via coke

For processes where the catalyst deactivates due to coke deposition on its surface, the TZFBR provides an opportunity to regenerate the catalyst in the lower zone via an oxidizing agent such as O_2 or CO_2 after deactivation in the upper zone, where the main reaction takes place. Some of these reactions include methanol to hydrocarbons [54,57], steam reforming of glycerol [64], methane [63] or ethanol [81], methane aromatization [59,60,68], propane dehydrogenation [65,82], glycerol dehydration to acrolein [83], dry reforming of biogas [50,55,56,70], propane aromatization [84], and direct transformation of crude oil to olefins [74]. It has also been used to upgrade gases from biomass gasification [85], where the TZFBR combines the removal of tar from the products with the steam reforming of hydrocarbons.

2.4. Intensified TZFBR designs

Several modifications have been made to the original TZFBR design to enhance its performance and increase the viability of the reactor for other processes favoring their intensification. Some changes focus on solving the problems above, removing limitations, or increasing the desired product yield.

2.4.1. Oxygen substitution

As previously mentioned, a significant concern associated with using the TZFBR is the explosion risk arising from the potential mixing of oxidizing agents (typically oxygen) and reactants (commonly hydrocarbons), as demonstrated in Fig. 6 for the oxidative coupling of methane. These results indicate that a significant concentration of oxygen is present with methane in the TZFBR point of the injection of the latter.

This risk increases if reaction parameters are not carefully selected or little information about the process is known. Even though it is easily avoidable using suitable technical safety systems (*e.g.*, oxygen sensors and actuated flow cut-off valves), it could be one reason why this reactor has yet to be implemented industrially. However, one advance made with the TZFBR is replacing oxygen with another regenerative stream, such as CO_2, H_2O [59,64,79,90,91] or even H_2 [92,93]. At the same operating conditions, O_2 reacts faster with coke than CO_2 or H_2O [55,59,

64,68]. This difference could be related to the available oxygen that can remove carbon and the strength of their bonds—also, the use of different agents results in other regeneration products—. The applicability of CO_2 or H_2O as regenerative streams could decrease reactor performance in processes where coke forms rapidly [54,58]. However, if coke forms at low rates [55,57], slow regeneration could counteract this formation.

2.4.2. Two-section TZFBR

The TZFBR's initial cylindrical design allows good movement of the solid inside and between zones. However, the amount of gas required for catalyst regeneration is usually smaller than the flow rate of the main reactant. Excessive gas flow introduced in the upper section of a reactor with a constant cross-section could cause catalyst elutriation and a change from smooth or bubbling fluidization to a turbulent regime, favoring gas back-mixing.

To reduce or even avoid this effect, a two-section cylindrical reactor was proposed [51,52,68,74,86–88,94]. In this system, depicted in Fig. 4 (center), the transversal area of the upper zone is larger than in the lower zone, and a higher gas volumetric flow rate may be introduced in the upper zone. The physical change between reactor zones can be characterized by a parameter α, which reflects the smoothness of the transition. A value of α close to 0° indicates an abrupt transition, leading to defluidization issues where solid particles near the corner remain stationary, creating a 'dead zone'. Conversely, when α approaches 90°, the transition becomes smoother, significantly reducing or eliminating defluidization (Fig. 7). Notably, defluidization is influenced by various factors. Julian et al. explored this phenomenon through a combination of simulation and visualization experiments, discovering that increasing α to over 80°—considered a conservative threshold—along with the gas flow rate and the size of catalyst particles, can effectively mitigate this issue (Fig. 8) [51,52,68,86].

In addition to defluidization, modifying the reactor section between zones could also produce channeling or slugging. Channeling could develop under specific conditions, mainly related to low relative gas velocities and particle-particle and particle-wall forces. This phenomenon becomes significant when the u_r in the upper section is insufficiently high, preventing tiny bubbles from dragging particles upward to facilitate effective solid circulation. Conversely, slugging is particularly relevant in narrow lab-scale reactors and is typically observed in systems where the gas velocity is high in the lower zone but low in the upper zone. This disparity in gas velocities between the two zones hampers the mixing rate of solids, leading to slugging. However, this issue can be mitigated by ensuring that the gas velocities in both zones are similar.

This concept of a multi-section fluidized bed is also applied to other reactor designs, such as the diameter-transformed fluidized bed reactor [95]. In this design, the reactor vessel is built with different sections to modify the gas velocity and favor specific reactions over others (*e.g.,* cracking or catalytic conversions in processes such as fluid catalytic cracking or methanol to olefins).

2.4.3. TZFBR with membranes

One recent development in TZFBR technology has been its coupling with membranes, as shown in Fig. 4 (right). Typically, membrane reactors achieve higher conversion and yield by removing one of the reaction products, which helps shift the equilibrium towards the released product. However, this improvement could increase coke formation [96,97]. FBRs with selective membranes have already been proposed [98–101], but its operation with the TZFBR allows for combining three processes in one device: reaction, regeneration, and separation.

In the TZFBR + MB configuration, the TZFBR operates as previously described. However, for effective functionality, the membrane must be strategically positioned in the upper zone of the FBR, where the main reaction occurs [55,82,88,89]. Within the TZFBR + MB system, the gas permeation rate and membrane configuration emerge as critical parameters. The size of the bubbles ascending in the upper zone plays a pivotal role in fluidization and the movement of solids. Extracting a high product flow through the membrane could significantly lead to defluidization in certain sections of the solid bed, such as near the reactor wall or at the transition between zones, especially where the relative gas velocity might fall below one [88,99].

However, the membrane configuration also influences performance. For example, when the membrane is positioned as a vertical (or horizontal) rod in the bed's center, it promotes solids axial mixing. In contrast, when integrated into the reactor wall, it provides a larger permeation area for selective gas removal [88].

Unfortunately, one significant drawback of using membranes in FBRs is their fragility, as they can be damaged by high temperatures, certain chemical substances, or the attrition caused by the movement of the catalyst. This poses a particular challenge for membranes with a thin layer of active material on the side of the fluidized bed containing moving solids. Despite some relevant advances in this area [102–105], producing a selective and durable membrane that can operate effectively for an extended period remains challenging.

2.5. TZFBR experimental studies for fluid dynamics

As the bubble evolution is crucial for suitable application and proper reactor design of the TZFBR, we emphasized the experimental studies regarding fluid dynamics in this section.

Visualization of the TZFBR is proven to improve understanding of fluid dynamics. Combining two non-intrusive techniques, digital image analysis (DIA) and particle image velocimetry (PIV), allowed for studying fluid dynamics in a pseudo-2D TS-TZFBR with five different transition angles and several solid particle types [52,86,87]. Experimental findings revealed that the reactor geometry affects the average equivalent bubble diameter, bubble velocity profiles, and particle circulation between the two zones. Based on these findings, a non-parametric correlation for predicting bubble size reduction as a function of transition section angle, relative gas velocity, and particle type was proposed. This correlation successfully predicted the experimental bubble size evolution in a range of relative velocities. The same visualization system was used to evaluate the hydrodynamic behavior in the lower zone of the TZFBR, testing six different tube bank configurations at several superficial gas velocities [51]. This assessment estimated solid axial mixing and the effect of the internals on gas-solid mass transfer. A five-staggered tube bundle configuration could reduce the average bubble size by 30 % within the lower bed zone at the usual TZFBR gas flow rate without significantly increasing the solids circulation time.

2.6. TZFBR modeling studies

To characterize the complex features of the TZFBRs, simplifications have been applied to develop various mathematical models to describe the fluid dynamics and reaction kinetics. Computational fluid dynamics is another useful way to understand the multi-phase phenomenon.

2.6.1. Mathematical model

After a detailed review [48] of ICFBR applications and the TZFBR, efforts were made to develop a mathematical model for simulating FBR with two zones [75]. These models aim to understand the system and predict the effect of the primary process parameters. In the TZFBR, the solid flows between both reaction zones through the bubble, wake, and emulsion phases. The experimental data from a bench-scale plant serve as the basis for understanding the reactor behaviors, which can be adopted for further simulation with the fluid dynamic model and appropriate kinetic models. The fluid dynamics in the TZFBR as a bubbling bed, based on the description of the three-phase model (bubble, wake, and emulsion), have been validated with experiments, and the coupling of reaction kinetics leads to a better understanding of the behavior of reactors and reactions. However, certain parameters, such as the velocity of solid circulation and the oxidation state of the catalyst,

which cannot be experimentally determined, have proven to be among the most crucial variables related to the reactor.

In similar research, other authors developed a mathematical model for the dry-reforming methane across three different reactors, including a TZFBR and a TZFBR + MB [70]. This model accounts for variables such as methane conversion, H_2 yield, H_2 selectivity, and the H_2/CO ratio, along with their evolution over time-on-stream. The model's predictions indicate an improvement in stability when transitioning from a conventional fluidized bed to a TZFBR and further enhancements in yield when incorporating membranes into the TZFBR. Comparisons with previous experimental results demonstrate the model accuracy in accurately predicting the effects of varying operating conditions.

Modeling TZFBR is a complex task as it involves the composition variation in the gas phase due to catalytic processes, as well as the variation in the solid's composition with height, either due to a change in its oxidation state or a change in the concentration of coke deposited on it. The mathematical modeling of the TZFBR reactor must include both a proper fluid dynamic model and a kinetics model of the reactions taking place in the reaction and regeneration zones of the bed (*i.e.*, above and below the intermediate feeding point).

As previously mentioned, the mathematical modeling of the TZFBR's fluid dynamics follows the classical three-phase (bubble, emulsion, and cloud) gas flow model by Kunii and Levenspiel [106]. In this model, gas rises through the emulsion phase at the minimum fluidization velocity (u_{mf}), while bubbles rise at a velocity (u_b), carrying some solids upward in their wake. Upon reaching the bed surface, these solids enter the emulsion phase and descend. The fluid dynamic parameters that delineate the interactions among these phases, including the bubble rise velocity (u_b), the gas exchange coefficient between the bubble and emulsion (K_{be}), the coefficient of solids exchange between wake and emulsion (K_{we}), and others [70], are intricately linked to the bubble size (d_b).

In an initial approach, it is posited that the bubble size (d_b) remains constant throughout the bed [53]. This study presupposes isothermal conditions and a steady flow of solids within the bubbles, independent of bed height (z). The model incorporates a gas exchange between the bubble and emulsion phases as delineated by Davison and Harrison [107], and a solid exchange between the wake and emulsion following the model proposed by Chiba and Kobayashi [108]. This modeling framework has been effectively employed in studying the oxidative dehydrogenation of butane in a TZFBR. Notably, the model necessitates two variables to describe the oxidation state of the solid at any given point: one for a fraction of selective active centers and another for a fraction of non-selective active centers, as per the Mars van Krevelen dual kinetic model [109] for that reaction.

However, the fluid dynamics accuracy of the model is noticeably improved when a variable bubble size with the bed height z [47] is considered, for example, using the equations proposed by Mori and Wen [110] that suppose an exponential growth of bubbles from an initial diameter (d_{bo}), according to equation (1).

$$d_b = d_{bm} - (d_{bm} - d_{bo})\exp\left(-\frac{0.3z}{D_i}\right) \tag{1}$$

In a subsequent refinement, the assumption of a constant d_b was reconsidered. A more robust model [75] incorporated the variation of d_b with bed height (z), in line with the equation proposed by Horio and Nonaka [111]. This consideration implies that both the bubble velocity and the rate of solid flow rising in the wake phase (and descending in the emulsion phase) change. Consequently, the mass balance for the solid becomes more complex, necessitating the inclusion of a term to account for the variation in flow rate, as detailed subsequently. The predictions from this model showed strong agreement with experimental findings on propane dehydrogenation and butane oxidation to maleic anhydride in a TZFBR.

Apart from these conventional considerations, a key point in modeling a TZFBR is properly describing the effect of the intermediate feed entry at a height z_f on both the bubble size d_b and phase distributions. As mentioned in section 2.2, bubble size and velocity are related to gas backmixing and the possible formation of explosive mixtures. This safety concern makes modeling the bubbles a key advancement with this reactor because it allows us to know the limits to ensure a safe operation. Although considering the d_b variation with bed position (z) marked a significant advancement, it is important to note that the existing correlations for bubble size *versus* height were not specifically devised for a TZFBR. Addressing this gap, Julian et al. [86] introduced a novel correlation based on experimental data from a TZFBR. This work led to the estimation of d_b using the newly proposed JHM correlation. Notably [70], applied this correlation within a reactor model for the dry reforming of methane, considering systems both with and without hydrogen-selective membranes. The correlation introduces an equation (2), derived from an initial equation (1), for modeling the lower zone of the bed beneath the feed entry ($z < z_f$), typically referred to as the regeneration zone.

$$d_{b,1} = d_{bm,1} - (d_{bm,1} - d_{bo})\exp\left(-\frac{0.3z}{D_i}\right) \tag{2}$$

with:

$$d_{bo,1} = 3.77(u_{sg,1} - u_{mf})^2 g^{-1} \tag{2a}$$

$$d_{bm,1} = 1.49 g^{-0.2}\left[\pi D_i^2 (u_{sg,1} - u_{mf})\right]^{0.4} \tag{2b}$$

For the upper zone of the bed, situated above the feed entry point ($z > z_f$), which is typically the reaction zone, equation (3) is applicable. It is posited that the gas added at the feed entry point (z_f) instantaneously mixes with the gas stream emanating from the lower zone. Consequently, this mixed gas is evenly distributed between the bubble and emulsion phases. Such an assumption aligns more closely with experimental observations [75] compared to the alternative hypothesis that the introduced gas solely contributes to forming new bubbles.

$$d_b = \frac{d_{b,2}^3 + d_{b,orif}^3}{d_{b,2}^2 + d_{b,orif}^2} \tag{3}$$

with:

$$d_{bo,2} = d_{b,1}(z = z_f) \tag{3a}$$

$$d_{bm,2} = 1.49 g^{-0.2}\left[\pi D_i^2 (u_{sg2} - u_{mf})\right]^{0.4} \tag{3b}$$

$$d_{b,2} = d_{bm,2} - (d_{bm,2} - d_{bo,2})\exp\left(-\frac{0.3z}{D_i}\right) \tag{3c}$$

$$d_{b,orif} = d_{bm,2} - (d_{bm,2} - d_{orif})\exp\left(-\frac{0.3z}{D_i}\right) \tag{3d}$$

Once the d_b at each bed height (z) is determined, the gas exchange coefficients between the three phases (K_{be}, K_{bc}, K_{ce}) and the solid exchange coefficient (K_{we}) between wake and emulsion can be accurately estimated using the expressions provided by Kunii and Levenspiel [112], or analogous methodologies. Similarly, conventional correlations can be employed to calculate the volume fraction of the bed occupied by bubbles (δ) [70,113].

Given the variation in bubble size and velocity with bed height, both the value of δ and the distribution of gas flow between the bubble and emulsion phases vary along the bed. Specifically, changes in the volumetric flow rate within the bubble phase necessitate a compensatory net flow of gas or solid, either from the emulsion to the bubble-wake or in the reverse direction. Consequently, a term to account for the transversal flow—reflecting the movement of solids between the wake and emulsion due to changing bubble properties—can be integrated into the model [114,115], as outlined in equation (4):

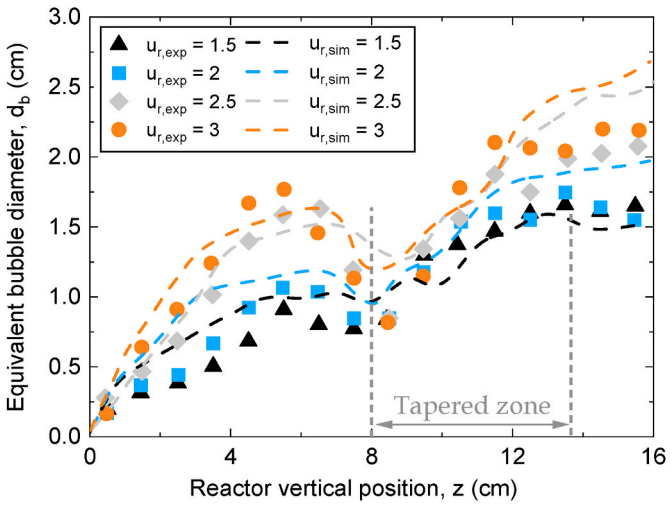

Fig. 9. Comparison between experimental and CFD simulated bubble size profiles as a function of the relative gas velocity in a TS-TZFBR. Experimental parameters: $\alpha = 80^{o}$, $z_f = z_{sc} = 8$ cm. Reproduced with permission from Ref. [87].

$$\left(\lambda_1 C_{x,y} + \lambda_2 C_{x,y}\right)\frac{\partial(f(\delta)u_b)}{\partial z} \tag{4}$$

with:

$$\lambda_1 = 1;\ \ \lambda_2 = 0 \text{ when } \frac{\partial(f(\delta)u_b)}{\partial z} < 0 \tag{4a}$$

$$\lambda_1 = 0;\ \ \lambda_2 = 1 \text{ when } \frac{\partial(f(\delta)u_b)}{\partial z} \geq 0 \tag{4b}$$

To close the mathematical model of the TZFBR, it is essential to incorporate the kinetic models for chemical reactions occurring within both the gas and solid phases. These models should detail the reaction kinetics by expressing the rate of reaction ($r_{i,x}$) for compound i in phase x (bubble, wake, or emulsion) as a function of its concentration and that of other compounds within the same phase. Beyond the basic reaction kinetics, the model must also account for the kinetics of regeneration processes or those involving catalyst reduction and oxidation, particularly if the catalyst serves as an oxygen carrier. This includes, for example, kinetic models for the combustion of coke (with O_2) or its gasification (with CO_2), depending on the reactor configuration.

In a TZFBR, mass balances must be carried out for both the gas and solid phases. For the solid phase, solid particles can rise with the bubbles (in the wake and with the cloud accompanying the bubbles) and descend in the emulsion phase. Therefore, it is necessary to consider mass balances for both gas and solid in the bubble phase, as well as in the emulsion phase, and for the solid in the wake and emulsion. Considering the fluid dynamic and kinetic models, mass balances in a non-steady-state can be made in a differential reactor volume element with a length ∂z. Thus, the continuity equation for compound i includes terms such as accumulation, inputs, outputs, transfer, and reactions. Applying the fluid dynamic properties previously stated, the resulting partial differential equations for gas and solid and the different bed phases are shown in equations (5)–(8). Furthermore, there is a balance of the gaseous species at the point of feeding the reactants ($z = z_f$).

Gas phase.

- *Bubble (b) + Wake (w):*

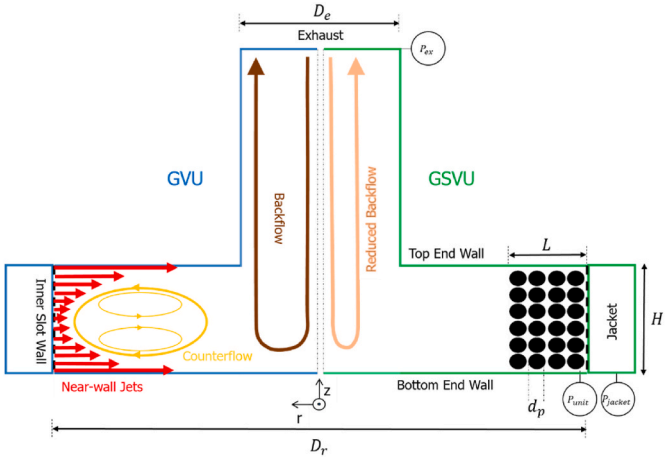

Fig. 10. Schematic representation of GVU and GSVU flow patterns in a vortex unit (front view of a vertical axis unit). Gas flows radially inward from the jacket. Reproduced with permissions from Ref. [118].

$$\begin{aligned}&\left(\delta + \delta f_w \varepsilon_{mf}\right)\frac{\partial C_{i,b}}{\partial t} = \\ &-\frac{\partial\left(\left(\delta + \delta f_w \varepsilon_{mf}\right)u_b C_{i,b}\right)}{\partial z} + \left(\lambda_1 C_{i,b} + \lambda_2 C_{i,e}\right)\frac{\partial\left(\left(\delta + \delta f_w \varepsilon_{mf}\right)u_b\right)}{\partial z} \\ &- K_{b,e}\left(\delta + \delta f_w \varepsilon_{mf}\right)\left(C_{i,b} - C_{i,e}\right) + r_{i,b}\rho_{cat}\left(1 - \varepsilon_{mf}\right)\delta f_w\end{aligned} \tag{5}$$

- *Emulsion (e):*

$$\begin{aligned}&\left(1 - \delta - \delta f_w\right)\varepsilon_{mf}\frac{\partial C_{i,e}}{\partial t} = -\frac{\partial\left(\left(1 - \delta - \delta f_w\right)\varepsilon_{mf} u_e C_{i,e}\right)}{\partial z} \\ &- \left(\lambda_1 C_{i,b} + \lambda_2 C_{i,e}\right)\frac{\partial\left(\left(\delta + \delta f_w \varepsilon_{mf}\right)u_b\right)}{\partial z} + K_{b,e}\left(\delta + \delta f_w \varepsilon_{mf}\right)\left(C_{i,b} - C_{i,e}\right) \\ &+ r_{i,e}\rho_{cat}\left(1 - \delta - \delta f_w\right)\left(1 - \varepsilon_{mf}\right)\end{aligned} \tag{6}$$

Solid phase.

- *Wake (w):*

$$\begin{aligned}&\left(1 - \varepsilon_{mf}\right)\delta f_w\frac{\partial C_{j,w}}{\partial t} = \\ &-\frac{\partial\left(\left(1 - \varepsilon_{mf}\right)\delta f_w u_b C_{j,w}\right)}{\partial z} + \left(\lambda_1 C_{j,w} + \lambda_2 C_{j,e}\right)\frac{\partial\left(\left(1 - \varepsilon_{mf}\right)\delta f_w u_b\right)}{\partial z} \\ &- K_{w,e}\left(1 - \varepsilon_{mf}\right)\delta f_w\left(C_{j,w} - C_{j,e}\right) + r_{j,w}\left(1 - \varepsilon_{mf}\right)\delta f_w\end{aligned} \tag{7}$$

- *Emulsion (e):*

$$\begin{aligned}&\left(1 - \varepsilon_{mf}\right)\left(1 - \delta - \delta f_w\right)\frac{\partial C_{j,e}}{\partial t} = -\frac{\partial\left(\left(1 - \varepsilon_{mf}\right)\left(1 - \delta - \delta f_w\right)u_s C_{j,e}\right)}{\partial z} \\ &- \left(\lambda_1 C_{j,w} + \lambda_2 C_{j,e}\right)\frac{\partial\left(\left(1 - \varepsilon_{mf}\right)\delta f_w u_b\right)}{\partial z} + K_{w,e}\left(1 - \varepsilon_{mf}\right)\delta f_w\left(C_{j,w} - C_{j,e}\right) \\ &+ r_{j,e}\left(1 - \varepsilon_{mf}\right)\left(1 - \delta - \delta f_w\right)\end{aligned} \tag{8}$$

2.6.2. Computational fluid dynamics model

A CFD study employing an Eulerian two-fluid approach was conducted to simulate the hydrodynamics within a pseudo-2D TZFBR [87]. The model successfully predicted the characteristic bubble shrinkage occurring in the transition section of the bed and the eventual emergence of defluidized regions, as depicted in Fig. 9. Additionally, it examined the impact of various TZFBR design features, such as the angle of the transition section, the superficial gas velocity, and the placement of the immersed gas distributor, on the hydrodynamic behavior. The

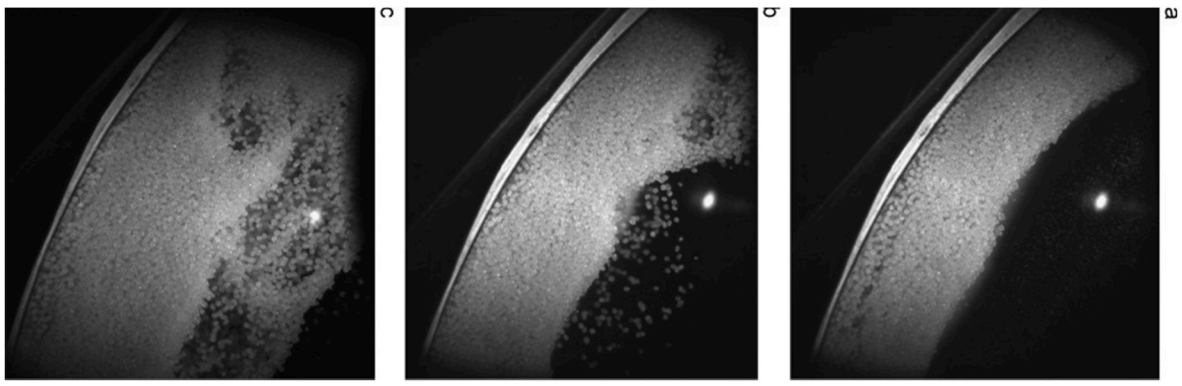

Fig. 11. Bed behavior with increasing solids capacity. (a) 3 kg; (b) 4 kg; and (c) maximum capacity (5.4 kg). HDPE (ρ_s = 950 kg m^{-3}), d_p = 1.5 mm, $u_{g,inj}$ = 110 m s^{-1}. Reproduced with permission from Ref. [120].

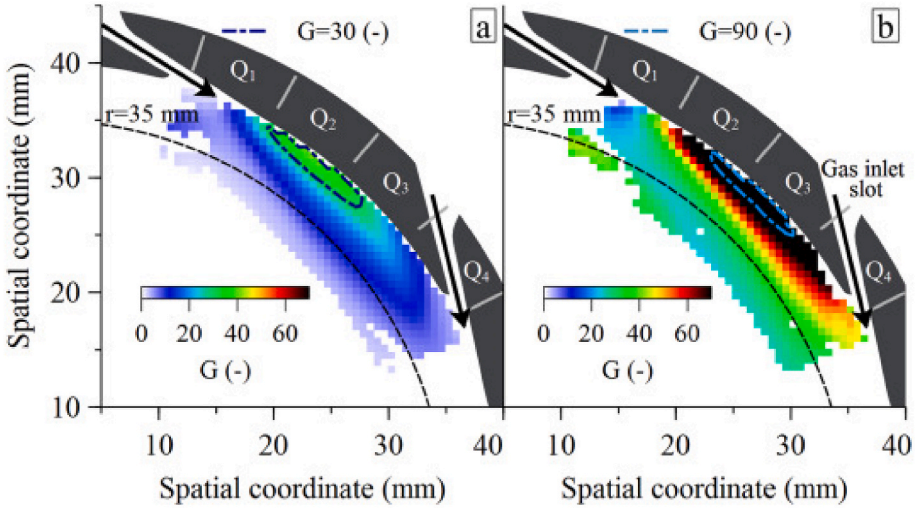

Fig. 12. Dimensionless centrifugal acceleration, G, for the air inlet velocity 101 m s^{-1}: a) aluminum spheres with a diameter of 0.5 mm and particle density of 2700 kg m^{-3}, and b) walnut shell particles in the sieve fraction of 0.50–0.56 mm with a particle density of ≈700 kg m^{-3}. In both cases, the results correspond to the mean from at least 100 2D PIV pairs. The dash-dot lines represent isoacceleration contours, and the light gray radial lines divide the arc distance between the gas inlet slots into quarters designated as Q_{1-4}. This figure is reproduced with permission from Ref. [121].

findings were compared with experimental data, showing reasonably good agreement. This comparison was validated using the standard Eulerian-Eulerian model for accurately simulating bubble hydrodynamics within the TZFBR across a broad spectrum of operational conditions.

The two-fluid model simulations applied the commercial CFD software Ansys CFX and Fluent to the TZFBR with membranes to examine the effect of gas extraction on fluid dynamic behavior. Simulated bubble properties and bed dynamics were analyzed and compared among different membrane reactor configurations, including reactor-wall and immersed tubular membranes. The immersed tubular membranes' configuration is the most suitable to enhance the gas-particle contact and favor the solids' axial mixing for *in situ* catalyst regeneration purposes based on the solids' holdup distribution at different fluidization regimes and permeation fluxes. However, the reactor-wall membrane configuration provides a greater permeation area for selective gas removal and is preferred to enhance purification.

3. Vortex reactor

3.1. Concept and functionality

Gas-solid vortex reactors (GSVRs) are centripetally operated FBRs achieved by injecting high-velocity gas in a circular shape where solids are added and rotated along the perimeter. The rotation is influenced by a radially inward drag force (typically a destabilizing force) and a radially outward centrifugal force (considered stabilizing). This review focuses on distinguishing the discussed reactors, known as rotating fluidized beds in static geometry (RFB-SG), from other devices that operate on a similar principle. Notably, these reactors lack mechanical moving parts. However, a short global overview of two types of centrifugal FBRs is given: the rotating fluidized bed and the stator-rotor reactor.

3.1.1. Single and multiphase flow fundamentals

Several studies have provided the most accurate hydrodynamic description of vortex reactors operating with single and two phases (gas-solid) through computational-experimental effort [116]. Recently, the validity of these flow phenomena has also been proven in gas-liquid operations [117]. Fig. 10 pictorially represents all these phenomena. Single-phase flow is characterized by the presence of near-wall jets arriving from the inwardly swirling gas flow, along with counterflow and backflow resulting from the near-wall interactions of these jets. These flow characteristics are primarily responsible for more significant pressure drops across the reactor as the gas flow undergoes multiple rotations, sudden changes in the flow plane, and reduced cross-sectional area before reaching the reactor outlet. The behavior of gas-only flow adheres to the cyclostrophic balance, as captured by equation (9), which

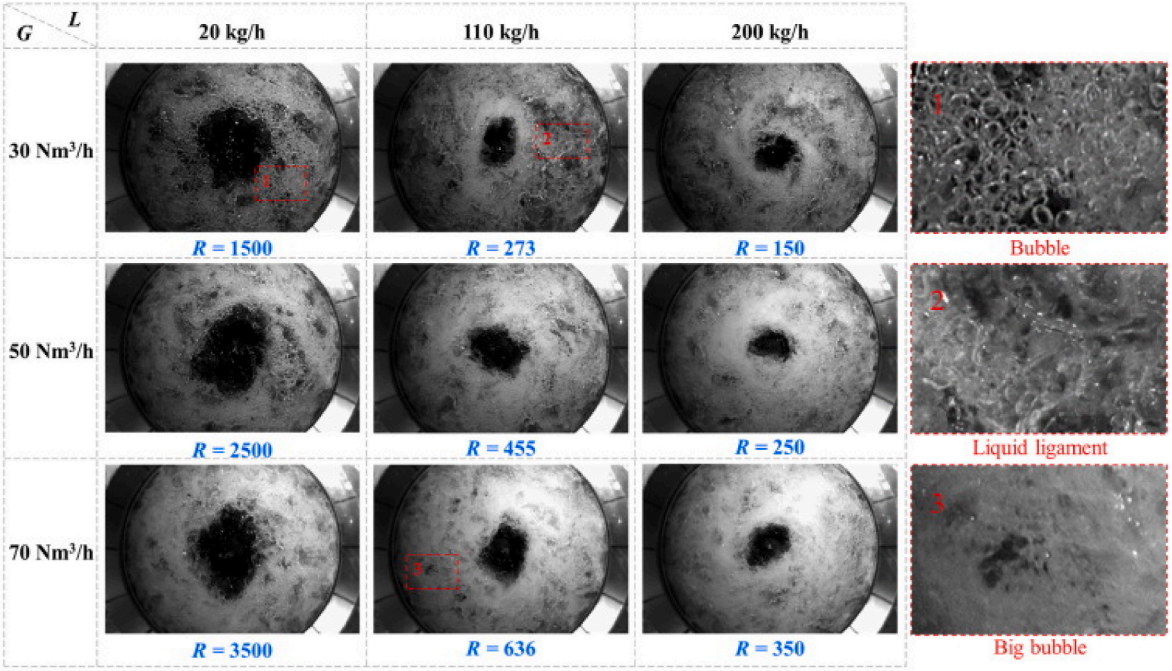

Fig. 13. Gas-liquid flow images from a high-speed camera and enlarged views of gas-liquid flow patterns for various combinations of gas-liquid flow rates. *G*: gas flow rate, *L*: liquid flow rate, *R*: gas-liquid volumetric flow ratio. Reproduced with permission from Ref. [117].

elucidates that the radial pressure gradient within the vortex reactor balances the centrifugal force.

$$\frac{\partial P}{\partial r} = \frac{\rho U_\theta^2}{r} \tag{9}$$

Gas-solid flows are relatively straightforward as other flow features are suppressed except for marginal backflow. This transition from single to multiphase flow occurs through a transitional flow regime called vortex suppression, achieved by feeding a minimum solid (or liquid) to the gas flow. In addition to establishing a rotational solid flow, vortex suppression also reduces the pressure drop through the reactor.

The gas flow behavior in gas-solid units differs substantially from the single-phase flow. The average gas residence time does not change from gas-only to gas-solid flows; only the gas residence time distribution is altered [118]. Most of the momentum is transferred to solids, which reduces the gas velocity by 70–80 % of its value in the gas-only flow [118]. Upon exiting the solids bed in the freeboard, the gas will almost immediately leave the unit via the central exhaust.

On the other hand, solids in the GSVU rotate under the action of outward centrifugal force and inward drag force. Depending on the unit geometry, gas flow rates, solids properties, etc., the range of minimum-maximum solid capacities can vary considerably, with slugging, channeling, and wobbling flow regimes [119] also observed, similar to those of classical FBRs (see Fig. 11 for experimental images of these bed behaviors).

Changes in gas flow rates and solids loading across these regimes result in a change in local solids volume fractions and a variation of the average azimuthal velocity of the solids bed in a vortex unit. However, the overall behavior of gas and solids remains relatively the same; the gas exits the unit from the freeboard without completing a turn, while solids keep rotating along the inner slot wall of the unit. Gonzalez-Quiroga [121] proposed that the aerodynamic response time of the particles (τ_p in seconds; equation (10)) is an important parameter that relates the particle physical properties to the solid bed-reactor outer wall interactions, which, in turn, affects the solids' azimuthal and radial velocity. For instance, low τ_p indicates radial velocities and bed voidage fluctuations, while a high value refers to a case of elevated solids-wall

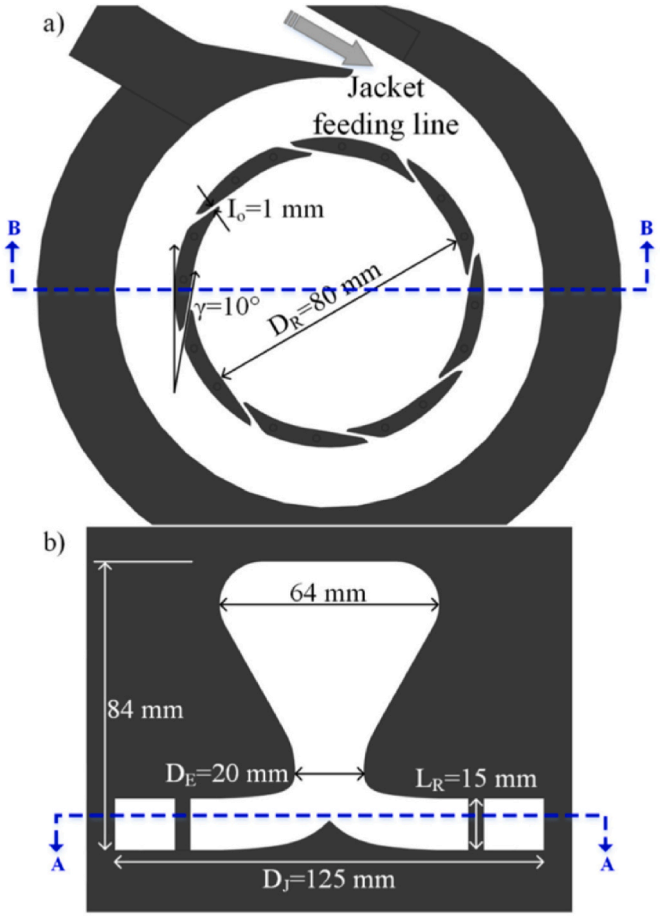

Fig. 14. Top and front views of a vortex reactor. Reproduced with permissions from Ref. [125].

friction and, therefore, lowered solid azimuthal velocity:

$$\tau_p = \frac{\rho_s d_p^2}{18\,\mu_g}\ (s) \tag{10}$$

Based on equation (10), the azimuthal acceleration of solids between the consecutive slots was defined and measured using the PIV technique, as illustrated in Fig. 12.

Replacing the solids with liquids does not significantly alter the phase dynamics. A highly dispersed, turbulent gas-liquid mixture is seen rotating within the reactor, and the gas passes through this liquid "bed" before exiting the reactor without completing a single rotation [122]. Liquid flow regimes can evolve through bubbling flow and annular flow, with a micromixing time recorded across these regimes from 10^{-3} to 10^{-4} s [117]. Fluid velocities and liquid back-mixing exhibit their peak intensities near the slot mouth, where the liquid behavior closely mimics that of a CSTR, facilitating high mass transfer rates. Conversely, the gas phase exhibits behavior akin to a PFR in the freeboard area and near the exhaust. The average liquid residence time, inferred from the overall phase holdup, is marginally greater than that of the gas phase, which remains largely unaffected by changes in the liquid feed rate [122]. Similarly to solids, the liquid bed remains in a state of rotational fluidization as long as gas flow into the reactor continues. It is noteworthy that, akin to the entrainment of fines due to attrition, the exiting gas is also likely to carry fine liquid droplets. Ouyang et al. captured this behavior using a high-speed camera, as shown in Fig. 13.

3.1.2. Solid capacity of reactors

A fundamental aspect of vortex reactor operation is understanding its minimum and maximum solids capacity. While seemingly straightforward, determining solids loading is intricately linked to several factors, including gas flow rate, reactor dimensions, and the physical properties of the solids. Friedle [123] synthesized correlations from a range of published experimental data, offering a method to predict the operational solids capacity of a vortex reactor.

$$\lambda_{max} = (4 \pm 0.4)10^{-3} Re_{p,R}^{(0.443\pm0.011)} S^{(0.454\pm0.018)} \tag{11}$$

$$\lambda_{min} = (1.15 \pm 0.05)10^{-4} Re_{p,R} \tag{12}$$

where λ_{max} and λ_{min} refer to the maximum and minimum solids capacity; $Re_{p,R}$ is the particle Reynolds number based on superficial velocity, and S is the swirl ratio.

These expressions can be used to determine the solids capacity of a vortex reactor. It should be noted that an implicit assumption in these laws is that the gas-solid flows are stable under the tested operating conditions. Therefore, the minimum solids capacity refers to the solid holdup at a steady state and fully established gas-solid flow in a vortex reactor. By definition, this capacity is different (slightly higher) than the vortex-breaking solids loading predicted by Kulkarni et al. [118]. The latter can be estimated by considering the number of solids in a monolayer at the inner slot wall of a given reactor, as shown in equation (13). In this respect, gas-liquid vortex reactors are still in the early stages of development. However, estimating the liquid holdup is relatively easy by measuring the liquid bed thickness, as demonstrated by Ouyang et al. [117].

$$V_{monolayer} = \pi\left(D_i^2 - \left(D_i - d_p\right)^2\right)H \tag{13}$$

where D_i and d_p are the reactor and particle diameters, respectively, and H is the reactor length (axial direction).

Table 2
Comparison of rotating fluidized bed and stator-rotor reactors.

Design feature	Rotating fluidized bed reactor	Stator-rotor reactor
Rotation source	Reactor chamber connected to a motor	Gas impinging on the reactor chamber
Gas feed	Optional; application-based	Mandatory; source of rotation
Scale-up possibilities	Limited; as higher sizes drive higher power costs	Practically not-constrained
Particle entrainment	Low to none as independent solids outlet is often undesired	Unavoidable as gas is implicitly used as source of fluidization
Gas-solid velocities	Can be independently controlled through separated feeds	Difficult to control without extensive design modifications
Technology maturity	Fully developed yet faces challenges for industrial applications	In early stages of development with lot of potential for applications

3.2. Vortex reactor configurations

Although the concept of vortex reactors is general (*i.e.*, FBRs that operate centripetally by injecting a high-velocity gas in a circular shape vessel), there are several configurations or operation modes to choose depending on the application. These and their particularities are shown in this section.

3.2.1. Gas-solid vortex reactor

A metered gas flow is sent to the reactor assembly through single or multiple inlet gas pipes. Although a single gas inlet shows minor velocity and pressure fluctuations [124], the number of channels is mainly inconsequential to the overall flow stability inside the vortex reactor. The gas brought by the inlet pipes is distributed over an annular space called a jacket, designed to distribute the gas uniformly over the entire circumference. The predominantly azimuthal flow direction is imparted to the gas beyond the jacket using a slotted ring, one of the essential geometrical features of the vortex devices. The slotted ring consists of I_N number of slots, each having a width of I_0 mm and is angled at γ degrees concerning the tangent to the main reactor. These geometrical features accelerate the incoming gas from the jacket and enforce a strongly tangential flow to establish in the reaction chamber, which is often referred to as the reactor. The reactor has a cylindrical shape due to the two closely spaced end-walls separated axially by H, marking the axial length of the reactor. The resulting gas flow in the reactor (for gas-only operation) is a strongly swirling flow that follows the laws of free-swirl motion, and its velocity increases as the reactor radius decreases. Finally, the gas exits via the central exhaust, which is positioned on either (or both, in rare cases) end plates, depending on the application. Fig. 14 shows an example of a vortex reactor from the literature [125].

In this developed gas flow in the reactor, solids are added pneumatically using a dedicated inlet positioned inside the reactor [126]. Solids are added against the adverse pressure gradients using a small amount of purge gas that can be inert or the same as the main gas. The

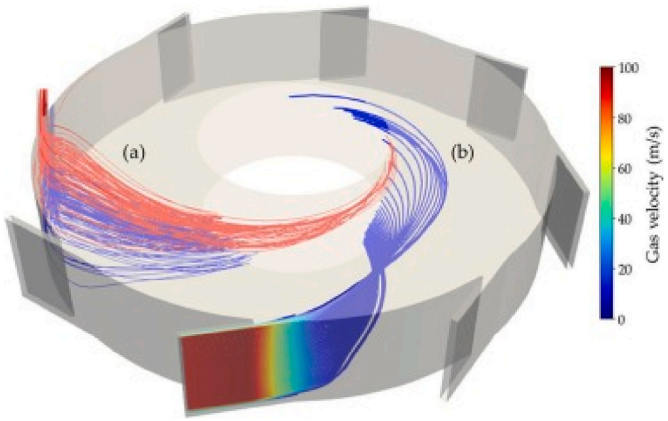

Fig. 15. Streamlines of time-averaged gas velocity (a) colored by reactor height, where blue and red represent the bottom and top half of the reactor unit, respectively, and (b) colored by mean gas velocity magnitude. Reproduced with permission from Ref. [116].

fluidization gas transfers most of its momentum to the solids, which then rotate along the outer wall of the reactor to form a rotating bed of solids with a thickness of L mm inside the GSVRs. Because the gas experiences reduced velocities after contact with the solids, it exits the reactor with a little swirl through the central exhaust. A continuous gas feed is necessary to maintain the solid continuous rotation. However, a constant solids feed is optional since vortex reactors can operate equally efficiently with a batch feed of solids. Denser solid beds rotating with a higher width-to-height ratio can be sustained in vortex reactors compared to traditional FBRs.

Notably, other designs conforming to the principle of rotating beds in static geometry, such as TORBED and fluidized jet mills, also exist in the literature. The latter has a design similar to that of the vortex reactor and is commonly used in the pharmaceutical sector as a grinding mill utilizing high momentum of incoming gas with continuous solid inlet and outlet. For further details, readers are referred to the relevant literature [127–129]. TORBED reactors also have a similar working principle to the vortex reactor, achieving a toroidal circular movement of particles through gas flowing through openings between stationary blades beneath the solids bed. The key difference is that in the vortex reactor, the gas flow direction is in the same plane as the solids, while it is orthogonal in TORBEDs [130,131].

3.2.2. Rotating fluidized bed reactor (RFBR)

An RFBR is a centrifugal reactor in which a motor provides momentum to a cylindrical reactor. One of the advantages of operating in such a dynamic geometry is the ability to independently control gas velocity and rotational speeds. This independent adjustment not only improves bed stability but also allows for higher solid loadings within the RFB. However, the mechanical components in motion can lead to vibrations and significant wear on seals. Fluidization in an RFB is primarily achieved through reactor rotation, enabling operation at lower gas flow rates compared to a traditional GSVR. This reduced gas-solid mass ratio renders the RFBR particularly suitable for processes where the gas phase does not participate in the reaction, such as in drying operations and the powder coating of materials [132–134].

3.2.3. Stator-rotor reactor

This reactor generates a homogeneous and densely packed bed of particles within a rotating reactor using momentum transfer from the gas phase [121]. Unlike the GSVR, the momentum is not directly imparted to the solid particles but rather to a series of angled blades appended to the reactor. Through proper blade design, the energy efficiency of the reactor improves compared to that of the GSVR. The increased energy efficiency reduces the required gas-solid mass ratio for sufficient fluidization. Therefore, the stator-rotor reactor has advantages and disadvantages similar to the RFBR. Although no external motor is needed for a stator-rotor reactor setup, available research uses an engine to have more control over the rotating speed [121]. The stator-rotor reactor is currently in the early stages of development, necessitating extensive investigation both experimentally and in modeling to fully realize and refine this innovative reactor design.

Table 2 shows the main differences between the rotating fluidized bed and the stator-rotor vortex reactor designs.

3.3. Advantages and limitations

The introduction of centrifugal force enhances various flow phenomena in vortex reactors, and the key ones are listed here.

1. Firstly, the slip velocities between gas and solid, which are otherwise limited in gravitationally operated devices, can be increased by a few orders of magnitude in the centrifugal field. The slip velocity is the vector difference between the gas and solid velocities at any location in the bed. In a vortex reactor, both contributions to slip velocities are higher, thereby increasing the overall magnitude. This direct

Table 3
Summary of vortex reactor-based applications (A: article; P: patent; E: experimental; M: reaction modeling; C: computational fluid dynamics).

Vortex reactors for Gas-solid applications				
Authors	Application	Type	Highlights	Comments
Kopp et al. [146]	Cocoa processing	P (E)	Single-step processing of cocoa beans and shells to produce cocoa products, without moving parts, shows improvements over typically used rotational devices.	Design and operation can be optimized for an industrial level of operation, indicating the potential for scalability.
Wu et al. [147]	Atomic layer deposition (ALD)	P (–)	Conceptual work, grounded in understanding vortex devices, provides detailed designs for (ALD in vortex reactors on thin wafers.	Multiple patents from the same authors suggest a strong intellectual property position, though the work is primarily conceptual, lacking experimental validation.
Grant et al. [148]	Chemical Vapour Deposition	P (C)	Swirling flow, generated by tangential injection of chemical vapors, deposits on the wafers attached to the reactor's top/bottom walls. Eliminated the need for moving parts, unlike competing technologies.	No experimental proof or data provided. The semiconductor industry reported as a possible target market.
Ma et al. [149]	Plasma-assisted ALD	P	Materials that can be deposited include ruthenium, tantalum, tantalum nitride, tungsten, and tungsten nitride.	Concerns about etching damage to substrates and compatibility with certain chemical precursors highlight the need for additional hardware to mitigate these risks.
Eliaers et al. [137]	Biomass drying	A (E, M)	An experimental drying study indicated the shrinking core model as the most suitable for capturing the drying process. Device scale-up studies suggested air flow reduction and multi-zone vortex operations from an industrial applications perspective.	Scale-up strategies could extend beyond drying applications, notably by adopting multi-stage vortex reactors to minimize gas usage or maximize the efficiency of gas feeds.
Fang et al. [150]	Lipid–Polymer Hybrid Nanoparticles synthesis	A (E)	Particles fabricated via this process display characteristics,	Scaling up the formulation involves balancing

(continued on next page)

Table 3 (*continued*)

Vortex reactors for Gas-solid applications				
Authors	Application	Type	Highlights	Comments
			such as small size, low polydispersity, and excellent stability, comparable to those made at the lab scale.	production yield against the desired particle characteristics.
Marchisio et al. [151]	Production of TiO_2 nanoparticles	A (E, C)	Particle sizes largely depend on the mixing effectiveness, which can be controlled.	Qualitative study
Hirsch and Steinfeld [152]	Catalytic H_2 production from natural gas	A (E)	Harnessing solar energy through vortex-type reactors reduced CO_2 emissions compared to other technologies.	The technology and device, still in developmental stages, could benefit from geometry optimization, potentially through CFD simulations to enhance design and functionality.
Kraupl et al. [153]	Combined ZnO-reduction and CH_4-reforming ($ZnO + CH_4 \rightarrow Zn + 2H_2 + CO$)	A (E, C)	High-temperature applications using solar energy demonstrated efficient heat transfer. Zinc conversion rates of up to 90 % were achieved, along with high-quality syngas production.	Same as above.
Trujillo and De Wilde [154]	Fluidized Catalytic Cracking (FCC)	A (C)	A significant process intensification was established compared with riser reactors for fluid catalytic cracking, suggesting potential optimization of gasoline and light gas selectivity.	2D CFD simulations performed; lacks experimental validation
Eliaers et al. [145]	Particle coating	A (E)	Uniform particle coating without agglomeration was demonstrated, even amidst high turbulence, resulting in minor cracks in the coated layer.	The inevitable loss of Geldart-C-type particles and the need for continuous solid feeding underscore the importance of optimizing the coating solution-solids flow to prevent slugging and ensure effective coating.
Ashcraft [142]	SO_2/NOx adsorption	A (C)	The SNAP process in GSVR proved as efficient as a riser for the same amount of solid sorbent used, with process intensification quantified at approximately 100–120 times per reactor unit volume.	A mismatch between experimental and simulation results, especially for the ΔP and local bed voidage irregularities, suggests limitations in current CFD model ability to capture complex physical phenomena.
Kulkarni et al. [24]	Biomass fast pyrolysis	A (C)	Demonstrations achieved around 70 % bio-oil yields for pine feed using 3D CFD simulations, with continuous segregation of unreacted biomass and generated char.	Proof of concept work, later validated by Nunez et al. Considering energy efficiency, replacing nitrogen with steam could offer significant advantages.
Vandewalle et al. [135]	Oxidative coupling of methane (OCM)	A (C)	Detailed 3D CFD simulations of OCM in vortex reactors also highlighted the potential for OCM at much lower temperatures through steady-state multiplicity.	Computational studies have shown the feasibility of OCM operations in vortex reactors with reduced hot spots and possibly enhanced C_2 yields.
Nunez et al. [138]	Biomass fast pyrolysis	A (E)	Experimental demonstrations showed 72 % bio-oil yields for pine feed, with continuous segregation leading to high bio-oil and low char yields.	Proof of concept work demonstrating the reactors' capability at operating temperatures around 550 °C with continuous feeding and char removal of pine/poplar.
Vortex reactors for Gas-liquid(-solid) applications				
Ryazantsev et al. [155]	Wastewater treatment (H_2S oxidation)	A (E)	Intensified oxidation rate observed. The oxidation of hydrosulfide ions is not controlled by the dissolution of oxygen in solution due to the large gas-liquid interface.	The rotating chamber, instead of a stationary one, could present challenges in scaling up device capacities.
Qian et al. [156]	Selective H_2S removal	A (M)	Selective H_2S removal over CO_2 using MDEA from a mixture was observed, with scale-up showing promise compared to packed bed reactors.	Rotating device and need for solid packing to improve gas-liquid contact.
Ouyang et al. [117]	CO_2 sequestration	A (E)	Reactive CO_2 absorption in alkali was	Quantifying gas throughput per reactor volume

(*continued on next page*)

Table 3 (*continued*)

Vortex reactors for Gas-solid applications				
Authors	Application	Type	Highlights	Comments
			demonstrated. Higher mass transfer coefficients were demonstrated compared to other technologies.	is essential for benchmarking the process intensification achieved through these designs.
Loftus et al. [144]	Particulate scrubber	A (E)	Gas-liquid vortex scrubbers efficiently removed fines from coal combustor flue gas, achieving >99 % efficiency for 3 μm fly ash particles with low-pressure drop and stable operation.	Further optimization is required to navigate the complex interplay between device throughput, liquid bubble sizes, cleanup efficiency, and pressure drop.

effect is anticipated to significantly enhance inter- and intra-phase heat and mass transfer [24,117]. In vortex reactors operating at room temperature, solids (and liquids) have been observed to reach velocities up to 10 m s^{-1}, a phenomenon that is difficult to achieve in traditional reactors.

2. Secondly, the centrifugal force exerted on particles within vortex reactors causes them to form a densely packed arrangement near the outer wall. This compacted bed, rotating with the primary gas phase, facilitates interactions between the gas and solids in a confined space. The average volume fraction of solids in this environment can reach 0.5–0.6 for spherical particles and potentially higher for irregularly shaped solids, compared to the 0.2–0.3 typically seen in conventional fluidized beds, depending on the operating regime.
3. Increasing the gas flow in vortex reactors leads to the stabilization of solid beds, which is attributed to the enhanced centrifugal components. This contrasts with FBRs, where increasing fluidization flow eventually causes solid beds to entrain.
4. The formation of closely packed beds, alongside higher slip velocities and greater gas throughput per reactor volume, allows for a reduction in reactor size compared to conventional designs. Moreover, vortex reactors can process larger quantities of materials per unit volume.
5. Vortex reactors are characterized by effective thermal back-mixing while limiting species back-mixing. This feature, combined with a plug-flow-like residence time distribution, facilitates control over intermediate product concentrations in processes where secondary reactions are undesirable [135]. Wery et al. [116] conducted simulations on the behavior of two gas-phase species introduced from the top and bottom of the slot, respectively. Their findings demonstrated the absence of lateral mixing between these two streams, as evidenced in Fig. 15.

Compared to reactors with rotating zones, vortex reactors are less energy-intensive without compromising the process intensification obtained. However, vortex technology also has disadvantages.

1. Vortex reactors require significantly larger quantities of gas to initiate and maintain fluidization, offering advantages over FBRs of equivalent volume. These gas volumes may appear excessive, especially when gas does not serve as a reactant, necessitating the recycling of outlet gas and increasing CAPEX costs. However, this limitation can be mitigated in applications where gas is a reactant, such as in CH_4 oxidative coupling or CO_2 sequestration. In such scenarios, vortex reactors can process higher volumes of gas per reactor volume more efficiently than alternative technologies [24,125].
2. Solid particles experience high shear due to intensified particle-particle and particle-wall interactions, leading to the attrition of solids. This causes loss of solids during operation and requires the deployment of solids recovery systems downstream of the reactor or intermittent feeding to replenish lost solids. However, attrition incurs additional costs and negatively impacts the process by changing the space velocities. Therefore, from a catalysis point of view, it is essential that a catalyst can sustain the high-shear environment in vortex reactors. At the same time, it must be ensured that metal-support interactions are strong enough to prevent metal loss and reduce catalytic activity.
3. Continuous solids operation is also challenging for several reasons. Solids feeding is assisted by a purge gas, which can be up to 10 % of the primary gas flow rate but may unintentionally dilute the reaction mixture. Solid removal can also lead to unwanted reaction mixture leaks that are difficult to quantify. The location of the solids outlet is also challenging to predetermine, as the bed thickness is directly related to solids loading and inversely related to the gas flow rate.
4. Fluidizing Geldart C-type particles is difficult, as most of the particles fed to the reactor, regardless of the start-up method, end up entraining with the gas.

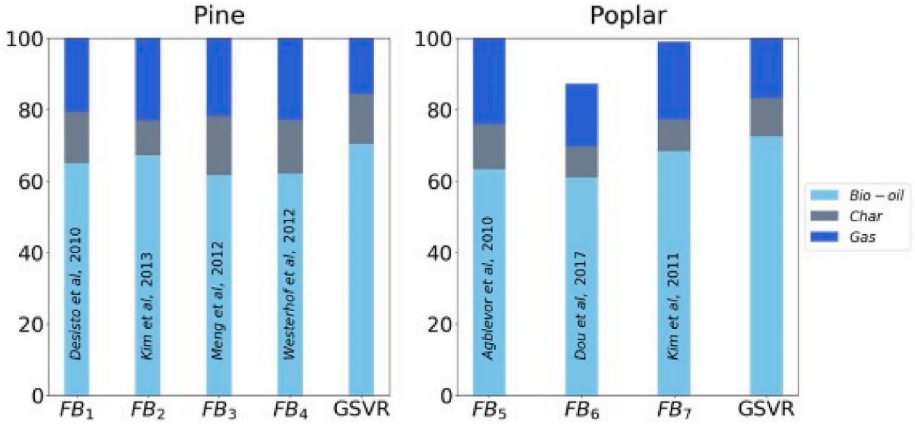

Fig. 16. Comparison of product yields on feed basis for the fast pyrolysis of pine and poplar in conventional FBR and the GSVR. Reproduced with permission from Ref. [138].

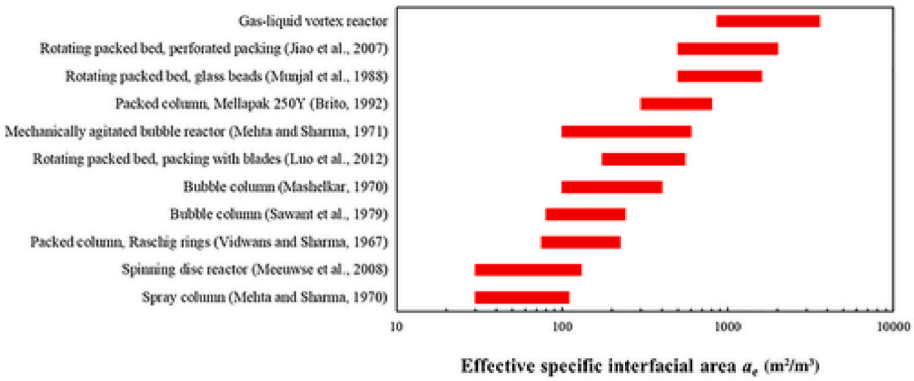

Fig. 17. Comparison of published ranges for the effective specific interfacial area for various gas-liquid reactors against the gas-liquid vortex reactor. Reproduced with permission from Ref. [117].

3.4. Applications of vortex reactors

Vortex reactors have been implemented for various applications, either computationally, experimentally, or both as seen in Table 3. While the predominant use of vortex devices has been in unit operations such as drying, recent years have seen a shift toward reactive applications [136,137]. This is partly because vortex reactors are a relatively new technology and partly due to factors such as the lack of a suitable catalyst and the recognition of process intensifications from vortex reactors. Since this review focuses primarily on applications, only a brief overview is given here; refer to for details on all the conceptual and implemented applications.

3.4.1. Reactive applications

Reactive applications combining high gas throughput and short contact times are attractive for vortex technology. Examples of such applications include adsorption processes, gas-phase polymerization, biomass (or coal) gasification, and fast catalytic partial oxidation of hydrocarbons. Reactive tests of vortex-based applications mainly focus on fast biomass pyrolysis, oxidative coupling of methane, and CO_2 reactive absorption. Despite the variation in operating conditions, feedstocks, and targeted products, these processes have similar requirements: short yet effective gas-solid contact times and high heat transfer rates. Biomass fast pyrolysis benefits greatly from the rapid heating of solid particles and the concurrent removal of generated char, which otherwise might catalyze undesirable product degradation. Computational fluid dynamics (CFD) studies on fast pyrolysis biomass have forecasted bio-oil yields of up to 70 % from biomass feedstock, facilitating *in situ* separation of char from unreacted biomass [124]. These predictions have recently been experimentally validated by Manzano [138], who achieved a 72 % (w/w) bio-oil yield from pine at 500 °C using a vortex reactor, with char yields around 10 %. The produced bio-oil was notably rich in phenolics, syringols, and catechols, with no aromatics detected. Fig. 16 summarizes the product yields from

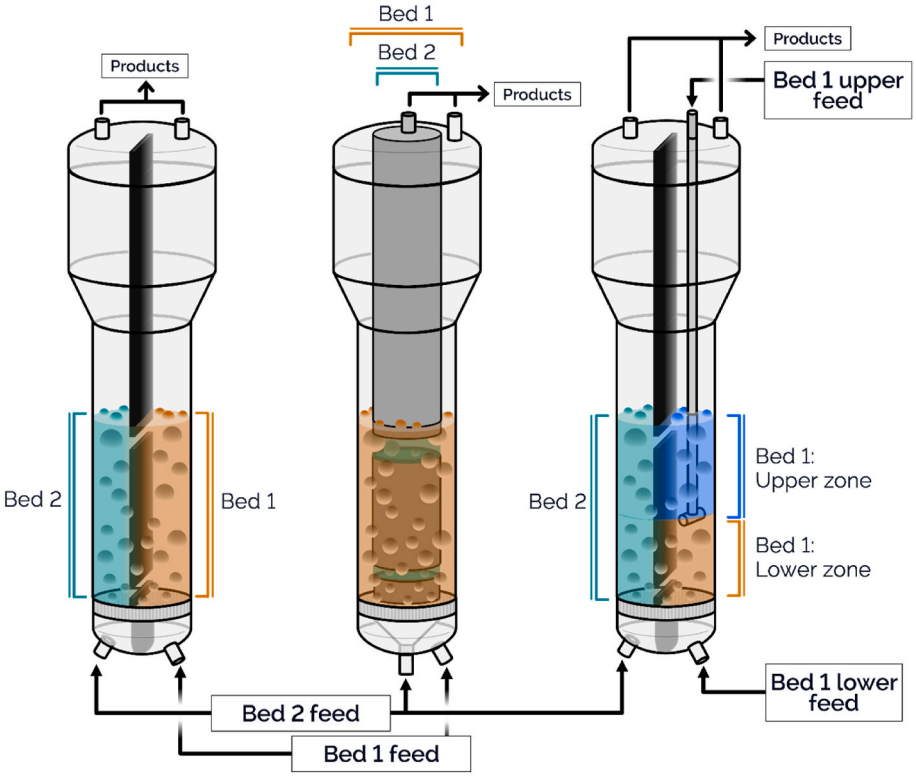

Fig. 18. Schematic representation of ICFBR configurations: plate (left), tube (center), and plate + TZFBR (right). Blue and green arrows represent the movement of the solids.

these experiments and compares them with data from various reactor types using the same biomass feed.

Catalytic oxidative coupling of methane also requires short contact times between methane-oxygen and the catalyst. However, effectively removing the exothermic reaction heat for high olefin yields is crucial for OCM. Several CFD and mathematical studies have predicted C_2 yields exceeding 25 % from OCM conducted in a GSVR [139]. Recently, a proof-of-concept experimental study demonstrated OCM at 850 °C in a vortex reactor and predicted a 6 % C_2 yield for a N_2:O_2:CH_4 feed of 20:1:4 [140]. The study employed a SiC-based Sr–La catalyst that enabled it to withstand the highly attrition-prone reactor environment, paving the way for other high-temperature catalytic applications. Similar studies investigating the thermal conversion of natural gas to lower olefins were recently conducted in a vortex-like device known as ANJEVOC (Novel Annular Jet Vortex Reactor). Pannala et al. computationally predicted C_2 yields as high as 28 %, with excellent scalability [141]. Vortex reactors are also attractive for OCM as the fluidizing gas is a reactant, unlike fast pyrolysis biomass. Thus, the high volumetric gas flows can potentially result in a high throughput compared to other reactor choices for OCM.

Computationally, an industrial SO_2/NOx adsorption process (SNAP) was also studied by Ashcraft [142] and demonstrated excellent process intensification compared to the conventionally preferred riser reactors. The vortex reactors removed 0.93 and 0.33 mol^{-1} $m^3_{reactor}$ of SO_2 and NOx, respectively, compared to 0.0086 and 0.0027 mol^{-1} $m^3_{reactor}$ in a riser due to the densely packed solid bed and larger surface area available. The authors further showed the potential for process enhancement by incorporating feed recycling.

Carbon capture via CO_2 sequestration proceeds through reactive absorption in an alkali. The effectiveness of CO_2 removal in all the absorption processes is directly proportional to the interfacial surface area available in the reactor. Ouyang et al. [117] experimentally demonstrated that a GLVR (gas-liquid vortex reactor) can generate high interfacial areas per reactor volumes of the order of 5000 m^2 m^{-3}, which is several orders of magnitude higher than those achieved in conventional bubble or packed column reactors. Additionally, vortex reactors provide 1 to 2 orders of magnitude higher mass transfer coefficients than other reactor types when comparing the volumetric mass transfer coefficient against the total energy dissipation (Fig. 17). Thus, vortex reactors offer absorption intensification without needing a mechanical stirrer.

3.4.2. *Non-reactive applications*

The intense centrifugal action inside the vortex forces the absorbed moisture (used for the liquid content inside solids) out and entrains it in the outgoing gas, making vortex devices primarily used in various drying operations. Additionally, spherical solid particles are typically obtained from vortex reactors due to centrifugal forces and wall-solid-fluid

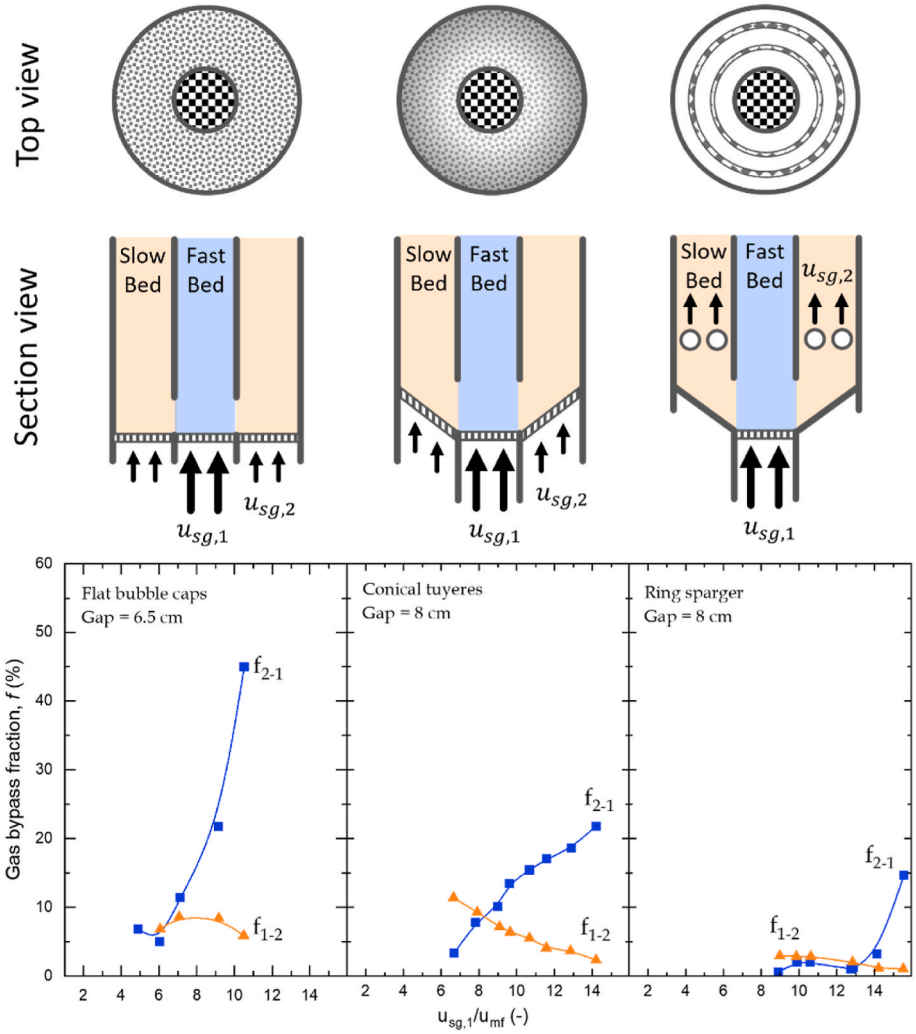

Fig. 19. Diagram of tube-type ICFBR gas distributors (top) and their respective gas bypass fraction as a function of superficial-to-minimum fluidization gas velocity ratio (bottom). $u_{sg,2}/u_{mf}$ = 0.7, $f_{1\text{-}2}$: gas bypassing fraction from section 1 to section 2, $f_{2\text{-}1}$: gas bypassing fraction from section 2 to section 1. Reproduced with permission from Ref. [168].

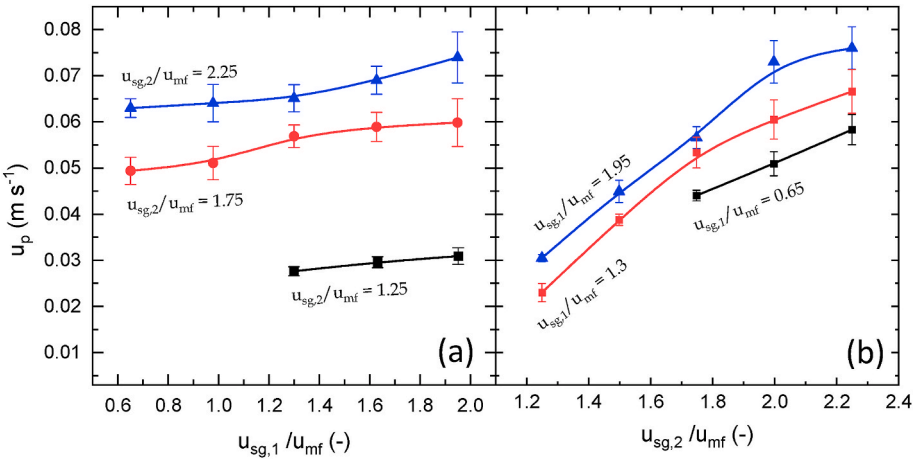

Fig. 20. Effect of superficial-to-minimum fluidization gas velocity ratio over particle velocity for (a) draft tube and (b) annulus section of a tube-type ICFBR. Reproduced with permission from Ref. [172].

Table 4
Summary of internal circulating fluidized bed reactors applications (A: article; P: patent; E: experimental; M: reaction modeling; C: computational fluid dynamics).

Authors	Application	Type	Highlights	Comments
M. Kuramoto et al. [157]	Fluid dynamics by cold flow visual observation	Plate (A, E)	The circulation rate of solids in reactors is significantly influenced by reactor design, gas velocity, and static pressure.	
M. Kuramoto et al. [158]	Fluid dynamics by cold flow visual observation	2D plate (A, E)	Model for the circulation rate of solids	
J. Cao et al. [176]	Bio-oil production from waste pyrolysis	Plate (A, E)	Proof of concept	
Y. Feng et al. [163]	Fluid dynamics by CFD	2D plate (A, C)	Model for solid and gas flows. Effect of reactor geometry and internal tubes bundle	
D. Thiemsakul et al. [183]	Dry reforming of methane	2D plate (A, C)	Proof of concept, experimental and simulated effects of reactor geometry and gas feeding system.	
P. U. Foscolo et al. [174]	Biomass gasification	2D plate (A, E)	Proof of concept, design, and coldflow modeling.	
X. Xiao et al. [164]	Biomass gasification	Plate (A, E)	Low-temperature profiles, heat exchange between profiles, and the use of pressure balance to separate gas streams.	Triple chamber reactor
X. Yang et al. [177]	Sorption-enhanced ethanol steam reforming	2D plate (A, E, M, C)	Fluid dynamic and kinetic models and improved heat management.	
J. Herguido et al. [169]	Hydrogen separation from H_2/CH_4 mixtures by steam-iron process	Plate (A, E, M)	Effect of reactor geometry on gas and solid flows.	Coupled with kinetic data
O. C. Snip [184]	Adsorption-desorption for SO_2 and NO_X removal	Plate (A, E)	Reduced solid attrition, a more compact system, and lower consumption due to the absence of solid transport lines.	Comparison with a NOXSO traditional process
L. Mleczko et al. [180]	Catalytic oxidative coupling of methane	Draft tube (A, E)	Proof of concept, greater safety, and stability with similar product yields (in FBRs).	Proposed an industrial-scale draft for this system
Z. Meng et al. [185]	Fluid dynamics by Ansys Fluent ®	Draft tube (A, Em C)	Effect of reactor design and operating conditions on gas and solid flows	
L. Mukadi et al. [175]	Thermal treatment of industrial waste	Draft tube (A, C)	Mathematical model for the effect of reactor design and operation.	
A. Hong-Sik et al. [186]	Fluid dynamics by cold flow	Draft tube (A, C)	Effect of reactor design and operating conditions on gas and solid flows.	Solid circulation rate measurement by thermal tracers
P. Li et al. [172]	Fluid dynamics for polysilicon granules production	Draft tube (A, E, C)	Less particle segregation (different sizes), lower gas bypass, and mathematical correlations to describe the system.	Solid circulation rate measurement by solid holdup and average particle velocity
S. D. Kim et al. [159]	Fluid dynamics by cold flow	Draft tube (A, E, C)	Effect of operating conditions and solid properties on gas and solid flows.	Solid circulation rate measurement by thermal tracers and pressure drop
J. Herguido et al. [48]	Catalytic oxidations (catalyst acts as an oxygen carrier) and dehydrogenation processes (the catalyst becomes deactivated by coke)	Plate + TZFBR (A, E)	Increases safety and selectivity and improves the control of catalyst oxidation.	
O. Rubio et al. [162]	Oxidative dehydrogenation of butane	Plate + TZFBR (A, C, M)	Proof of concept and mathematical model for estimating operating conditions	
J. Gascon et al. [65]	Catalytic propane dehydrogenation	Plate + TZFBR (A, E)	Proof of concept, similar yields to propylene as in other reactor configurations, better heat management from coke regeneration, and more stable operation	
J. Gascon et al. [75]	Fluid dynamics for catalytic propane dehydrogenation and butane partial oxidation	Plate + TZFBR (A, E, C, M)	Model for reactor design and operating conditions.	Fluid dynamics by the three-phase model coupled with kinetic models

attrition. Therefore, vortex devices are preferred for drying paddy [143], woody biomass [136,137], and other granular materials.

Loftus et al. [144] used a gas-liquid vortex reactor as a scrubber for fine fly ash particles in the incoming gas stream, mimicking the flue gas from industrial coal combustors and achieving 99 % efficiency in removing particles as small as 3 μm (particles an order of magnitude smaller were removed with ~90 % efficiency). The confined vortex scrubber showed favorable scale-up compared to conventional inertial separators, allowing pressure drops through the scrubber to be optimized using inlet gas flow, particle load, liquid amount, and bubble sizes. Eliaers [145] demonstrated particle coating using a gas-solid-liquid vortex reactor, resulting in a uniform layer of whey protein (70 μm; 260 kg m^{-3}; Geldart-C-type) particles by an aqueous maltodextrin solution (50 wt%). The work paved the way for the fluidization of Geldart-C-type particles and concluded that continuous solids feeding is necessary for cohesive particle fluidization in vortex reactors.

4. Internal circulating FBR (ICFBR)

Circulating fluidized beds are a particular category among fluidized beds, and they can circulate particles externally (conventional circulating beds or CFB) or internally (ICFBR). In the following sections, the latter are described, including their advantages and disadvantages, applicability, modifications to enhance them, and visualization and simulation studies.

4.1. Concept and functionality

ICFBRs are single vessels where particles move following an established path [157] by dividing the reactor into two zones with a plate (baffle type ICFBR) [157–161]. The circulation of particles between two distinct zones is facilitated by applying varying fluidizing gas velocities, typically distinguished as the fast bed and slow bed. This variation in gas velocity results in different porosities within the beds, thereby creating a pressure gradient at the reactor bottom. This gradient drives the movement of particles between zones through openings located at both the top and bottom of the zones [158,162–164].

This reactor exemplifies process intensification because this geometry allows it to operate in two different atmospheres in the same vessel while differentiating from the TZFBR because the separation between zones is physical and delimited. A schematic representation of the ICFBR is shown in Fig. 18 (left).

It is essential to consider that solid recirculation is the critical parameter to control when designing an ICFBR. The solid flow through each one and between sections is mainly affected by superficial gas velocity, specifically the ratio between both zones, particle size, bed height, and the size and shape of the connection between zones [159,160,163,165–167].

4.2. Advantages and shortcomings

ICFBRs have multiple advantages over conventional FBRs. The most apparent advantage is their capacity to maintain two separate atmospheres where reactants and products do not mix. This increases safety and selectivity and simplifies the circulation of solids compared to TZFBR. In the ICFBR, bubbles carry the movement of solids through and between beds, allowing for the maximum downward flow of solids without producing gas back-mixing. The separation between zones is physical, and the movement of solids between zones is driven by pressure perpendicular to gas movement. Proper connections and small dead-volume valves prevent gas mixing between zones. However, leakage could be significant in reactor configurations without restrictions on the gas flow between both zones through the upper and lower connecting holes (Fig. 19). One challenging aspect of the ICFBR is reaching an operating window with a high flow rate of solids and a minimum gas shortcut.

The mixing of the currents from each zone is evident in configurations without a separation plate in the freeboard (Fig. 18). This is crucial when maintaining two separate atmospheres throughout the reactor is required, such as the separation of H_2 from gas streams through the steam-iron process, an example of a reduction-oxidation system [169].

Properly designing the connection between zones and maintaining a significant difference in gas velocities of both zones can prevent gas back-mixing and promote greater solid flow [163,165,166,170,171]. While this strategy offers promising advantages, it also introduces safety concerns. For instance, solids might not flow as intended (*e.g.*, plugged solid flow or failure in controlling gas feed to each zone), potentially allowing an oxidizing agent to reach the reaction zone. However, it is important to recognize that this issue is not unique to the ICFBR but can occur in any conventional reactor handling gas-phase oxidations. One of the key characteristics of the ICFBR is its enhanced solid circulation. The clearly defined path for solids from one zone to another allows for straightforward control of solid flow by employing varying gas velocities in the two zones (Fig. 20). This approach helps prevent issues like particle segregation by size or gas back-mixing, enabling the reactor to operate at higher gas velocities than other configurations [159,161,162,165,172,173]. However, solid circulation does not only depend on gas

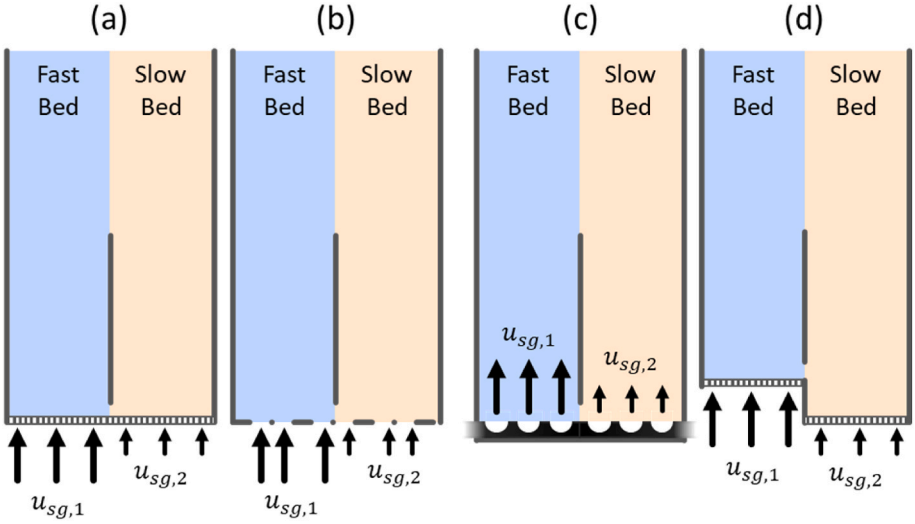

Fig. 21. Different geometries of 2D ICFBR gas distributors: (a) plate, (b) perforated, (c) tubular, and (d) raised plate. Adapted from Ref. [167].

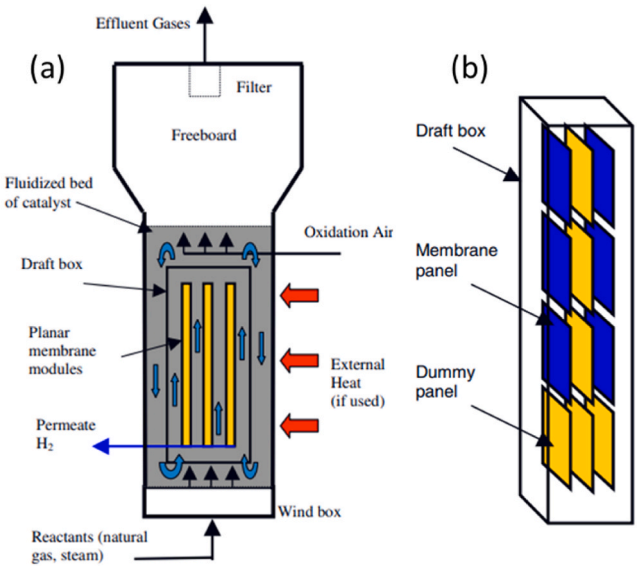

Fig. 22. (a) Schematic representation of an ICFBR with membranes and (b) the isometric view of its core. Reproduced with permission from Ref. [178].

velocity but is also affected by particle properties, the size of the orifice between zones, and reactor geometry and design [159,161,163,165,170,174], making it challenging to achieve optimal operation if the solid does not flow as designed.

The system also enhances energy transfer between zones. As a result of the high flow of solids between both zones, the reactor can be considered isothermal. This characteristic is particularly advantageous for processes involving one exothermic and one endothermic reaction. In such cases, one zone generates heat, which is then transported by the solid to the other zone, where it can be utilized [162,164,172,175]. However, despite a thorough understanding of reaction rates for each zone, energy transfer is significantly influenced by catalyst properties, such as thermal conductivity and size. This can lead to high-temperature gradients between beds, even with high solid circulation rates [175].

4.3. Applications of ICFBRs

ICFBRs have attracted attention for several reactions due to their advantages over conventional fluidized reactors as seen in Table 4. The geometries range from basic ICFBR configurations, such as baffler-type designs, to more advanced ones, described in the subsequent section. Potential applications for the ICFBR include coal or biomass gasification [164,174–176], ethanol or hydrocarbon reforming [177–179], oxidative coupling of methane [180], hydrocarbon dehydrogenation [162,181,182], partial oxidation of butane to maleic anhydride [182], dry reforming of methane [183], among others [169].

4.4. Process intensification

The original design of the ICFBR has been modified to enhance its capability and performance. These changes encompass two main directions: modifying the original system design and coupling the system with other technologies.

4.4.1. Design modifications

The most common design modification involves changing the geometry of the physically separated zones from a plate-type to a tube-type design, as shown in Fig. 18 (center) [159,172,183,185,187]. This variation changes the flow of solids from a 2D movement to a 3D axial direction, in which the solids move upwards through the internal face of the tube and downwards through the external front of it. Changing the movement of solid flow presents two advantages over the original path. First, the flow of solids could be enhanced because the movement of the solids is not confined to a single direction, eliminating solid clogging at the connection point between zones. Second, heat and energy transfer are improved due to an increased contact area (per unit of volume) between zones [188].

Another modification involves the gas distributor (Fig. 21), which can be elevated in one of the beds [167,172,183], inclined at a certain angle to facilitate solid movement from one zone to another [159,166,187], or even altered from a flat plate to different geometries [159,167].

4.4.2. Coupling ICFBR with other technologies

The original design of the ICFBR employs either smooth or bubbling fluidization regimes for both zones, where the flow of solids can be modulated by the difference in gas velocity between them. A notable modification to this design incorporates alternative fluidization regimes for one or both zones, specifically fast fluidization, such as riser or downer regimes [175,180,183,185]. Integrating draft-tube geometries within the ICFBR, combined with riser and downer regimes, could enhance control over solid flow and improve contact between the solid and gas phases.

Owing to its superior management of solid flow between zones, ICFBRs can be integrated with other technologies where controlling solid flow is challenging. One such technology is the TZFBR, where managing solid flow, driven by ascending bubbles, is a critical operational parameter. The synergy of these two technologies, illustrated in Fig. 18 (right), allows for precise control of catalyst flow through the reactor by adjusting the gas velocity ratio between the zones [162,171,181–183]. This integration not only enhances the overall process but also serves as a prime example of process intensification, with each technology addressing a limitation of the other.

Furthermore, the adaptation of membrane technology represents a promising enhancement to the ICFBR system. Although research in this domain is relatively limited, some studies have demonstrated its viability for methane steam reforming (Fig. 22). In these studies, the membrane facilitated a higher yield of targeted products (in this context, H_2) by shifting the reaction equilibrium. Concurrently, the optimized solid flow and heat transfer characteristics of the ICFBR mitigated heat transfer limitations associated with reforming [178,179,189].

4.5. ICFBR experimental and mathematical models

Although the ICFBR promotes solid circulation within a single vessel, predicting the solid recirculation rate quantitatively is challenging due to multiple factors such as geometry, operating conditions, and gas/solid properties [165].

Experimental systems have been used to investigate reactor hydrodynamics [157,160,165,166,190,191], while physical and numerical models help optimize the design and operating conditions and allow for trial changes in operating conditions and geometrical configurations [163,170,185]. Measuring solid flows or circulation rates underlies many experimental studies with cold-flow transparent ICFBRs concerning dynamic behaviors, including direct calculation, non-intrusive, optical probes, and combined methods.

4.5.1. Direct calculation methods

These methods determine the solid circulation rate by measuring the weight of the collected solids in a specific system location within the consumed time. In an early work, an ICFBR was developed and used to study the effects of several parameters [157]. These parameters were the superficial gas velocities introduced through various injection ports, the static pressure, and the coarse foreign solids' movement under various operating conditions. The results showed the same advantages as conventional dual-circulation systems with the feasibility of pressurized operation, which is almost impossible to achieve using traditional methods.

4.5.2. Non-intrusive method

Non-intrusive methods involve obtaining results from visualizing tracer-like particles. In these methods, colored or marked particles are introduced into a transparent reactor (with two or three-dimensional geometries) to obtain time-dependent movement vector fields, which can be translated into models and correlations through software.

Some authors described a non-intrusive radiotracer-based method for determining the solids circulation rate in a cold-flow four-cell ICFBR. This method directly measures the residence time of a single radioactive glass bead (radiotracer particle) in two adjacent cells [190]. It can be achieved by labeling solid particles with radioactive ^{24}Na or ^{192}Ir and monitoring them with two external NaI scintillation detectors. The solid circulation rate between the interconnected cells is determined by calculating the radiotracer particle's mean residence time and the solid mass. For this method to be effective, the characteristics of the radiotracer particle and the solids in the cell should be as similar as possible, including particle size, shape, density, and possibly electrostatic properties. This technique accurately measures the RTD of the particles, independent of other processes occurring within the system, such as the generation of static electricity during fluidization.

Other researchers have utilized a twin fluidized bed solid circulation system where two adjacent beds exchange solids [160]. In this system, a high-speed digital video camera records the particle flow in the lower orifice through the transparent reactor wall. Using a computer correlation analysis method, the recorded video can determine particle flow velocity, and the total solid flow rate can be obtained based on the measured particle velocities at different times. Experiments on a small-scale setup have shown that bed material properties, gas velocities of the two beds, orifice size, and distance are the main factors affecting the solid circulation rate.

Another approach to studying solid flow characteristics and circulation rate in an ICFBR is to use a single fluorescent sphere as a tracer and record its trajectories with a camera [165]. In this setup, the fluidized bed is placed in a dark room to observe the fluorescent movement more clearly. A tool like MATLAB can be used to process the images to determine the particle positions, velocity and solid circulation rate. This method can yield results that align with experimental measurements in literature and predictions using the correlation based on Bernoulli's equation.

Table 5
Summary of simulations in internal circulating fluidized bed reactors.

Authors	Physical model	Methodology	Classification
Feng et al. (2012) [163]	2D geometry with baffle	Two-fluid model with kinetic theory of granular flow	CFD
Lou et al. (2013) [160]	3D geometry in rectangle shape	Gas flow by large eddy simulation while solid kinematics by soft-sphere model	CFD-DEM
Solnordal et al. (2015) [161]	3D geometry in rectangle shape	Eulerian solution for fluid phase with a Lagrangian-based approach for the particle phase	CPFD
Hassan et al. (2016) [167]	2D geometry with baffle	Two-fluid model with kinetic theory of granular flow	CFD
Hassan et al. (2019) [170]	2D geometry with baffle	Two-fluid model with kinetic theory of granular flow	CFD
Meng et al. (2020) [185]	Industrial scale reactor	Two-fluid model with kinetic theory of granular flow and EMMS drag model	CFD
Thiemsakul et al. (2022) [183]	2D geometry with baffle	Two-fluid model with kinetic theory of granular flow, modified Gidaspow drag model and reaction kinetics	CFD with UDF

4.5.3. Intrusive methods

Intrusive methods, which affect the measurement of solid or gas flow development through the reactor, include gas sampling tubes and optical probes but have advantages such as gas concentration or direct velocity measurements.

One method to determine the solids circulation rate involves measuring the particle's downward velocity in the moving bed by employing two thermistor probes to trace heated bed material [168]. When hot sand particles interact with the probe, a change in resistance is converted into voltage through a bridge circuit. The particle's downward velocity can be estimated by measuring the time lag between the peak-to-peak distances of two distinct signals. It is assumed that the particle velocity measured at the center of the annulus represents the average bulk velocity within the annulus. Similarly, thermistor probes can also be utilized to investigate solid circulation in a cold-mode transparent ICFBR equipped with an orifice-type square draft tube [191].

A similar procedure can be used to obtain the solid circulation rate across a two-compartment fluidized bed. This system, divided by a pair of V-valves and a riser, exhibits solid flow characteristics that depend on various design and operating parameters [192]. In this case, calculations were performed based on the heat balance of circulating solids under steady-state conditions by measuring the average temperature of the upstream bed and the inlet and outlet gas temperatures. This method is akin to the one previously described but relies on the overall heat balance rather than the heat transfer of individual particles.

Other research in this field involves a cold-flow ICFBR utilized to explore gas-solid flow characteristics in a novel furnace design, employing reflective-type optical probes and differential pressure transmitters for measurements [193]. This study focused on examining the particle internal circulation rate and solid holdup in the furnace's upper space by varying the height of the partition wall, initial static bed height, and fluidization air velocity in the main zone. The findings indicated that the particle internal circulation rate decreases with an increase in the partition wall height but increases with the initial static bed height in the main zone and reaches a maximum with a certain fluidization air velocity. However, although the solids holdup in the upper space of the ICFBR cold system constituted only 1–4% of that in a conventional CFBR, the proportion of particle external circulation rate was relatively low in the circulating system.

4.5.4. Combined method

A combined method utilizes both non-intrusive (radioactive tracer) and intrusive (metallic sampling probes) approaches [194]. Tracer-tracked particle trajectories generate a set of solid dynamic properties. Solid falling in the annulus zone is collected and measured by the sampling probe. Solid RTD measurements are taken in the volume space delimited by the external column of the ICFBR. With the solid concentration and solid RTD at the exit zone, the effects of the riser exit geometry on pressure drop and solid behavior inside the ICFBR are studied. Solid RTD results and axial solid hold-up profiles provide clear evidence that the separator device at the riser exit significantly affects the hydrodynamics of the ICFBR riser. The V-shaped riser exit geometry is optimal among the configurations studied (Λ, V, double cone, and none).

4.6. Reactor simulations

Physical and numerical models are often used to test modifications in operating conditions and geometrical configurations due to the limitations of visual methods at larger scales. These models have proven helpful for adequately designing and operating ICFBR systems based on a better understanding of the phenomena involved.

Particle circulation between two fluidized beds can be investigated using an open-loop circulating apparatus with two compartments separated by a partition plate [195]. A model for calculating driving and

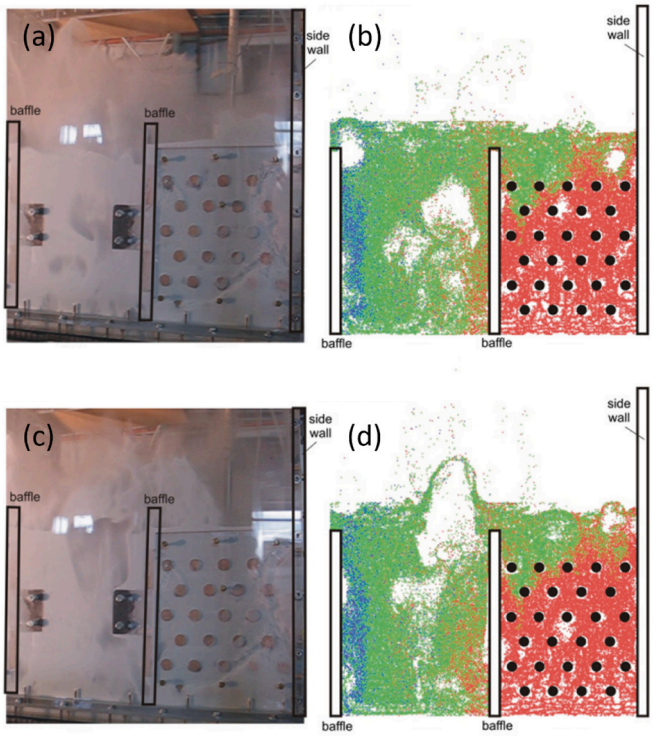

Fig. 23. Comparison between experimental observation (a, c) and model prediction of ICFBR bubbles (b, d) at two different times. Colors for tracking particle flow paths from two of the three chambers (red: right chamber, green: central chamber, and blue: left chamber located out of the pictures). Reproduced with permission from Ref. [161].

resisting forces can be developed by measuring pressure gradients and bed porosities. Experimental results indicated that the most efficient method to control the circulation rate of solids was by varying the vertical resisting force in the down-flowing compartment. This was achieved by adjusting the gas velocity and, thus, the fluidization regime in this area. Furthermore, a mathematical model [196] described the flow of solid and gas through an orifice between two aerated beds, where one operated in a reduced fluidization mode (u_g/u_{mf} close to 1) while the other is fully fluidized. The model was qualitatively and, to a certain extent, quantitatively validated. It demonstrated good agreement with the data and the trends documented in the literature [195]. Another mathematical model [144] calculated the particle flow rate through the orifice in a TZFBR solid circulation system, considering the effects of bed material, pressure gradient, and gas velocity. This model achieved a relative deviation between calculation and experimental data of less than 15 %. Additionally, other researchers have found that the bypassing gas fraction can be correlated with gas velocities of the fluidized and moving beds, opening area ratio, particle diameter, and solid height in the bed [191].

All these models and correlations could be integrated with CFD modeling, which captures the complexities of hydrodynamics, physical properties, operating conditions, and chemical reactions. Therefore, various variations in physical design and operational parameters can be tested and refined until an optimum performance design is identified [200]. Table 5 summarizes the different simulation methodologies and features in the ICFBRs by 2D and 3D geometries at the laboratory and industrial scales. Fluent has been an efficient way to simulate the hydrodynamics in the ICFBRs by the two fluid Eulerian-Eulerian model with different settings of granular flow and drag models ([163,167,170,185]), for which the reaction kinetics can also be included [183]. The two–fluid model has limited prediction accuracy due to the assumption of pseudo–fluid rheological properties of particles, so DEM [160] and CPFD [161] have been adopted to better describe the particle interactions. As DEM models each individual particle as a separate entity, it is computationally resource–consuming. The CPFD method based on the Eulerian–Lagrangian scheme has become one of the most practicable approaches for studying gas–solid interactions in fluidized bed reactors with the convenience of less computational resources and scale–up feasibility.

4.6.1. *Pure hydrodynamic models*

Pure hydrodynamic models aim to predict and explain phenomena in ICFBRs by considering the properties and movement of both solids and gas through the different zones of the reactor. No reaction is assumed in these models, so the solid and gas flux/flows do not change.

One study investigated gas and solid dynamics in an ICFBR using the Eulerian-Eulerian model alongside the kinetic theory of granular flow (KTGF) in Fluent® [163]. Simulations were performed to assess the effect of changes to four different parameters: gas distributor plate angles, the presence of a heat exchange tube bundle, superficial gas velocities, and initial packed solid heights based on a two-dimensional geometry. The mechanism governing the solid recirculation in an ICFBR is explained, and the effect of those parameters can be quantified in terms of the solid recirculation rate. From the parametric study, superficial gas velocities and initial packed solid height significantly affect the solid circulation rate. Moreover, the presence of a tube bundle reduced the solid recirculation rate by 20 %, while a 1.5° inclination angle had minimal effect on the recirculation rate.

Other studies also utilize Fluent® to model the behavior of bed particles [167,170]. The first employed a two-fluid model in a two-dimensional baffle-type ICFBR to assess the effects of gas distributor types, superficial gas velocity, and zone height elevation on solid circulation. The second study used a multi-fluid Eulerian model to simulate the solid circulation rate, focusing on a binary mixture of solids (two particle types with different sizes and densities) in a twin-zone ICFBR. The effects of varying gas velocities, mix of solids, and mixture composition were investigated. Results indicated that the ICFBR exhibited a higher capacity for solid mixing than a conventional bubbling fluidized bed, which aligns with the previously mentioned advantageous feature of this type of reactor.

Another model can be generated by numerically investigating the gas-solid flow dynamics in a three-dimensional baffle-type ICFBR using CFD-discrete element methods (CFD-DEM) [160]. In this approach, gas flow is modeled using large eddy simulation (LES), while solid kinematics are addressed through the soft-sphere model. Gas-solid dynamics and parameter sensitivity analysis elucidate the mechanisms driving specific circulation behaviors. The pressure difference between the two zones acts as the driving force for solid circulation through the gap, while bubble evolution, breakup, and gas flow diversion stimulate solid circulation over the baffle.

When employing CPFD Barracuda software to simulate a three-zone ICFBR at room temperature, a comparison between visual experiments and modeling (Fig. 23) indicated that the multiphase particle-in-cell (MP-PIC) method could qualitatively predict the overall ICFBR behavior [161]. This encompassed the relative degree of fluidization between the central reaction zone and the two heat exchange zones, the bubbling dynamics, and both the relative and absolute bubble sizes within each zone. Thus, the MP-PIC technique was affirmed as a valid tool for simulating isothermal bubbling fluidized bed systems containing Geldart B solids. However, quantitative accuracy diminishes when gas velocities approach u_{mf}, primarily due to less defined and more homogeneous bubbles.

Other authors had also employed the two-fluid model to examine the effects of operating gas velocity, particle diameter, and reactor configuration on fluidization behavior in an ICFBR [172]. This study specifically focused on the solid circulation rate, gas bypass fraction, and solid circulation pattern, all integral to ICFBR performance. Furthermore, the transition in the solid circulation pattern was found to be closely linked

to the gas bypassing behavior. The energy minimization multi-scale drag model was utilized in Fluent® to simulate industrial-scale ICFBRs equipped with central downcomers [185]. Based on the two-fluid model, this research aimed to analyze the impacts of various outlet structures to develop a model capable of predicting outcomes closely aligned with experimental observations. The findings indicated that the solid mass flux circulation is significantly influenced by the reactor design.

4.6.2. Models involving reaction

Models involving reaction must consider that gas concentration and flow may change during the reaction. Therefore, the evolution of these factors through the reactor must be included in the model, as they may also impact the flow of solids. In the two-dimensional Eulerian-Eulerian model used in Fluent®, the mass, momentum, and energy governing equations are solved together with KTGF to describe gas-solid hydrodynamic characteristics, like in this example of an ICFBR [183]. This work considered the dry reforming of CH_4 and coke oxidation, which were included in a CFD model using user-defined functions (UDFs). The analysis of variance revealed [196] that the length of the loop seal and the gas outlet diameter have significant negative and positive effects on methane conversion, respectively. The interaction between the size of the loop seal and the gas outlet diameter also significantly impacts methane conversion.

5. Considerations and perspectives

Notably, multifunctional FBRs will attract greater attention in multiphase process intensification in the coming decades [197]. This section discusses some common considerations and potential enhancements to make their implementation more seamless.

5.1. Common considerations

As stated in previous sections, FBRs are an exciting alternative to traditional packed beds. Although their use is less widespread, they offer undeniable advantages in laboratory and industrial scales. However, certain considerations should be considered when using FBRs, especially multifunctional designs like the ones described herein.

5.1.1. Geldart's classification and fluidization regimes

When using solid particles in FBRs, one of the first considerations is their physical properties, such as particle size and density, which significantly affect how the solid behaves in the fluidized bed and how easily the desired fluidized regime for specific applications can be achieved. To characterize the solid type, it is common to refer to Geldart's classification, which typically requires knowledge of the gas, particle density, and particle size. Powders can be classified into four groups (aeratable, bubbling, cohesive, and spoutable) [33,198].

The type of powder significantly influences how it fluidizes with increasing gas velocity. Aeratable and bubbling solids generally transition from smooth to bubbling to turbulent fluidization, cohesive solids exhibit channeling before entering turbulent fluidization, and spoutable solids initially demonstrate spouted fluidization before transitioning to a turbulent regime. After reaching turbulent fluidization, all powder types progress to fast fluidization and ultimately to pneumatic transport [199]. It is important to consider this because some reactors discussed in this review require specific fluidization regimes for optimal operation. The two-zone and the internal circulating reactors are designed to facilitate the vertical movement of solids by gas bubbles, rendering them suitable only for the bubbling regime. In lower gas velocity regimes, such as smooth fluidization, no gas bubbles are present to transport the solid [14,200], while at higher gas velocities, in a turbulent regime, gas back-mixing becomes pronounced [201–203].

Interestingly, the direct application of the Geldart classification to vortex reactors has sparked extensive debate due to the dissimilarity in the driving forces at play: 1 G in traditional fluidized beds versus several orders of G in a vortex reactor. This difference is the main reason for the hesitancy to directly apply the Geldart classification; the experimental literature indicates a transition from Geldart B-type to D-type particles as the centrifugal force increases in a rotating fluidized bed, where both the vessel and solid bed rotate [204,205]. Despite these findings, the Geldart classification is often used for vortex devices due to its simplicity and the lack of alternative classifications. However, a detailed experimental campaign is necessary to fully map the fluidization regimes under the influence of high-gravitational environments.

Unpublished experimental data from the Laboratory for Chemical Technology at Ghent University have revealed potential fluidization behaviors for C-type particles in vortex reactors. Preliminary fluidization trials with a batch feed of flour-like material and developed gas flow indicated a transient bed formation prone to entrainment. However, at steady state, a thin layer of solids was observed to rotate near the inner walls of the reactor, constituting less than 20 % of the feed mass. Similar observations were also recently made for an OCM catalyst, highlighting the challenges of sustaining a bed of Geldart C-type particles under ambient and reactive conditions [140]. Therefore, understanding the transition between fluidized regimes is crucial in reaction engineering and reactor design, as it elucidates the phenomena occurring inside the reactor, especially the interaction between gas and solid phases.

5.1.2. Solid attrition, wear, and fines entrainment

Particle attrition occurs when particles break into smaller ones due to abrasion or stress caused by impacts, reactions, or thermal changes. Wear (also known as erosion) refers to the loss of material from the particle's surface through continuous contact with gas or other solids. Both effects are relevant in fluidized systems, but wear is particularly important in systems with high local gas and entrained particle velocities, such as the vortex reactor [206,207]. Corrosion and scaling can exacerbate these phenomena, which are relevant for processes with high chlorine or sulfur content, a lack of oxidation control, high temperatures, and a reducing atmosphere. While the formation of fines is usually problematic, in some fluidization regimes, it can be advantageous. In smooth and bubbling regimes, adding or generating fines can improve fluidization by reducing the interaction between particles and walls, reducing u_{mf} [208,209].

However, the formation of fines is detrimental to bed stability in vortex reactors, leading to material loss through entrainment. Dynamic image processing and sieve analysis of attrited-entrained particles from a vortex reactor have shown increased particle roundness and decreased Feret diameter (the longest diagonal measurement). Surface abrasion was reported as the primary attrition mechanism for the Sr–La–O/SiC particles in the GSVR. However, the breakup of larger particles also seems to contribute, albeit insignificantly, to attrition-led entrainment [140]. To achieve a complete understanding and better predict attrition mechanisms in vortex reactors, more detailed experimental studies combined with physical characterization techniques are required.

5.1.3. Solid flow control

Solid flow control is another important phenomenon. However, there are two types of solid flows to consider. The first type occurs inside the reactor (typically called G_S) and is described as the internal circulation of solids between different zones. The control of this solid flow is significant in reactors, where it forms a closed loop, meaning no solid is added or removed from the reactor vessel. The flow of solids in the TZFBR and ICFBR is critical because it determines the residence time in each reaction section, directly affecting reactor performance. In these systems, the flow of solids is influenced by the cloud-bubble-wake interaction, and its behavior depends on strict control of the size, velocity, and distribution of bubbles throughout the bed.

The second type involves continuous solid flow, with solids being fed into and removed from the reactor during continuous operation. This is crucial in certain fluidization regimes, such as spouted and pneumatic

transport fluidization, and influences parameters like residence and contact time between gas and solid. Continuous solids operation in vortex reactors is challenging for various reasons. Solids feeding must be assisted by purge gas, which can constitute up to 10 % of the primary gas flow rate, potentially leading to unintentional dilution of the reaction mixture. Conversely, solids removal can also result in unintended quantification challenges for the reaction mixture. Determining the precise location for the solids outlet is difficult, as the bed thickness is directly related to solids loading and inversely proportional to the gas flow rate. Therefore, while continuous solids operation for vortex devices is appealing, it remains unachievable without significant design considerations or modifications to reactor geometry.

5.1.4. Gas back-mixing

Gas back-mixing presents a common issue in gas-solid reactors, occurring when the movement of solids drags gas along with it and is often attributed to operating at incorrect conditions or in a sub-optimal fluidization regime. The main consequence of gas back-mixing is the unwanted mixing of gas streams, resulting in the formation of secondary products. This is particularly problematic in the TZFBR and ICFBR, which usually maintain different atmospheres in each section. Uncontrolled mixing of gas streams due to back-mixing can negatively impact both the process's performance and safety.

A prime example is the continuous reaction-regeneration operation in the TZFBR for the MTO process [16,54]. If hydrocarbons produced in the upper section mix with oxygen fed to the lower section, it could create an explosive environment, leading to the loss of valuable products and damage to the reactor. Based on their operating principles, vortex reactors operate with limited or no species back-mixing and are, therefore, ideal for thermally sensitive chemistries involving several series-parallel reactions.

5.1.5. Electrostatics

Electrostatic forces become significant during operations involving small particles (less than 100 μm) in fluidized systems. These forces are generated when two particles come into contact and are separated or when a charged particle interacts with a conductor surface, such as the metallic reactor wall. They can lead to considerable operational challenges, such as particle agglomeration or adhesion to the reactor wall, causing deviations from desired operation, defluidization, and necessitating shutdowns for cleaning [206,210,211]. The formation and intensity of electrostatic forces typically depend on various characteristics of the fluidization system, including temperature, pressure, particle material and size, reactor wall material, and the velocity and humidity of the gas [212–214].

5.1.6. Gas distribution systems

The behavior of a reactor is significantly influenced by the gas feed method to the fluidized bed. The gas distribution system determines the fluidization regime—such as bubbling, riser, downer, or spouted—and directly impacts the efficiency of gas-solid contact, thereby affecting performance. In bubbling reactors, such as the TZFBR and the ICFBR, gas is typically introduced upwards through a porous plate, facilitating uniform bubble formation and distribution [159,167,185,215]. However, in the TZFBR, the upper gas feed mechanism involves not a porous plate but a rod whose shape and dimensions significantly influence gas distribution [47,74,87]. In contrast, gas distribution in vortex reactors adopts a unique approach, utilizing a multi-point feed design through azimuthal slots, which obviates the need for traditional gas distributors.

5.1.7. Reactor design features

Reactor design is a crucial aspect of reaction engineering and requires careful consideration to create an optimal FBR.

The fluidization regime at which the reactor operates is one of the key factors in the design process. The reactor design will differ depending on whether it operates in the smooth, bubbling, or turbulent regime, where the solid bed remains inside the reactor body, or in the pneumatic transport regime, where solid removal occurs continuously. Since both the TZFBR and the ICFBR operate in the bubbling regime, they are considered bubbling columns, and their design is based on a cylindrical reactor body. Although one is essentially similar to the other, both reactors have their particularities. On the one hand, the TZFBR is vertically divided into sections with different diameters but not separated by a physical barrier. Each section has an additional gas feed, arranged vertically: one at the bottom of the vessel and the other at the top. On the other hand, the ICFBR is usually divided radially, and its sections, which can be of different sizes, are separated by a physical system (plate or tube). In this reactor, the gas feed to each section is at the bottom of the vessel. Owing to their design, the transition zone between sections is one of the most critical features in these reactors. In the TZFBR, this zone has a cylindrical or conical geometry and affects the gas and solid dynamics between zones, especially if there is a change in reactor diameter [51,86,87] The ICFBR has a gap shape and mainly affects the flow of solids between sections [158,186].

The use of internals is a common practice in reactor technology, mainly used to improve gas and, sometimes, solid flow control. In bubbling reactors such as the TZFBR and ICFBR, the shape, size, and location of the internals aim to break the bubbles and improve gas-solid contact. However, they also hinder the movement of solids, an effect that must be considered carefully in reactors where it can produce defluidization and dead zones [6,51,161,185,215,216]. For larger-scale systems, these internals are usually heat exchangers in the shape of tube banks [215,217], and their effect on bubbles, solid flow, and heat profiles must also be considered.

Reactor size selection is relevant and can be divided into two categories. The first concerns reactor diameter, where two approaches can be taken. First, the ratio between the reactor diameter and particle size (D_R/D_p) is usually associated with small-scale systems, where particle-particle and particle-wall interactions significantly affect gas and solid flow patterns in the bed [218,219]. These phenomena are especially relevant in bubbling beds because such interactions can produce agglomeration, defluidization, and channeling, worsening gas-solid contact and producing severe heat and mass gradients along the bed. The second category considers the influence of reactor size on hydrodynamics. For bed diameters commonly used at the laboratory scale, 20 cm or smaller, there is a zone of preferred bubble flow near the bed walls at lower bed heights.

In contrast, bubbles grow and move toward the center, ascribable to coalescence, higher up in the bed [220,221]. For the reactors considered in this review, bubble development is a crucial concern for both TZFBR and ICFBR because it influences the solid flow between zones. The objective is to maintain a good bubble size and distribution throughout the bed. In vortex reactors, the particle diameter should always be smaller than the slot opening to prevent losing momentum due to particle rotation around its axis. It is postulated that the slots could be replaced by multiple, narrow holes through which the fluidizing gas can enter the reactor zone (provided the area of all holes is the same as the total area of all the circles), achieving more uniform fluidization. CFD simulations have reported a lack of significant axial-radial mixing between the gas from the bottom and the top of the slots [135,222]. This feature could be utilized to study processes such as chemical looping or fluid catalytic cracking. The second category concerns the solid bed height, which is closely related to gas flow development. This parameter affects residence and contact time and is particularly important in the TZFBR, where the height of each zone affects conversion, product yields, and safety because both zones share the same solid bed.

5.2. Perspectives and future scope

Although the multifunctional reactors presented in this study offer several enhancements over traditional fluidized beds, there is still room for improvement. Process, design, or catalyst-based modifications could

enhance the performance of multifunctional FBRs. This section explores these enhancements for each type of reactor.

5.2.1. Process-based enhancements

Solid segregation is common in fluidized systems, where attrition, fines production, electrostatics, and solid flow control are crucial parameters. Segregation can occur in systems with solids of the same size but different densities or solids of different sizes and the same density. In the first case, the bed segregates rapidly, and the dense material forms a relatively pure bottom layer, while the upper layer always contains some uniformly dispersed denser solids. In the second case, particles of different sizes but the same density segregate more slowly. Particles with a bimodal and narrow size distribution will mix uniformly under moderate bubbling conditions, while less segregation is expected with a broader size distribution [216]. Rising bubbles are considered the primary mechanism for particle segregation since they carry up solids in their wake. However, only larger, denser particles move down the bed through the temporarily disturbed region (wake) as a bubble passes [223]. Gas velocity is the main process parameter to consider for avoiding or reducing the effects of segregation. Segregation can be severe at gas velocities close to the u_{mf}, but increasing the velocity can significantly reduce this phenomenon [216,223–225]. Particle segregation is a significant concern in systems like the TZFBR and ICFBR because it disrupts the solid flow through different sections of these reactors. However, segregation can be advantageous in processes with *in situ* regeneration. In these cases, segregation is caused by increased coke content in solid particles, which makes the particles denser and favors their downward movement to the regeneration section. This is favorable only in the TZFBR because the solid flow between sections is axial, unlike in the ICFBR, which is radial. Focusing on processes similar to biomass fast pyrolysis, where one of the reaction products is a fine solid that can be entrained by reactor hydrodynamics, could be more applicable in vortex reactors. Such applications eliminate the need for additional solids outlets and can function conveniently in continuous mode. Conversely, solids of different densities and diameters can form radially separated, rotating beds under dissimilar centrifugal-drag forces [24], paving the way for using vortex reactors as solid separators.

Selecting the optimal fluidization regime is important in both TZFBR and ICFBR operations, as they both target bubbling fluidization, where bubbles transport the solid between zones. Bubbles' size and velocity are mainly determined by the gas velocity, which controls the operation by needing to be above the minimum bubbling velocity but below the critical velocity, where the turbulent fluidization regime starts, and gas back-mixing becomes relevant [33,34,215,226].

Numerous methods reduce erosion, such as using internals to minimize direct contact with particles or lower gas velocities, which apply directly to the bubbling reactors in this study. However, to operate under the best conditions, other effects like bubble formation or solid flow disruption must be considered along with erosion. In vortex reactors, lowering gas velocity is sometimes not ideal because it affects momentum.

Typical strategies to cope with corrosion include using low-oxygen combustion, ensuring a uniform distribution of combustion air and fuel, avoiding local hot spots, injecting additives, controlling the flue temperature at the furnace outlet, and utilizing corrosion-resistant alloys.

An additional perspective unique to vortex reactors is that liquid feeding is much simpler than solid feeding due to its free flowability and ability to feed against adverse pressure gradients. A highly bubbling liquid bed has been experimentally demonstrated for easily dispersed, low-surface tension liquids like H_2O [122]. However, using high-viscosity liquids, such as oil or honey, may result in annular, core-annular (or radially stratified) gas-liquid flow patterns. The physical properties of a given liquid can be modified to better suit the gas-liquid flow regime required for a specific application by controlling temperature, pressure, and additives. Additionally, by leveraging the incompressible nature of liquids, the operating pressure offers another degree of freedom in pursuing process intensification. Introducing liquids as a secondary phase in vortex reactors opens new horizons, presenting possibilities that are not as readily apparent in gas-solid applications. Liquid feeding via a pump can also eliminate the need for purge gas, which is necessary for solids feeding.

Heat transfer enhancement is also relevant in fluidized systems, which can be improved by introducing heat exchangers in the reactor, typically in the form of tube bundles. However, adding these systems as internals can disrupt the flow of gas and solids, potentially leading to defluidization and dead zones in the solid bed [51,217,227,228]. This concern is particularly significant in the TZFBR and the ICFBR, where solid flow and its contact with bubbles are critical, especially for processes with *in situ* regeneration. Computational studies mostly support these claims made for vortex reactors, but an experimental heat transfer model/correlation is needed to validate them numerically. Such a model can help predict the exact particle temperature for a given application with sufficient accuracy. However, developing such a model is more practical, as it requires simultaneously recording the particle temperature of a high-velocity bed, and both measurements rely on high-speed cameras.

Despite efforts to quantify process intensification, head-to-head comparisons against traditional reactors are still necessary for applications. Doing so will provide a holistic view of using multifunctional reactors for a given application across the scales.

5.2.2. Design-based enhancements

Reactor design in reactor engineering is crucial for carefully designing multifunctional reactors to operate under optimal conditions. However, almost every design parameter affects others, resulting in tradeoffs. For instance, in the case of the TZFBR reactor, changing the reactor section influences gas velocity in both zones. Similarly, altering the gas feed to one section affects gas velocity, fluidization, and solid exchange between the top and bottom zones. Moreover, modifying the upper gas distribution system impacts fluidization, bubble formation and development, the upwards-downwards flow of solid, and the contact between gas and solid [48,68,70,182]. The Menéndez-Herguido group at the University of Zaragoza [48,61] has primarily conducted TZFBR design studies, focusing on fluid dynamic studies [65,86,87], changes in gas feeding systems [56,64], and modeling [51,70,75,87].

Despite having similar features, the ICFBR has a physical separation between zones, making its design and operation easier. In this system, changing some design parameters do not affect others; for example, changing gas velocity in one zone has little effect on the other. However, designing the ICFBR depends mainly on the hole or gap that separates both zones because its optimal operation is defined by the correct exchange of solids between them. Several features have been proposed to improve its design, including modifying the gas distributor [163,167,188], introducing internals [161,163], or changing the geometry of the gap or reactor [163,174,183,186].

Gonzalez-Quiroga et al. [125] have demonstrated the effective use of CFD simulations to optimize the design of a GSVR for biomass-fast pyrolysis. Based on the CFD simulations, the following modifications were made to the bare reactor geometry: the use of a single gas inlet to the jacket (without any observable non-uniformity in the flows, pressure, or velocities in the jacket-slots-reactor zone [124]); rounding off the slot edges (minimizing streamline curvature and reducing pressure drop); profiling the bottom end wall of the reactor (reducing backflow region); and implementing a converging-diverging exhaust, among others. Similar design optimization iterations can be applied to other applications through targeted numerical studies. Recent experimental and computational studies have shown the possibility of further improving the utilization of incoming gas momentum using stator-rotor-type designs [125]. Design improvements include equipping the reaction zone with multiple paddles, where the incoming gas rotates, significantly increasing the solid velocity compared to conventional designs.

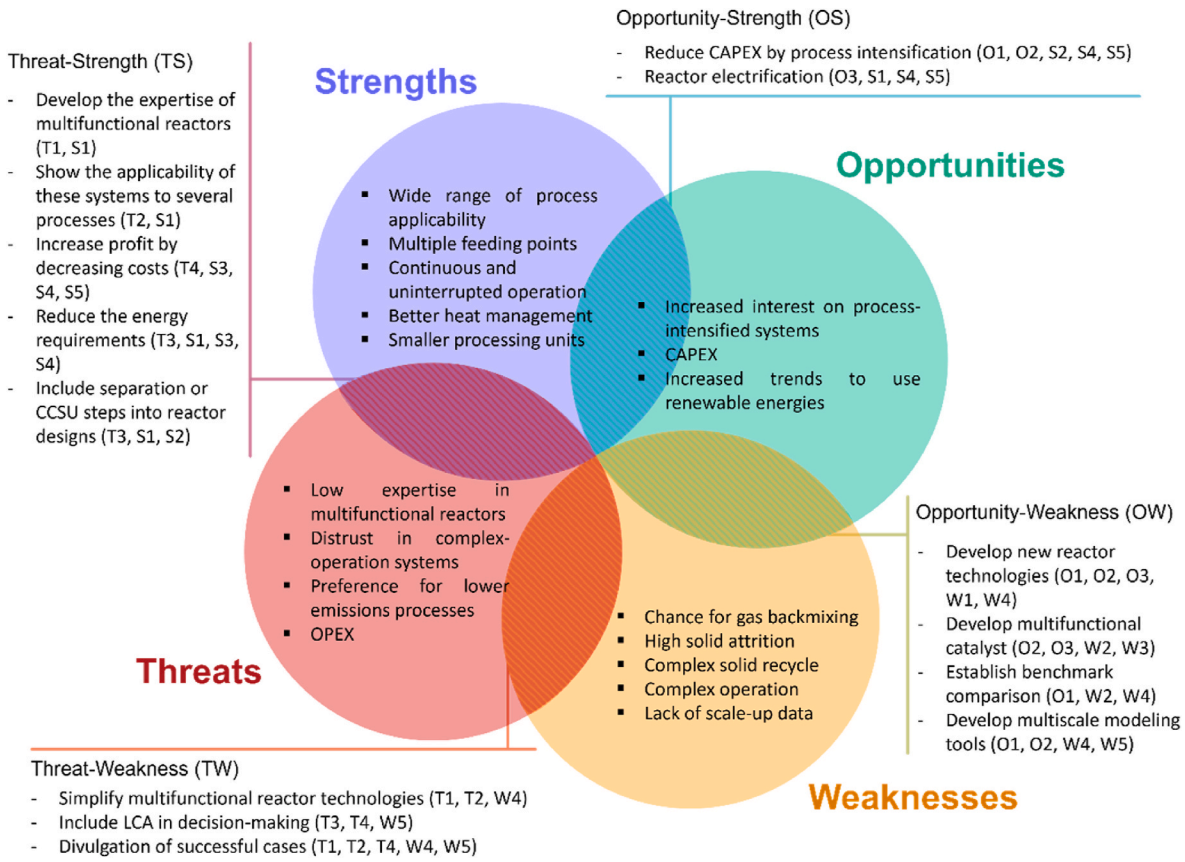

Fig. 24. Strengths, weaknesses, opportunities, and threats analysis for TZFBR, vortex, and ICFBR multifunctional reactors.

Although these designs offer enhancements, their implementation for reactive applications is pending the development of suitable designs that allow effective solids handling at high temperatures.

Preference should be given to the vertical central axis design rather than the horizontal one. Reactors with a vertical axis are prone to axial non-uniformities but are limited only to the bed length. Horizontal axis designs, on the other hand, are more susceptible to the effect of gravity on the bed shape, as reported by various studies [120,229,230]. It is further postulated that the downwards-oriented reactor exhaust assists in the solids of the vertical-axis design. It should be noted that this configuration might result in a lower solid capacity than the vertically upward outlet design because solids in the freeboard region are due to the gravitational force overcoming centrifugal force.

5.2.3. *Catalyst-based enhancements*

One important aspect to consider in fluidized beds is the solid properties, especially their resistance to attrition. The constant movement of solids in fluidized beds can cause high attrition in solid particles depending on the fluidization regime. This effect is particularly significant in vortex reactors, where the gas velocity is so high that the formation and elutriation of fines could cause operational problems. To minimize this, some strategies can be applied in catalyst design, including agglomeration [59,60,231], spray drying [232–237], and even spouted bed [238–241] preparation techniques.

Enhancing the solid flow through the reactor can be achieved by favoring the fluidization of the solids. There are two main ways to achieve this. First, fluidization is preferred if the catalyst is designed with a spherical shape (or close to $\phi = 1$) because of the lower drag coefficient and smoother particle-particle interaction [242–244]. Second, if the solid size distribution is wide, or some fines are added to the bed, fluidization can be improved due to the reduction in rubbing between particles and, thus, bed viscosity [208,209,245].

Another aspect to consider when testing fluidization with small particles is the electrostatic behavior of the solid, which can affect fluidization and produce problems such as cluster formation or channeling. To avoid these issues, the catalyst can be designed as large particles with high electrical conductivity or operated with mild humidity to facilitate discharge through hydrogen bridges of H_2O between particles. However, this latter method could only be applied in some processes [211,213,214].

Exploring a durable and efficient operation of vortex reactors still requires addressing shortcomings in developing an active yet mechanically stable catalyst that can withstand the high-attrition environment of the vortex reactor. Tharakaraman recently demonstrated that using SiC along with the conventional Sr–La catalyst (without binders), oxidative coupling of methane could be performed in a vortex reactor at 850 °C [140]. Silicon carbide provided the necessary mechanical strength and desired porosity for catalytic activity [246]. The use of SiC as a support for OCM has already been established in the literature [247,248], and a recent demonstration in vortex reactors further encourages translating this information to other relevant processes and scales.

To achieve these broader aims, the shape-memory synthesis method for beta-SiC synthesis introduced by Phaam-Huu et al. [249] presented a unique opportunity to synthesize more extensive catalytic supports without the need to use binders to enlarge the catalyst size required for industrial-level reactors. By avoiding binders, the structural integrity of catalysts is enforced, even under high shear and attrition, which benefits advanced fluidized reactors such as the vortex, TORBEDS, and others. Additionally, introducing binders for larger catalytic pellets might adversely affect other relevant physical properties, such as the thermal conductivity of the resulting catalyst, which could be detrimental to the process, especially if there is a mismatch in the physical properties of the binder and the support/active phase. SiC without a binder, as synthesized during the scaled-up SMS process, is also crucial for recovering

precious metals from a spent catalyst point of view [250]. This property enhances the re-usability of the support, which is relevant for reactors where catalyst size reduction by attrition leading to loss by entrainment is a known issue, such as FBRs or even vortex reactors.

To develop catalysts that are more resistant to attrition, it is necessary to understand the mechanism of attrition in vortex reactors. Attrition occurs through three main routes of contact: gas-solid, solid-solid, and solid-wall. However, the exact contributions of each of these modes still need to be discovered, which is crucial for tailor-making resistant materials for catalytic applications in vortex reactors.

5.3. Other process intensification opportunities

In addition to the considerations and perspectives mentioned earlier, other opportunities for process intensification are common to all multifunctional FBRs discussed in this review. We propose a strengths, weaknesses, opportunities, and threats (SWOT) analysis to identify them, as schematized in Fig. 24.

The multifunctional fluidized bed reactors presented in this review reveal several advantages that can be translated into suitable industrial opportunities. These multifunctional FBRs have the potential to modify the CAPEX of a process by reducing the number of units necessary, improving heat management, or operating with multiple streams simultaneously. However, their feasibility remains open for discussion due to their dependence on the specific case considered. Therefore, an opportunity for multifunctional reactors lies in benchmarking a given process with an existing, state-of-the-art industrial counterpart. Another relevant opportunity to consider is reactor electrification, which addresses the increased interest in using renewable sources of energy by making better use of heat, operating smaller units, and increasing the versatility of these multifunctional designs. Both topics are discussed in more detail later in this section.

There are opportunities to motivate the reduction of weaknesses. The first relates to new technologies that avoid gas backmixing and simplify reactor operation. However, this strategy would require strong resource investment and may not be profitable in the short term. Similarly, developing new multifunctional catalysts that operate in these reactors looks promising, even though finding more robust and fluidizable materials simultaneously possessing catalytic activity would require great effort. Establishing benchmarks is another aspect to consider because they directly compare traditional and intensified processes. Lastly, it is mandatory to develop specialized multiscale modeling tools that reduce investment in designing and building replicas of these reactors, as well as provide useful data across different scales. Many of these aspects appear circular, meaning solving one problem would likely lead to a possible solution for the next challenge. For example, developing multiscale-multiphase modeling tools would not only provide a deeper understanding of the reactor/process but also provide quantifiable avenues for a head-to-head comparison with current industrial standards, a requirement for benchmarking.

Strategies that minimize weaknesses and avoid threats are crucial when developing new technologies. The most direct strategy includes simplifying current designs, which can reduce distrust about using new, intensified systems while helping the industry familiarize itself with them. Divulging previous successful cases can also achieve this goal, which is our objective with this review. Finally, life cycle assessment (LCA) studies can provide some context to the decision-making process when implementing large-scale reactor technologies, particularly for high-emissions processes. This approach allows for a more closed-loop comparison from reactants to products and can be presented for high-level decision-making.

These multifunctional reactors have several advantages that can help overcome the challenges to their implementation. On one hand, it is crucial to demonstrate the applicability of these systems to a wide range of processes and to develop expertise in them, both experimentally and computationally. These two strategies are closely related and can be achieved simultaneously by incorporating multifunctional FBRs into conferences, publications, or even classrooms. On the other hand, reducing both capital and operating costs should be a top priority. This could be achieved by reducing capital costs (using lower volume units

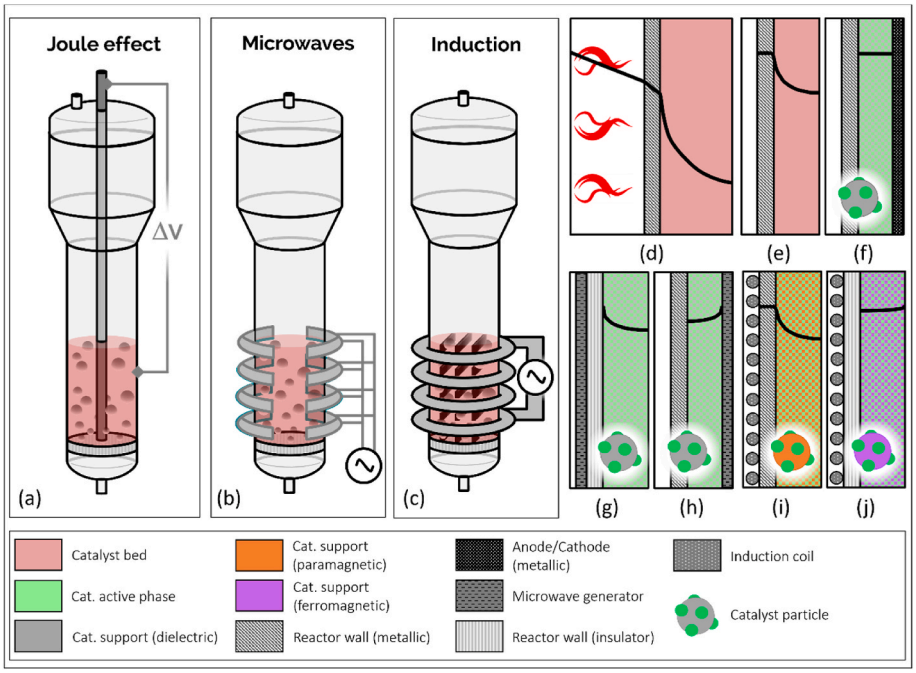

Fig. 25. Schematic representation of electrification strategies for FBRs: (a) Joule effect, (b) microwaves, and (c) induction. Radial temperature profiles (solid lines) as a function of the way of supplying energy to the reactor: (d) conventional fired reactor, (e) Joule heating by using the reactor body as resistance, (f) Joule heating by using the catalyst as the resistance between anode and cathode, (g) external microwave heating when the catalyst absorbs the radiation, (h) internal microwave heating when the catalyst absorbs the radiation and it is reflected inwards by the reactor body, (i) induction inwards heating of the reactor wall, and (j) induction outwards heating of the catalyst.

with more efficient energy supply methods) or by decreasing operating costs (recycling reactants or products, reducing energy requirements, reducing the number of operating units, or improving overall heat management). Finally, one of the most important strategies is the implementation of carbon capture, storage, and utilization steps. This could be achieved by adding subsequent steps downstream or directly incorporating them into the multifunctional reactor design. However, both approaches involve additional costs that must be carefully considered to avoid the emergence of new weaknesses and threats.

Among these strategies, cost analysis (CAPEX and OPEX), electrification, and CCSU are currently in focus because they aim towards current global trends.

5.3.1. CAPEX and OPEX

Cost estimation is one of the most useful tools for analyzing the feasibility of a proposed process and identifying areas where process intensification could be successfully applied. CAPEX and OPEX estimations serve as key tools for decision-making, especially in cases involving unconventional technologies like the multifunctional reactors discussed in this review. From the viewpoint of systems that carry out more than one process in the same vessel, opposite forces affect capital cost estimation, such as the TZFBR or ICFBR. Although reducing the number of units required to perform the same processes could have a positive impact, the complexity of these designs might increase costs in the design and fabrication stages. This could also apply to vortex reactors, where higher production rates per unit of reactor volume are possible. Even though this could decrease CAPEX, the higher gas velocity needed for the appropriate fluidization regime could negatively impact OPEX. However, CAPEX and OPEX can vary significantly for the vortex reactor if the fluidization gas differs from the reactant gas. In the case of biomass pyrolysis, where N_2 is the inert fluidization gas requiring recycling after separation, this adds to both CAPEX and OPEX. For systems with favorable heat management, such as vortex or TZFBR and ICFBR operating in a reaction-regeneration mode, achieving lower fuel consumption and energy losses may be possible, significantly affecting OPEX.

5.3.2. Electrification

Electrification of chemical processes is a key goal the chemical industry has pursued in recent years. From all stages comprising a chemical process, the reactor stage offers a key opportunity for electrification [251,252]. Besides using electricity indirectly (*e.g.*, electrolyzing water to produce hydrogen used as fuel) or applying power to non-catalytic systems (plasma gas reactors [253–255]), there are several ways to electrify FBRs. These are shown in Fig. 25.

Systems based on the Joule effect produce heat through electrical losses, similar to how a resistance generates heat when an electric current passes through it [256–259]. These systems can utilize the reactor body as a source of heat (Fig. 25a and e), reducing temperature profiles from radiation-convection in the fired chamber and conduction through the reactor wall, which are currently the predominant methods (d). An alternative system follows a similar concept but uses the catalyst bed as a resistance [260–262]. In this approach, the bed closes the circuit between the reactor body and a metallic rod at its center, acting as an anode-cathode. When a current is applied between the metallic parts, the dielectric material formulated into the catalyst produces heat similar to a resistance (f). Other strategies could provide energy by utilizing radiating microwaves into the reactor (b). Although the heating is localized in this case, the catalyst bed must be able to absorb them and produce heat; thus, it must be dielectric [263]. Microwaves can be emitted from the exterior (g) or interior (h) of the reactor body. In the first case, the reactor wall needs to be an insulator, such as quartz or glass, to permeate the radiation, while in the second case, it could be a metallic material that reflects radiation back to the bed, thereby increasing heating efficiency. The last strategy is based on the induction phenomena (c), the heat produced by spinning magnetic moments under the effect of an alternating magnetic field [251,256,257]. This method of providing energy involves using a coil to generate an alternating magnetic field and a ferromagnetic material to be heated by it. Although generating the magnetic field is straightforward, the choice of ferromagnetic material can be based on a metallic reactor body (i) or a ferromagnetic catalyst (j), depending on the desired temperature profile. It is important to consider that the intensity of the magnetic field generated by the coil decreases radially, leading to an outward heating profile if the heating source is the ferromagnetic catalyst. However, this profile is likely to be smoother than that produced when heating the reactor wall because the heating is targeted where it is most needed.

These strategies not only enable the substitution of traditional burners, leading to lower fuel consumption and emissions, but also result in smoother temperature profiles, extended lifetimes of materials, and sometimes improved performance. Additionally, replacing the external furnace with a quartz-based material allows visual access to the reactors, which is typically impossible with conventional heating sources.

5.3.3. Carbon capture, storage, and utilization (CCSU)

CCSU is a mitigation technology that aims to reduce the impact of carbon-based emissions from the chemical industry. Although it is one of the pillars supporting current trends, its tandem development with the reactor technology is far behind the industry's needs. CCSU consists of three main parts: capturing carbon-related emissions where they are produced, their transport and storage, and/or their use for several purposes. Carbon capture is typically conducted on-site through chemical or physicochemical processes (*e.g.*, adsorption) of the flue gas, which usually contains only around 10 % CO_x, depending on its source (*e.g.*, fuel combustion or process streams). While the common approach involves a gas separation stage through sorption, it is essential to consider the energy demand of this stage, which increases with the dilution of CO_x in the stream. Therefore, carbon capture processes are more energy-efficient when the flue gas has a high CO_x concentration [264]. In addition to the energy cost of capturing CO_x, factors such as solubility, density, reactivity, heat capacity, and pressure sensitivity are also critical and could influence the choice of capture technology for each process [265,266]. After the separation/capture stage, carbon-based pollutants can be managed through various methods, including sequestration in deep geological reservoirs, mineral carbonation into thermodynamically stable carbonates, or ocean storage [267,268]. Although this strategy is crucial in CCSU strategies, its discussion is beyond the scope of this work due to its limited relation to reactor technology. Carbon utilization involves using streams derived from the carbon separation and capture steps, either totally or partially. The state of these carbon streams (solid, slurry, or gas phases) will determine the most suitable strategy. Direct utilization of carbon-rich gaseous streams in chemical synthesis is particularly attractive because it provides a cost-effective and abundant C1 feedstock. Promising applications include dry reforming of methane, methanol production by hydrogenation, dimethyl carbonate synthesis, and oxidative dehydrogenation of ethane [265,268].

The use of CCSU technologies alongside multifunctional fluidized beds opens up a whole new question concerning their feasibility, depending on the system. Applying CCSU technologies to the TZFBR design could be challenging due to the dilution of the gas stream in the interzone. At that point, gases from the bottom zone mix with those fed to the upper zone, which increases the energy cost of the separation and capture stage. However, improved TZFBR designs can operate with embedded membranes, enabling *in situ* CO_x separation and producing highly concentrated streams. Optimizing this strategy involves equipping each reactor zone with its membranes, which is particularly relevant considering the high CO_x production in the lower zone typically designated for catalyst regeneration. This approach enhances the separation and capture stage, making the process more efficient and potentially feasible. Moreover, the catalyst regeneration can be performed with CO_2, allowing the recycling of a fraction of the separated flue gas

back to the bottom zone to produce a mixture of CO_2 and O_2 as a regenerative stream. Vortex reactors can directly sequester CO_2 by using an alkali to replace the solid phase, providing a high interfacial area for gas-liquid contact and converting CO_2 into other chemicals more effectively than previously discussed technologies. In terms of CO_2 separation in gas-solid-based reactive applications, the complexity of separation varies depending on the similarity of feed and fluidization gas and downstream reactor concentrations. The physical separation in ICFBR chambers allows for the production of streams with different CO_x concentrations, making the application of CCSU technologies more feasible for gas-solid applications than in the TZFBR or vortex reactor. Unlike the latter, the flue gas obtained in the ICFBR is not mixed with gases in the reaction chamber, meaning it is not diluted and can be sent directly to a capture stage, concentrated with membranes, or partially recycled to the regeneration chamber.

6. Conclusions

Multifunctional fluidized reactors, such as the TZFBR, ICFBR, and vortex reactor, offer advanced technologies that overcome the limitations of traditional fluidized beds and allow for multiple processes within a single vessel. These reactors have the potential for process intensification, space reduction, and cost and energy savings.

Among these reactors, the TZFBR is particularly notable for its ability to operate efficiently over extended periods due to simultaneous reaction and regeneration within the same vessel, making it an alternative for chemical processes prone to catalyst deactivation. However, despite its advantages, no industry has implemented the TZFBR since its first description over 40 years ago. This lack of implementation could be due to factors such as the complexity associated with the design and operation of fluidized solid-gas catalytic systems, the risk of explosion associated with feeding oxygen to a hydrocarbon mixture, or the ease of access to other well-established technologies. Nevertheless, certain factors could facilitate the implementation of the TZFBR on an industrial scale. These include the many successful processes tested in the TZFBR, the extended knowledge of the system after over 40 years of research, the advantages it offers in different designs (*e.g.*, two-section reactors or coupling them with membranes), and the possibility of substituting regenerative streams such as H_2O or CO_2 for oxygen. Although implementing this reactor could decrease CAPEX by reducing the number of units required to complete a process, the complex design of the TZFBR might increase capital costs in the design and build phases. Additionally, this multifunctional fluidized bed is distinguished by its superior heat management, which could lower energy consumption and, consequently, operating costs. Considering these factors, the TZFBR could garner interest for certain industrial applications. Once adopted on an industrial scale, its adoption could encourage others to follow suit, potentially making it a standard technology.

Vortex reactors are beneficial for thermally sensitive reactions and *in situ* separations of dissimilar solids, as they overcome gravitational forces and promote efficient gas-solid or gas-liquid heat and mass transfer. With improved designs incorporating continuous solids feeding-removal and the development of robust catalysts, these reactors hold promise for widespread applications in the chemical industry. ICFBRs emerge as promising technologies for solid-gas catalytic reactions, offering the advantage of producing 2 atm with different reactant and product concentrations, thereby enhancing operational safety and accessibility. Furthermore, new designs solve some of the most relevant solid movement problems of these reactor configurations, increasing their appeal for new reactions and processes. Implementing ICFBR technology could be an attractive alternative to other methods, and the possibility of coupling them with other technologies (*e.g.*, riser-downer, TZFBR, or membranes) makes ICFBRs a beacon for process intensification.

CRediT authorship contribution statement

D. Zapater: Writing – original draft, Methodology, Formal analysis, Conceptualization. **S.R. Kulkarni:** Validation, Investigation, Data curation, Conceptualization. **F. Wery:** Writing – original draft, Formal analysis, Data curation. **M. Cui:** Writing – original draft, Visualization, Methodology, Data curation. **J. Herguido:** Writing – review & editing, Supervision, Data curation. **M. Menendez:** Writing – review & editing, Validation, Methodology. **G.J. Heynderickx:** Writing – review & editing, Validation, Methodology. **K.M. Van Geem:** Writing – review & editing, Validation, Supervision, Formal analysis. **J. Gascon:** Writing – review & editing, Validation, Project administration. **P. Castaño:** Writing – review & editing, Supervision, Resources, Project administration, Conceptualization.

Declaration of competing interest

The authors declare that they have no known competing financial interests or personal relationships that could have appeared to influence the work reported in this paper.

Data availability

Data will be made available on request.

Acknowledgments

The authors gratefully acknowledge the financial support, resources, and facilities provided by the King Abdullah University of Science and Technology (KAUST, BAS/1/1403). FW acknowledges the Fund for Scientific Research Flanders (FWO) under application number 1S97521 N.

Nomenclature and subscripts

8.1. Nomenclature

FBR	Fluidized bed reactors
TZFBR	Two-zone fluidized bed reactor
TS-TZFBR	Two-section two-zone fluidized bed reactor
TZFBR + MB	Two-zone fluidized bed reactor with membranes
TS-TZFBR + MB	Two-section two-zone fluidized bed reactor with membranes
ICFBR	Internally circulating fluidized bed reactor
CFB	Circulating fluidized bed
GSVRs	Gas-solid vortex reactors
RFB	Rotating fluidized bed
RFB-SG	Rotating fluidized beds in static geometry
CSTR	Continuous stirred tank reactor
PFR	Plug-flow reactor
GVU	Gas vortex unit
GSVU	Gas-solid vortex unit
GVR	Gas vortex reactor
GSVR	Gas-solid vortex reactor
GLVR	Gas-liquid vortex reactor
LSVR	Liquid-solid vortex reactor
PIV	Particle image velocimetry
DIA	Direct image analysis
CFD	Computational fluid dynamics
RTD	Residence time distribution
KTGF	Kinetic theory of granular flow
CAPEX	Capital expenditures
OCM	Oxidative coupling of methane
HDPE	High density poly ethylene
SWOT	Strengths, weaknesses, opportunities, and threats
TS	Threat-Strength
TW	Threat-Weakness

OS	Opportunity-Strength
OW	Opportunity-Weakness
LCA	Life Cycle Assessment
CCSU	Carbon capture, storage, and utilization
z	Bed height [cm]
z_f	Height of the intermediate feed entry [cm]
z_{sc}	Height of the section change [cm]
L	Bed thickness for vortex reactors [mm]
h_i	Height of the zone i [cm]
d_b	Bubble diameter [cm]
d_{bm}	Maximum bubble diameter [cm]
D_i	Internal reactor diameter [cm]
d_{orif}	Diameter of the orifice of the feed entry located at height z_f [cm]
H	Reactor length [cm]
t	Time on stream [h]
t_f	Final time on stream [h]
u_b	Bubble rise rate [cm s^{-1}]
u_e	Gas velocity in emulsion [cm s^{-1}]
u_{mf}	Minimum fluidization velocity [cm s^{-1}]
u_s	Downward velocity of solid in emulsion [cm s^{-1}]
u_{sg}	Gas velocity [cm s^{-1}]
$u_{sg,1}$	Gas velocity in the zone 1 – regeneration zone [cm s^{-1}]
$u_{sg,2}$	Gas velocity in the zone 2 - reaction zone [cm s^{-1}]
u_{ga}	Superficial gas velocity in the annulus [m s^{-1}]
u_{gd}	Superficial gas velocity in the draft tube [m s^{-1}]
U_θ	Tangential velocity [m s^{-1}]
W	Weight of catalyst [g]
$G_{g\text{-}t}$	Mass flux of tracer gas [kg m^{-2} s^{-1}]
G_{sA}	Particle feed flow rate from inlet A [kg m^{-2} s^{-1}]
G_{sB}	Particle feed flow rate from inlet B [kg m^{-2} s^{-1}]
$C_{i,\,x}$	Concentration of i compound in phase x [mol cm^{-3}]
$r_{i,\,x}$	Reaction rate of i compound in phase x [mol g_{cat} s^{-1}]
K_{be}, K_{eb}	Gas exchange coefficient between bubble and emulsion and vice versa [s^{-1}]
K_{ew}, K_{we}	Solid exchange coefficient between wake and emulsion and vice versa [cm^{-1}]
f_w	Fraction of bubble volume occupied by the wake [-]
x_i	Conversion of i compound [%]
x_{i0}	Initial conversion of i compound [%]
R_{OH}	Oxygen/hydrocarbon ratio [-]
G	Centrifugal acceleration [-]
Re	Reynolds number [-]

8.2. Subscripts

b	Bubble
e	Emulsion
i	Gas species
j	Solid species (*e.g.*, coke)
w	Wake
s	Solid
p	Particle
o	Initial
f	Final
m	Maximum
orif	Orifice
sg, i	Superficial gas in zone i
mf	Minimum fluidization
g, inj	Gas at the injection point
i, x	Compound i in phase x

8.3. Greek letters

δ	Volume fraction of bed in bubbles [-]
ε_{mf}	Minimum fluidization porosity [-]
α	Transition section angle [°]
β	Defluidization angle [°]
μ	Viscosity [kg m^{-3} s^{-1}]
ρ	Density [kg m^{-3}]
λ	Solids operational capacity [-]
τ_p	Aerodynamic response time of the particles [s]

References

[1] Denbigh KG. Velocity and yield in continuous reaction systems. Trans Faraday Soc 1944;40:352.
[2] Kockmann N. A brief history of chemical reactor and reaction technology. Chem Ing Tech 2019;91:941–52.
[3] Sadeghbeigi R. Process description. In: Fluid catalytic cracking handbook. Elsevier; 2012. p. 1–42.
[4] Dogu O, Pelucchi M, Van de Vijver R, et al. The chemistry of chemical recycling of solid plastic waste via pyrolysis and gasification: state-of-the-art, challenges, and future directions. Prog. Energ. Combust. 2019;84:100901.
[5] Grace J, Bi X, Ellis N. Essentials of fluidization technology. John Wiley & Sons; 2020.
[6] Ruud Van Ommen J, Nijenhuis J, Coppens M-O. Four approaches to structure gas-solid fluidized beds. In: The 12th international conference on fluidization - new horizons in fluidization engineering; 2007.
[7] Zhao K, Thunman H, Pallarés D, et al. Control of the solids retention time by multi-staging a fluidized bed reactor. Fuel Process Technol 2017;167:171–82.
[8] Wu D, Gu Z, Li Y. Attrition of catalyst particles in a laboratory-scale fluidized-bed reactor. Chem Eng Sci 2015;135:431–40.
[9] Chourasia S, Alappat BJ. Experimental study on the attrition and size distribution of bed material in a recirculating fluidized bed. Chem Eng Commun 2017;204:1174–86.
[10] Santana D, Rodrıguez JM, Macıas-Machın A. Modelling fluidized bed elutriation of fine particles. Powder Technol 1999;106:110–8.
[11] Monazam ER, Breault RW, Weber J, et al. Elutriation of fines from binary particle mixtures in bubbling fluidized bed cold model. Powder Technol 2017;305:340–6.
[12] Ansart R, Neau H, Simonin O, et al. Elutriation from fluidized beds: comparison between experimental measurements and 3D simulation results. In: 10th international conference on circulating fluidized beds and fluidization technology, ECI symposium series; 2011.
[13] Van Landeghem F, Nevicato D, Pitault I, et al. Fluid catalytic cracking: modelling of an industrial riser. Appl Catal Gen 1996;138:381–405.
[14] Godfroy L, Larachi F, Chaouki J. Position and velocity of a large particle in a gas/solid riser using the radioactive particle tracking technique. Can J Chem Eng 1999;77:253–61.
[15] Zapater D, Lasobras J, Soler J, et al. Counteracting SAPO-34 catalyst deactivation in MTO process using a two zone fluidized bed reactor: reactor testing and process viability. Catal Today 2021;362:155–61.
[16] Zapater D, Lasobras J, Soler J, et al. Comparison of conventional and two-zone fluidized bed reactors for methanol to olefins. Effect of reaction conditions and the presence of water in the feed. Ind Eng Chem Res 2022;61:5757–65.
[17] Cordero-Lanzac T, Aguayo AT, Gayubo AG, et al. A comprehensive approach for designing different configurations of isothermal reactors with fast catalyst deactivation. Chem Eng J 2020;379:122260.
[18] Forzatti P, Lietti L. Catalyst deactivation. Catal Today 1999;52:165–81.
[19] Cerqueira HS, Caeiro G, Costa L, et al. Deactivation of FCC catalysts. J Mol Catal Chem 2008;292:1–13.
[20] Ibarra Á, Veloso A, Bilbao J, et al. Dual coke deactivation pathways during the catalytic cracking of raw bio-oil and vacuum gasoil in FCC conditions. Appl Catal, B 2016;182:336–46.
[21] Gibson I, Slim CJ, Zheng Y, et al. The continuous combustion of glycerol in a fluidised bed. Combust Flame 2019;200:60–8.
[22] Klaewkla R, Arend M, Hoelderich WF. A review of mass transfer controlling the reaction rate in heterogeneous catalytic systems. In: Mass transfer - advanced aspects. IntechOpen; 2011. p. 667–84.
[23] Kapteijn F, Moulijn JA, Krishna R. The generalized Maxwell-Stefan model for diffusion in zeolites: sorbate molecules with different saturation loadings. Chem Eng Sci 2000;55:2923–30.
[24] Kulkarni SR, Vandewalle LA, Gonzalez-Quiroga A, et al. Computational fluid dynamics-assisted process intensification study for biomass fast pyrolysis in a gas-solid vortex reactor. Energ. Fuels 2018;32:10169–83.
[25] Al-Mutairi EM. Optimal design of heat exchanger network in oil refineries. Chem Eng Trans 2010;21:955–60.
[26] Van Landeghem F, Nevicato D, Pitault I, et al. Fluid catalytic cracking: modelling of an industrial riser. Appl Catal Gen 1996;138:381–405.
[27] Pinheiro CIC, Fernandes JL, Domingues L, et al. Fluid catalytic cracking (FCC) process modeling, simulation, and control. Ind Eng Chem Res 2012;51:1–29.
[28] Aguayo AT, Ereña J, Sierra I, et al. Deactivation and regeneration of hybrid catalysts in the single-step synthesis of dimethyl ether from syngas and CO_2. Catal Today 2005;106:265–70.
[29] Chakraborty JP, Singh S, Maity SK. Advances in the conversion of methanol to gasoline. In: Hydrocarbon biorefinery: sustainable processing of biomass for hydrocarbon biofuels. Elsevier; 2021. p. 177–200.
[30] Patil CS, Van Sint Annaland M, Kuipers JAM. Experimental study of a membrane assisted fluidized bed reactor for H_2 production by steam reforming of CH_4. Chem Eng Res Des 2006;84:399–404.

[31] Patil CS, van Sint Annaland M, Kuipers JAM. Fluidised bed membrane reactor for ultrapure hydrogen production via methane steam reforming: experimental demonstration and model validation. Chem Eng Sci 2007;62:2989–3007.
[32] Deshmukh SARK, Laverman JA, Van Sint Annaland M, et al. Development of a membrane-assisted fluidized bed reactor. 2. Experimental demonstration and modeling for the partial oxidation of methanol. Ind Eng Chem Res 2005;44:5966–76.
[33] Kunii D, Levenspiel O. Fluidization and mapping of regimes. In: Fluidization engineering. Elsevier; 1991. p. 61–94.
[34] Teplitskii YuS, Tamarin AI. Laws governing gas-bubble motion in a fluidized bed. J Eng Phys 1978;34:270–6.
[35] Van Geem KM, Galvita VV, Marin GB. Making chemicals with electricity. Science 2019;364:734–5 (1979).
[36] Idakiev VV, Lazarova PV, Bück A, et al. Inductive heating of fluidized beds: drying of particulate solids. Powder Technol 2017;306:26–33.
[37] Idakiev VV, Marx S, Roßau A, et al. Inductive heating of fluidized beds: influence on fluidization behavior. Powder Technol 2015;286:90–7.
[38] Zheng X, Yin S, Ding Y, et al. Experimental study on high concentration entrainment of ultrafine powder. Powder Technol 2019;344:133–9.
[39] Lee JR, Hasolli N, Lee KS, et al. Fluidization of fine powder assisted by vertical vibration in fluidized bed reactor. Korean J. Chem. Eng. 2019;36:1548–56.
[40] Espin MJ, Valverde JM, Quintanilla MAS. Stabilization of fluidized beds of particles magnetized by an external field: effects of particle size and field orientation. J Fluid Mech 2013;732:282–303.
[41] Wang B, Tang T, Yan S, et al. Magnetic segregation behaviors of a binary mixture in fluidized beds. Powder Technol.; 397.
[42] Kleijn van Willigen F, Demirbas B, Deen NG, et al. Discrete particle simulations of an electric-field enhanced fluidized bed. Powder Technol 2008;183:196–206.
[43] Van Gerven T, Stankiewicz A. Structure, energy, synergy, time-the fundamentals of process intensification. Ind Eng Chem Res 2009;48:2465–74.
[44] Montgomery PD, Coeur C, Moore RN, et al. US 3965206. Production of stilbene and styrene. 1976.
[45] Hupp SS, Swift HE. Oxidative coupling of toluene to stilbene. Ind Eng Chem Prod Res Dev 1979;18:117.
[46] Ramos R, Herguido J, Menendez M, et al. Oxidation of hydrocarbons in an in situ redox fluidized bed reactor. J Catal 1996;163:218–21.
[47] Rubio O, Herguido J, Menéndez M. Two-zone fluidized bed reactor for simultaneous reaction and catalyst reoxidation: influence of reactor size. Appl Catal Gen 2004;272:321–7.
[48] Herguido J, Menéndez M, Santamaría J. On the use of fluidized bed catalytic reactors where reduction and oxidation zones are present simultaneously. Catal Today 2005:181–9.
[49] Soler J, Lopez Nieto JM, Herguido J, et al. Oxidative dehydrogenation of n-butane on V/MgO catalysts. Influence of the type of contactor. Catal. Letters 1998;50:25–30.
[50] Lachén J, Durán P, Menéndez M, et al. Biogas to high purity hydrogen by methane dry reforming in TZFBR+MB and exhaustion by Steam-Iron Process. Techno–economic assessment. Int J Hydrogen Energy 2018;43:11663–75.
[51] Julián I, Gallucci F, van Sint Annaland M, et al. Hydrodynamic study of a two-section two-zone fluidized bed reactor with an immersed tube bank via PIV/DIA. Chem Eng Sci 2015;134:238–50.
[52] Julián I, Gallucci F, van Sint Annaland M, et al. Coupled PIV/DIA for fluid dynamics studies on a two-section two-zone fluidized bed reactor. Chem. Eng. J. 2012;207–208:122–32.
[53] Callejas C, Soler J, Herguido J, et al. Catalytic dehydrogenation of n-butane in a fluidized bed reactor with separate coking and regeneration zones. Stud Surf Sci Catal 2000;130:2717–22.
[54] Zapater D, Lasobras J, Soler J, et al. Counteracting SAPO-34 catalyst deactivation in MTO process using a two zone fluidized bed reactor: reactor testing and process viability. Catal Today 2021;362:155–61.
[55] Ugarte P, Durán P, Lasobras J, et al. Dry reforming of biogas in fluidized bed: process intensification. Int J Hydrogen Energy 2017;42:13589–97.
[56] Durán P, Sanz-Martínez A, Soler J, et al. Pure hydrogen from biogas: intensified methane dry reforming in a two-zone fluidized bed reactor using permselective membranes. Chem. Eng. J. 2019;370:772–81.
[57] Sanz-Martínez A, Lasobras J, Soler J, et al. Methanol to gasoline (MTG): parametric study and validation of the process in a two-zone fluidized bed reactor (TZFBR). J Ind Eng Chem 2022;113:189–95.
[58] Zapater D, Lasobras J, Soler J, et al. Comparison of conventional and two-zone fluidized bed reactors for methanol to olefins. Effect of reaction conditions and the presence of water in the feed. Ind Eng Chem Res 2022;61:5757–65.
[59] Lasobras J, Soler J, Herguido J, et al. Methane aromatization in a fluidized bed reactor: parametric study. Front Energy Res; 7.
[60] Lasobras J, Medrano JA, Soler J, et al. Preparation of Mo/HZSM-5/Bentonite catalyst for methane aromatization in a fluidized bed reactor. Int J Chem React Eng 2017;15.
[61] Herguido J, Menéndez M. Advances and trends in two-zone fluidized-bed reactors. Curr. Opin. Chem. Eng. 2017;17:15–21.
[62] Rubio O, Mallada R, Herguido J, et al. Experimental study on the oxidation of butane to maleic anhydride in a two-zone fluidized bed reactor. Ind Eng Chem Res 2002;41:5181–6.
[63] Pérez-Moreno L, Soler J, Herguido J, et al. Stable hydrogen production by methane steam reforming in a two zone fluidized bed reactor: experimental assessment. J Power Sources 2013;243:233–41.
[64] Yus M, Soler J, Herguido J, et al. Glycerol steam reforming with low steam/glycerol ratio in a two-zone fluidized bed reactor. Catal Today 2018;299:317–27.
[65] Gascón J, Téllez C, Herguido J, et al. A two-zone fluidized bed reactor for catalytic propane dehydrogenation. Chem. Eng. J. 2005;106:91–6.
[66] Rischard J, Antinori C, Maier L, et al. Oxidative dehydrogenation of n-butane to butadiene with Mo-V-MgO catalysts in a two-zone fluidized bed reactor. Appl Catal Gen 2016;511:23–30.
[67] Pacheco ML, Soler J, Dejoz A, et al. MoO3/MgO as a catalyst in the oxidative dehydrogenation of n-butane in a two-zone fluidized bed reactor. Catal Today 2000;61:101–7.
[68] Gimeno MP, Soler J, Herguido J, et al. Counteracting catalyst deactivation in methane aromatization with a two zone fluidized bed reactor. Ind Eng Chem Res 2010;49:996–1000.
[69] Davidson JF, Harrison D. The behaviour of a continuously bubbling fluidised bed. Chem Eng Sci 1966;21:731–8.
[70] Zambrano D, Soler J, Herguido J, et al. Conventional and improved fluidized bed reactors for dry reforming of methane: mathematical models. Chem. Eng. J.; 393.
[71] Li J, Weinstein H. An experimental comparison of gas backmixing in fluidized beds across the regime spectrum. Chem Eng Sci 1989;44:1697–705.
[72] Namkung W, Done Kim S. Gas backmixing in a circulating fluidized bed. Powder Technol 1998;99:70–8.
[73] Kunii D, Levenspiel O. Bubbling bed model for kinetic processes in fluidized beds: gas-solid mass and heat transfer and catalytic reactions. Ind Eng Chem Process Des Dev 1986;7:481–92.
[74] Alabdullah M, Rodriguez-Gomez A, Shoinkhorova T, et al. One-step conversion of crude oil to light olefins using a multi-zone reactor. Nat Catal 2021;4:233–41.
[75] Gascón J, Téllez C, Herguido J, et al. Modeling of fluidized bed reactors with two reaction zones. AIChE J 2006;52:3911–23.
[76] Quanquan Z, Chaogang X, Weimin P, et al. CN 102443423 A. A petroleum hydrocarbon preparation that can produce more ethylene, propylene and light aromatics. 2010.
[77] Talebizadeh A, Mortazavi Y, Khodadadi AA. Comparative study of the two-zone fluidized-bed reactor and the fluidized-bed reactor for oxidative coupling of methane over Mn/Na2WO4/SiO2 catalyst. Fuel Process Technol 2009;90:1319–25.
[78] Soler J, López Nieto JM, Herguido J, et al. Oxidative dehydrogenation of n-butane in a two-zone fluidized-bed reactor. Ind Eng Chem Res 1999;38:90–7.
[79] Gimeno MP, Soler J, Herguido J, et al. Use of fluidized bed reactors for direct gas phase oxidation of benzene to phenol. Ind Eng Chem Res 2010;49:6810–4.
[80] Lobera MP, Téllez C, Herguido J, et al. Catalytic purification of H2-rich streams by CO-PROX over Pt-Co-Ce/γ-Al2O3 in fluidized bed reactors. Catal Today 2010:404–9.
[81] Pérez-Moreno L, Soler J, Herguido J, et al. Stable steam reforming of ethanol in a two-zone fluidized-bed reactor. Ind Eng Chem Res 2012;51:8840–8.
[82] Medrano JA, Julian I, Garcia-Garcia FR, et al. Catalytic propane dehydrogenation in a two zone fluidized bed reactor with hollow fibre palladium membrane. Procedia Eng 2012;44:288–9.
[83] Katryniok B, Meléndez R, Bellière-Baca V, et al. Catalytic dehydration of glycerol to acrolein in a two-zone fluidized bed reactor. Front Chem; 7.
[84] Roshanaei A, Alavi SM. Using two-zone fluidized bed reactor in propane aromatization over Zn/HZSM-5 catalyst. Fuel Process Technol 2018;176:197–204.
[85] García G, Campos E, Fonts I, et al. Gas catalytic upgrading in a two-zone fluidized bed reactor coupled to a cogasification plant. Energ. Fuel 2013;27:2835–45.
[86] Julián I, Herguido J, Menéndez M. A non-parametric bubble size correlation for a two-section two-zone fluidized bed reactor (TS-TZFBR). Powder Technol 2014;256:146–57.
[87] Julián I, Herguido J, Menéndez M. CFD model prediction of the two-section two-zone fluidized bed reactor (TS-TZFBR) hydrodynamics. Chem. Eng. J. 2014;248:352–62.
[88] Julián I, Herguido J, Menéndez M. Gas permeation effect on the two-section two-zone fluidized bed membrane reactor (TS-TZFBMR) fluid dynamics: a CFD simulation study. Chem. Eng. J. 2016;305:201–11.
[89] Gimeno MP, Wu ZT, Soler J, et al. Combination of a Two-Zone Fluidized Bed Reactor with a Pd hollow fibre membrane for catalytic alkane dehydrogenation. Chem. Eng. J. 2009;155:298–303.
[90] Cook B, Mousko D, Hoelderich W, et al. Conversion of methane to aromatics over Mo2C/ZSM-5 catalyst in different reactor types. Appl Catal Gen 2009;365:34–41.
[91] Ma H, Kojima R, Kikuchi S, et al. Effective coke removal in methane to benzene (MTB) reaction on Mo/HZSM-5 catalyst by H2 and H2O Co-addition to methane. Catal. Letters 2005;104:63–6.
[92] Laine J, Tosta M. Basic engineering of a two-stage process for Co-upgrading natural gas and petroleum coke. Adv. Chem. Engineer. Sci. 2015;5:129–33.
[93] Ohnishi R, Kojima R, Shu Y, et al. Highly stable performance of catalytic methane dehydro-condensation to benzene and naphthalene on Mo/HZSM-5 by addition and a periodic switching treatment of H_2. Stud Surf Sci Catal 2004;147:553–8.
[94] Menéndez Sastre M, Herguido Huerta J, Téllez Ariso C, et al. US 8697926 B2. Method for obtaining aromatic hydrocarbons from methane.
[95] Xu Y, Lu B, He M, et al. Diameter-transformed fluidized bed. Springer International Publishing; 2020.
[96] Basile A. Handbook of membrane reactors. Woodhead Publishing; 2013.
[97] Sanchez Marcano JG, Tsotsis TT. Catalytic membranes and membrane reactors. John Wiley & Sons -VCH; 2002.
[98] Deshmukh SARK, Laverman JA, Van Sint Annaland M, et al. Development of a membrane-assisted fluidized bed reactor. 2. Experimental demonstration and modeling for the partial oxidation of methanol. Ind Eng Chem Res 2005;44:5966–76.

[99] Deshmukh SARK, Laverman JA, Cents AHG, et al. Development of a membrane-assisted fluidized bed reactor. 1. Gas phase back-mixing and bubble-to-emulsion phase mass transfer using tracer injection and ultrasound experiments. Ind Eng Chem Res 2005;44:5955–65.
[100] Patil CS, Van Sint Annaland M, Kuipers JAM. Experimental study of a membrane assisted fluidized bed reactor for H2 production by steam reforming of CH4. Chem Eng Res Des 2006;84:399–404.
[101] Patil CS, van Sint Annaland M, Kuipers JAM. Fluidised bed membrane reactor for ultrapure hydrogen production via methane steam reforming: experimental demonstration and model validation. Chem Eng Sci 2007;62:2989–3007.
[102] Kikuchi E. Membrane reactor application to hydrogen production. Catal Today 2000;56:97–101.
[103] Arratibel A, Medrano JA, Melendez J, et al. Attrition-resistant membranes for fluidized-bed membrane reactors: double-skin membranes. J Memb Sci 2018;563:419–26.
[104] Arratibel Plazaola A, Pacheco Tanaka D, Van Sint Annaland M, et al. Recent advances in Pd-based membranes for membrane reactors. Molecules 2017;22:51.
[105] Liu T, Zhao W, Wang Y. Robust freeze-cast bilayer dual-phase oxygen transport membrane targeting chemical reactor application. ACS Appl Nano Mater 2018;1:3774–8.
[106] Kunii D, Levenspiel O. Fluidization engineering. Elsevier.
[107] Davidson JF, Harrison D. Fluidised particles. AIChE J 1964;10:783–5.
[108] Chiba T, Kobayashi H. Solid exchange between the bubble wake and the emulsion phase in a gas-fluidised bed. J Chem Eng Jpn 1977;10:206–10.
[109] Téllez C, Menéndez M, Santamaría J. Kinetic study of the oxidative dehydrogenation of butane on V/MgO catalysts. J Catal 1999;183:210–21.
[110] Mori S, Wen CY. Estimation of bubble diameter in gaseous fluidized beds. AIChE J 1975;21:109–15.
[111] Horio M, Nonaka A. A generalized bubble diameter correlation for gas-solid fluidized beds. AIChE J 1987;33:1865–72.
[112] Kunii D, Levenspiel O. Bubbling bed model for kinetic processes in fluidized beds. Gas-solid mass and heat transfer and catalytic reactions. Ind Eng Chem Process Des Dev 1968;7:481–92.
[113] Zhou Z, Han L, Bollas GM. Model-assisted analysis of fluidized bed chemical-looping reactors. Chem Eng Sci 2015;134:619–31.
[114] Srinivasan RA, Sriramulu S, Kulasekaran S, et al. Mathematical modeling of fluidized bed combustion - 2: combustion of gases. Fuel 1998;77:1033–49.
[115] Sriramulu S, Sane S, Agarwal P, et al. Mathematical modelling of fluidized bed combustion 1. Combustion of carbon in bubbling beds. Fuel 1996;75:1351.
[116] Wéry F, Vandewalle LA, Marin GB, et al. Hydrodynamic CFD-DEM model validation in a gas–solid vortex unit. Chem. Eng. J.; 455: 140529.
[117] Ouyang Y, Nunez Manzano M, Wetzels R, et al. Liquid hydrodynamics in a gas-liquid vortex reactor. Chem Eng Sci; 246: 116970.
[118] Kulkarni SR, Gonzalez-Quiroga A, Nuñez M, et al. An experimental and numerical study of the suppression of jets, counterflow, and backflow in vortex units. AIChE J; 65.
[119] De Wilde J, De Broqueville A. Rotating fluidized beds in a static geometry: experimental proof of concept. AIChE J 2007;53:793–810.
[120] Kovacevic JZ, Pantzali MN, Niyogi K, et al. Solids velocity fields in a cold-flow gas-solid vortex reactor. Chem Eng Sci 2015;123:220–30.
[121] Gonzalez-Quiroga A, Shtern V, Perreault P, et al. Intensifying mass and heat transfer using a high-g stator-rotor vortex chamber. Chem Eng Process 2023;169.
[122] Chen S, Ouyang Y, Vandewalle LA, et al. CFD analysis on hydrodynamics and residence time distribution in a gas-liquid vortex unit. Chem. Eng. J. 2022;446.
[123] Friedle M, Marin GB, Heynderickx GJ. Operational range of a gas-solid vortex unit. Powder Technol 2018;338:702–15.
[124] Kulkarni SR, Quiroga AG, Perreault P, et al. CFD-based biomass fast pyrolysis simulations in a gas-Solid vortex reactor demonstrating process intensification. Chem Eng Trans 2018;65:19–24.
[125] Gonzalez-Quiroga A, Reyniers PA, Kulkarni SR, et al. Design and cold flow testing of a Gas-Solid Vortex Reactor demonstration unit for biomass fast pyrolysis. Chem. Eng. J. 2017;329:198–210.
[126] Orozco-Jimenez AJ, Pinilla-Fernandez DA, Pugliese V, et al. Angular momentum Based-Analysis of Gas-Solid fluidized beds in vortex chambers. Chem. Eng. J.; 457.
[127] Scott L, Borissova A, Burns A, et al. Effect of grinding nozzles pressure on particle and fluid flow patterns in a spiral jet mill. Powder Technol 2021;394:439–47.
[128] Scott L, Borissova A, Burns A, et al. Influence of holdup on gas and particle flow patterns in a spiral jet mill. Powder Technol 2021;377:233–43.
[129] Bnà S, Ponzini R, Cestari M, et al. Investigation of particle dynamics and classification mechanism in a spiral jet mill through computational fluid dynamics and discrete element methods. Powder Technol 2020;364:746–73.
[130] Blissett R, Sommerville R, Rowson N, et al. Valorisation of rice husks using a TORBED® combustion process. Fuel Process Technol 2017;159:247–55.
[131] Shu J, Lakshmanan VI, Dodson CE. Hydrodynamic study of a toroidal fluidized bed reactor. Chem Eng Process 2000;39:199–506.
[132] Shi MH, Wang H, Hao YL. Experimental investigation of the heat and mass transfer in a centrifugal fluidized bed dryer. Chem. Eng. J. 2000;78:107–13.
[133] Watano S, Imada Y, Hamada K, et al. Microgranulation of fine powders by a novel rotating fluidized bed granulator. Powder Technol 2003;131:250–5.
[134] Lang X, Ouyang Y, Dutta S, et al. Hydrodynamic study of the operating window of a stator-rotor vortex chamber reactor. Powder Technol 2023;427:118749.
[135] Vandewalle LA, Van de Vijver R, Van Geem KM, et al. The role of mass and heat transfer in the design of novel reactors for oxidative coupling of methane. Chem Eng Sci 2019:268–89.
[136] Pati JR, Dutta S, Eliaers P, et al. Experimental study of paddy drying in a vortex chamber. Dry Technol 2016;34:1073–84.
[137] Eliaers P, Ranjan Pati J, Dutta S, et al. Modeling and simulation of biomass drying in vortex chambers. Chem Eng Sci 2015;123:648–64.
[138] Nunez Manzano M, Gonzalez Quiroga A, Perreault P, et al. Biomass fast pyrolysis in an innovative gas-solid vortex reactor: experimental proof of concept. J Anal Appl Pyrolysis 2021;156:105165.
[139] Vandewalle LA, Marin GB, Van Geem KM. CFD-based assessment of steady-state multiplicity in a gas-solid vortex reactor for oxidative coupling of methane. Chem Eng Process 2021;165:108434.
[140] Tharakaraman SS, Nunez Manzano M, Kulkarni SR, et al. Development of an active and mechanically stable catalyst for the oxidative coupling of methane in a gas-solid vortex reactor. Ind Eng Chem Res 2022;61:7748–59.
[141] Pannala S, Shtern V, Chen L, et al. Novel annular jet vortex reactor for high-temperature thermochemical conversion of hydrocarbons to acetylene. ACS Eng. Au 2022;2:406–20.
[142] Ashcraft RW, Kovacevic J, Heynderickx GJ, et al. Assessment of a gas-solid vortex reactor for SO_2/NO_x adsorption from flue gas. Ind Eng Chem Res 2013;52:861–75.
[143] Singh P, Kalita P, Mahanta P. Experimental study of food grain drying in a gas–solid vortex reactor. Dry Technol 2022;40:884–96.
[144] Loftus PJ, Stickler DB, Diehl RC. A Confined Vortex Scrubber for fine particulate removal from flue gases. Environ Prog 1992;11:27–32.
[145] Eliaers P, de Broqueville A, Poortinga A, et al. High-G, low-temperature coating of cohesive particles in a vortex chamber. Powder Technol 2014;258:242–51.
[146] Kopp GM, Pearson SM, Shah M, US 8067051 B2. Process for milling cocoa shells. 2011.
[147] Ma P, Shah K, Wu D, et al. US 7682946 B2. Apparatus and process for plasma-enhanced atomic layer deposition. 2010.
[148] Grant RW, Petrone BJ, Brubaker MD, et al. US 2004/0028810 A1. Chemical Vapor Deposition Reactor and Method for Utilizing Vapor Vortex; 2004.
[149] Ma P, Shah K, Wu D, et al. US 2007/0119370 A1. Apparatus and process for plasma-enhanced atomic layer deposition. 2007.
[150] Fang RH, Chen KNH, Aryal S, et al. Large-scale synthesis of lipid-polymer hybrid nanoparticles using a multi-inlet vortex reactor. Langmuir 2012;28:13824–9.
[151] Marchisio DL, Omegna F, Barresi AA. Production of TiO_2 nanoparticles with controlled characteristics by means of a Vortex Reactor. Chem. Eng. J. 2009;146:456–65.
[152] Hirsch D, Steinfeld A. Solar hydrogen production by thermal decomposition of natural gas using a vortex-flow reactor. Int J Hydrogen Energy 2004;29:47–55.
[153] Kräupl S, Steinfeld A. Experimental investigation of a vortex-flow solar chemical reactor for the combined ZnO-reduction and CH_4-reforming. Journal of Solar Energy Engineering, Transactions of the ASME 2001;123:237–43.
[154] Trujillo WR, De Wilde J. Computational fluid dynamics simulation of fluid catalytic cracking in a rotating fluidized bed in a static geometry. Ind Eng Chem Res 2010;49:5288–98.
[155] Ryazantsev AA, Malikov AS, Batoeva AA, et al. Liquid-phase oxidation of hydrogen sulfide in centrifugal bubbling apparatus. Russ J Appl Chem 2007;80:1544–8.
[156] Qian Z, Li Z-H, Guo K. Industrial applied and modeling research on selective H2S removal using a rotating packed bed. Ind Eng Chem Res 2012;51:8108–16.
[157] Kuramoto M, Furusawa T, Kunii D. Development of a new system for circulating fluidized particles within a single vessel. Powder Technol 1985;44:77–84.
[158] Kuramoto M, Kunii D, Furusawa T. Flow of dense fluidized particles through an opening in a circulation system. Powder Technol 1986;47:141–9.
[159] Kim SD, Kim YH, Roh A, et al. Solid circulation characteristics in an internally circulating fluidized bed with orifice-type draft tube. Korean J. Chem. Eng. 2002;19:911–6.
[160] Luo K, Fang M, Yang S, et al. LES-DEM investigation of an internally circulating fluidized bed: effects of gas and solid properties. Chem. Eng. J. 2013;228:583–95.
[161] Solnordal CB, Kenche V, Hadley TD, et al. Simulation of an internally circulating fluidized bed using a multiphase particle-in-cell method. Powder Technol 2015;274:123–34.
[162] Rubio O, Herguido J, Menéndez M, et al. Oxidative dehydrogenation of butane in an interconnected fluidized-bed reactor. AIChE J 2004;50:1510–22.
[163] Feng Y, Swenser-Smith T, Witt PJ, et al. CFD modeling of gas-solid flow in an internally circulating fluidized bed. Powder Technol 2012;219:78–85.
[164] Xiao X, Le DD, Morishita K, et al. Multi-stage biomass gasification in Internally Circulating Fluidized-bed Gasifier (ICFG): test operation of animal-waste-derived biomass and parametric investigation at low temperature. Fuel Process Technol 2010;91:895–902.
[165] Hu J, Liu D, Liang C, et al. Solids flow characteristics and circulation rate in an internally circulating fluidized bed. Particuology 2021;54:69–77.
[166] Fan H, Chen B, Yang R, et al. Experimental simulation of particle agglomeration in an internally circulating fluidized bed. Exp Therm Fluid Sci 2018;91:277–82.

[167] Hassan M, Schwarz MP, Yuqing F, et al. Numerical investigation of solid circulation flux in an internally circulating fluidized bed with different gas distributor designs. Powder Technol 2016;301:1103–11.
[168] Song BH, Kim YT, Kim SD. Circulation of solids and gas bypassing in an internally circulating fluidized bed with a draft tube. Chem. Eng. J. 1997;68:5–122.
[169] Herguido J, Peña JA, Carazo E. Experimental assessment of hydrogen separation from H_2/CH_4 mixtures by the "steam-iron process" in an interconnected circulating fluidized bed reactor. Int J Hydrogen Energy 2014;39:14050–60.
[170] Hassan M, Ahmad K, Rafique M, et al. Computational fluid dynamics analysis of the circulation characteristics of a binary mixture of particles in an internally circulating fluidized bed. Appl Math Model 2019;72:1–16.
[171] Herguido J, Menéndez M, Santamaría J. On the use of fluidized bed catalytic reactors where reduction and oxidation zones are present simultaneously. Catal Today 2005;100:181–9.
[172] Li P, Yu X, Liu F, et al. Hydrodynamic behaviors of an internally circulating fluidized bed with wide-size-distribution particles for preparing polysilicon granules. Powder Technol 2015;281:112–20.
[173] Formisani B, Girimonte R, Longo T. The fluidization process of binary mixtures of solids: development of the approach based on the fluidization velocity interval. Powder Technol 2008;185:97–108.
[174] Foscolo PU, Germanà A, Jand N, et al. Design and cold model testing of a biomass gasifier consisting of two interconnected fluidized beds. Powder Technol 2007; 173:179–88.
[175] Mukadi L, Guy C, Legros R. Parameter analysis and scale-up considerations for thermal treatment of industrial waste in an internally circulating fluidized bed reactor. Chem Eng Sci 1999;54:3071–8.
[176] Cao JP, Xiao X Bin, Zhang SY, et al. Preparation and characterization of bio-oils from internally circulating fluidized-bed pyrolyses of municipal, livestock, and wood waste. Bioresour Technol 2011;102:2009–15.
[177] Yang X, Wang S, Li B, et al. Evaluation of sorption-enhanced reforming over catalyst-sorbent bi-functional particles in an internally circulating fluidized bed. Adv Powder Technol 2020;31:2566–72.
[178] Boyd T, Grace J, Lim CJ, et al. Hydrogen from an internally circulating fluidized bed membrane reactor. Int J Chem React Eng 2005;3.
[179] Boyd T, Grace JR, Lim J, et al. In: Fluidization XII, editor. Cold modelling of an internally circulating fluidized bed membrane reactor; 2007. p. 521–8.
[180] Mleczko L, Marschall K-J. Performance of an internally circulating fluidized-bed reactor for the catalytic oxidative coupling of methane. Can J Chem Eng 1997;75: 610–9.
[181] Gascón J, Téllez C, Herguido J, et al. A two-zone fluidized bed reactor for catalytic propane dehydrogenation. Chem. Eng. J. 2005;106:91–6.
[182] Gascón J, Téllez C, Herguido J, et al. Modeling of fluidized bed reactors with two reaction zones. AIChE J 2006;52:3911–23.
[183] Thiemsakul D, Kamsuwan C, Piemjaiswang R, et al. Computational fluid dynamics simulation of internally circulating fluidized bed reactor for dry reforming of methane. Energy Rep 2022;8:817–24.
[184] Snip OC, Woods M, Korbee R, et al. Regenerative removal of SO_2 and NO_x for a 150 MWe power plant in an interconnected fluidized bed facility. Chem Eng Sci 1996;51:2021–9.
[185] Meng Z, Liu M, Ahmad N, et al. Hydrodynamics in commercial-scale internally circulating fluidized beds with different central downcomer outlets. Particuology 2020;51:120–31.
[186] Ahn H-S, Lee W-J, Kim S-D, et al. Solid circulation and gas bypassing in an internally circulating fluidized bed with an orifice-type draft tube. Korean J. Chem. Eng. 1999;16:618–23.
[187] Ahn H-S, Lee W-J, Kim S-D, et al. Solid circulation and gas bypassing in an internally circulating fluidized bed with an orifice-type draft tube. Korean J. Chem. Eng. 1999;16:618–23.
[188] Khan Wardag AN, Larachi F. Stability analysis of flat- and corrugated-wall bubbling fluidized beds: differential pressure, heat transfer coefficient, digital image analysis and CFD simulations. Chem. Eng. J. 2012;179:349–62.
[189] Boyd T, Grace JR, Lim CJ, et al. A novel autothermal reforming membrane reactor for high purity H_2. In: 16th world hydrogen energy conference; 2006.
[190] Abellon RD, Kolar ZI, Den Hollander W, et al. A single radiotracer particle method for the determination of solids circulation rate in interconnected fluidized beds. Powder Technol 1997;92:53–60.
[191] Jeon JH, Kim SD, Kim SJ, et al. Solid circulation and gas bypassing characteristics in a square internally circulating fluidized bed with draft tube. Chem Eng Process: Process Intensif 2008;47:2351–60.
[192] Das A, Bhattacharya SC. Circulating fluidised-bed combustion. Appl Energy 1990; 37:227–46.
[193] Song Y, Lu X, Wang Q, et al. Experimental study on gas-solid flow characteristics in an internally circulating fluidized bed cold test apparatus. Adv Powder Technol 2017;28:2102–9.
[194] Mabrouk R, Chaouki J, Guy C. Exit effect on hydrodynamics of the internal circulating fluidized bed riser. Powder Technol 2008;182:406–14.
[195] Fox WB. Determination of particle and gas convective heat transfer components in a circulating fluidized bed. University of North Dakota; 1997.
[196] Korbee R, Snip OC, Schouten JC, et al. Rate of solids and gas transfer via an orifice between partially and completely fluidized beds. Chem Eng Sci 1994;49:5819–32.
[197] Ouyang Y, Heynderickx GJ, Van Geem KM. Development of intensified reactors: a process intensification methodology perspective. Chem Eng Process 2022;181: 109164.
[198] Geldart D. Types of gas fluidization. Powder Technol 1973;7:285–92.
[199] Menéndez M, Herguido J, Bérard A, et al. Experimental methods in chemical engineering: reactors—fluidized beds. Can J Chem Eng 2019;97:2383–94.
[200] Stein M, Ding YL, Seville JPK, et al. Solids motion in bubbling gas fuidised beds. Chem Eng Sci 2000;55:5291–300.
[201] Namkung W, Kim SD. Gas backmixing in a circulating fluidized bed. Powder Technol 1998;99:70–8.
[202] Li J, Weinstein H. An experimental comparison of gas backmixing in fluidized beds across the regime spectrum. Chem Eng Sci 1989;44:1697–705.
[203] Davidson JF, Harrison D. The behaviour of a continuously bubbling fluidised bed. Chem Eng Sci 1966;21:731–8.
[204] Qian GH, Bágyi I, Pfeffer R, et al. Particle mixing in rotating fluidized beds: inferences about the fluidized state. AIChE J 1999;45:1401–10.
[205] Mutsers SMP, Rietema K. Fluidization in a centrifugal field. The effect of gravity upon bed expansion. Powder Technol 1977;18:249–56.
[206] Mehrani P, Sowinski A. Operating challenges. In: Essentials of fluidization technology. John Wiley & Sons, pp. 269–290.
[207] Bayham SC, Breault R, Monazam E. Particulate solid attrition in CFB systems – an assessment for emerging technologies. Powder Technol 2016;302:42–62.
[208] Kim SW, Yeo CE, Lee DY. Effect of fines content on fluidity of FCC catalysts for stable operation of fluid catalytic cracking unit. Energies 2019;12:293.
[209] Timsina R, Thapa RK, Moldestad BME, et al. Effect of particle size on flow behavior in fluidized beds. Int. J. Energy Prod. Manag. 2019;4:273–86.
[210] Song D, Mehrani P. Mechanism of particle build-up on gas-solid fluidization column wall due to electrostatic charge generation. Powder Technol 2017;316: 166–70.
[211] Lewis WK, Gilliland ER, Bauer WC. Electrostatics - 1949 - W.K. Lewis. Ind Eng Chem 1949;41:1104–17.
[212] Matsusaka S, Maruyama H, Matsuyama T, et al. Triboelectric charging of powders: a review. Chem Eng Sci 2010;65:5781–807.
[213] Mehrani P, Murtomaa M, Lacks DJ. An overview of advances in understanding electrostatic charge buildup in gas-solid fluidized beds. J. Electrostat. 2017;87: 64–78.
[214] Fotovat F, Bi XT, Grace JR. A perspective on electrostatics in gas-solid fluidized beds: challenges and future research needs. Powder Technol 2018;329:65–75.
[215] Yang W. Handbook of fluidization and fluid-particle systems. Marcel Dekker; 2003.
[216] Kunii D, Levenspiel O. Solid movement: mixing, segregation, and staging. In: Fluidization engineering. Elsevier, pp. 211–235.
[217] Glicksman LR, Yule T, Dyrness A. Prediction of the expansion of fluidized beds containing tubes. Chem Eng Sci 1991;46:1561–71.
[218] Liu X, Xu G, Gao S. Micro fluidized beds: wall effect and operability. Chem. Eng. J. 2008;137:302–7.
[219] Mabrouk R, Chaouki J, Guy C. Wall surface effects on particle-wall friction factor in upward gas-solid flows. Powder Technol 2008;186:80–8.
[220] Mabrouk R, Radmanesh R, Chaouki J, et al. Scale effects on fluidized bed hydrodynamics. Int J Chem React Eng 2005;3.
[221] Efhaima A, Al-Dahhan MH. Bed diameter effect on the hydrodynamics of gas-solid fluidized beds via radioactive particle tracking (RPT) technique. Can J Chem Eng 2017;95:744–56.
[222] Staudt N, De Broqueville A, Rosales Trujillo W, et al. Low-temperature pyrolysis and gasification of biomass: numerical evaluation of the process intensification potential of rotating-and circulating rotating fluidized beds in a static fluidization chamber. Int J Chem React Eng 2011;9.
[223] Rowe PN, Nienow AW. Particle mixing and segregation in gas fluidised beds. A review. Powder Technol 1976;15:141–7.
[224] Tabrizi HB, Panahandeh M, Saidi M. Experimental segregation of binary particles using gas-solid fluidized bed. In: Proceedings of the world Congress on engineering; 2013.
[225] Hameed S, Sharma A, Pareek V. Modelling of particle segregation in fluidized beds. Powder Technol 2019;353:202–18.
[226] Kunii D, Levenspiel O. High-velocity fluidization. In: Fluidization engineering. Elsevier, pp. 193–210.
[227] Sitnai O. Solids mixing in a fluidized bed with horizontal tubes. Ind Eng Chem Process Des Dev 1981;20:533–8.
[228] Hull AS, Chen Z, Agarwal PK. Influence of horizontal tube banks on the behavior of bubbling fluidized beds: 2. Mixing of solids. Powder Technol 2000;111:192–9.
[229] Kovacevic JZ, Pantzali MN, Heynderickx GJ, et al. Bed stability and maximum solids capacity in a Gas-Solid Vortex Reactor: experimental study. Chem Eng Sci 2014;106:293–303.
[230] Ekatpure RP, Suryawanshi VU, Heynderickx GJ, et al. Experimental investigation of a gas-solid rotating bed reactor with static geometry. Chem Eng Process: Process Intensif 2011;50:77–84.
[231] Michels NL, Mitchell S, Pérez-Ramírez J. Effects of binders on the performance of shaped hierarchical MFI zeolites in methanol-to-hydrocarbons. ACS Catal 2014;4: 2409–17.

[232] Zhao R, Sudsakorn K, Goodwin JG, et al. Attrition resistance of spray-dried iron F-T catalysts: effect of activation conditions. Catal Today 2002;71:319–26.
[233] Kim M, Chae HJ, Kim TW, et al. Attrition resistance and catalytic performance of spray-dried SAPO-34 catalyst for MTO process: effect of catalyst phase and acidic solution. J Ind Eng Chem 2011;17:621–7.
[234] Bukur DB, Carreto-Vazquez VH, Ma W. Catalytic performance and attrition strength of spray-dried iron catalysts for slurry phase Fischer-Tropsch synthesis. Appl Catal Gen 2010;388:240–7.
[235] Zhang Y, Zhong L, Wang H, et al. Catalytic performance of spray-dried Cu/ZnO/Al_2O_3/ZrO_2 catalysts for slurry methanol synthesis from CO_2 hydrogenation. J CO2 Util 2016;15:72–82.
[236] Ergin F. Effect of freeze drying, spray drying and electrospraying on the morphological, thermal, and structural properties of powders containing phage Felix O1 and activity of phage Felix O1 during storage. Powder Technol 2022;404:117516.
[237] Aghamohammadi S, Haghighi M, Ebrahimi A. Pathways in particle assembly by ultrasound-assisted spray-drying of kaolin/SAPO-34 as a fluidized bed catalyst for methanol to light olefins. Ultrason Sonochem 2019;53:237–51.
[238] Niksiar A, Nasernejad B. Activated carbon preparation from pistachio shell pyrolysis and gasification in a spouted bed reactor. Biomass Bioenergy 2017;106:43–50.
[239] Singh SKD, Lu K. SiOC coatings on yttria stabilized zirconia microspheres using a fluidized bed coating process. Powder Technol 2022;396:158–66.
[240] Dalai AK, Zaman J, Hall ES, et al. Preparation of activated carbon from Canadian coals using a fixed-bed reactor and a spouted bed-kiln system. Fuel 1996;75:227–37.
[241] Kamphuis AJ, Walls JR. Catalyst granule production in a spouted bed: opportunities for creative catalyst design. Stud Surf Sci Catal 1998;118:451–7.
[242] Gibilaro LG, Di Felice R, Waldram SP, et al. Generalized friction factor and drag coefficient correlations for fluid-particle interactions. Chem Eng Sci 1985;40:1817–23.
[243] Turton R, Levenspiel O. Short Communication A short note on the drag correlation for spheres. Powder Technol 1936;47:83–6.
[244] Karamanev DG. Equations for calculation of the terminal velocity and drag coefficient of solid spheres and gas bubbles. Chem Eng Commun 1996;147:75–84.
[245] Wang P, Jia H. Power-generation from Biorenewable resources: Biocatalysis in Biofuel cells. In: Bioprocessing for value-added products from renewable resources; 2007. p. 507–25.
[246] Kulkarni SR, Velisoju VK, Tavares F, et al. Silicon carbide in catalysis: from inert bed filler to catalytic support and multifunctional material. Catal Rev Sci Eng 2023;65:174–237.
[247] Lezcano G, Velisoju VK, Kulkarni SR, et al. Engineering thermally resistant catalytic particles for oxidative coupling of methane using spray-drying and incorporating SiC. Ind Eng Chem Res 2021;60:18770–80.
[248] Lezcano G, Kulkarni SR, Velisoju VK, et al. Effect of the particle blending-shaping method and silicon carbide crystal phase for Mn-Na-W/SiO_2-SiC catalyst in oxidative coupling of methane. Mol Catal 2022;527:112399.
[249] Pham-Huu C, Keller N, Ehret G, et al. The first preparation of silicon carbide nanotubes by shape memory synthesis and their catalytic potential. J Catal 2001;200:400–10.
[250] Lacroix M, Dreibine L, De Tymowski B, et al. Silicon carbide foam composite containing cobalt as a highly selective and re-useable Fischer-Tropsch synthesis catalyst. Appl Catal Gen 2011;397:62–72.
[251] Delikonstantis E, Cameli F, Stefanidis GD. Electrified chemical reactors for methane-to-ethylene conversion. Curr. Opin. Chem. Eng. 2023;41:100927.
[252] Van Geem KM, Galvita VV, Marin GB. Making chemicals with electricity. Science 2019;364:734–5.
[253] Scapinello M, Delikonstantis E, Stefanidis GD. Direct methane-to-ethylene conversion in a nanosecond pulsed discharge. Fuel 2018;222:705–10.
[254] Morais E, Delikonstantis E, Scapinello M, et al. Methane coupling in nanosecond pulsed plasmas: correlation between temperature and pressure and effects on product selectivity. Chem. Eng. J. 2023;462:142227.
[255] Lamichhane P, Pourali N, Scott L, et al. Critical review: 'Green' ethylene production through emerging technologies, with a focus on plasma catalysis. Renew Sustain Energy Rev 2024;189:114044.
[256] Kim YT, Lee J-J, Lee J. Electricity-driven reactors that promote thermochemical catalytic reactions via joule and induction heating. Chem. Eng. J. 2023;470:144333.
[257] Bolívar Caballero JJ, Zaini IN, Yang W. Reforming processes for syngas production: a mini-review on the current status, challenges, and prospects for biomass conversion to fuels. Appl. Energy Combust. Sci. 2022;10:100064.
[258] Wismann ST, Engbæk JS, Vendelbo SB, et al. Electrified methane reforming: a compact approach to greener industrial hydrogen production. Science 2019;364:756–9.
[259] Wismann ST, Engbæk JS, Vendelbo SB, et al. Electrified methane reforming: Elucidating transient phenomena. Chem. Eng. J. 2021;425:131509.
[260] Chen Y, Yuan L, Ye T, et al. Effects of current upon hydrogen production from electrochemical catalytic reforming of acetic acid. Int J Hydrogen Energy 2009;34:1760–70.
[261] Jung H, Yoon WL, Lee H, et al. Fast start-up reactor for partial oxidation of methane with electrically-heated metallic monolith catalyst. J Power Sources 2003;124:76–80.
[262] Ye T, Yuan L, Chen Y, et al. High efficient production of hydrogen from bio-oil using low-temperature electrochemical catalytic reforming approach over NiCuZn-Al_2O_3 catalyst. Catal. Letters 2009;127:323–33.
[263] Palma V, Barba D, Cortese M, et al. Microwaves and heterogeneous catalysis: a review on selected catalytic processes. Catalysts 2020;10.
[264] Bandilla KW. Carbon capture and storage. In: Future energy: improved, sustainable and clean options for our Planet. Elsevier; 2020. p. 669–92.
[265] Chung W, Lee JH. Application of nonlinear surrogate models on optimization of carbon capture and utilization network. In: Computer Aided chemical engineering. Elsevier B.V.; 2022. p. 1201–6.
[266] Davoodi S, Al-Shargabi M, Wood DA, et al. Review of technological progress in carbon dioxide capture, storage, and utilization. Gas Sci. Eng. 2023;117:205070.
[267] Aydin G, Karakurt I, Aydiner K. Evaluation of geologic storage options of CO_2: applicability, cost, storage capacity and safety. Energy Pol 2010;38:5072–80.
[268] Li L, Zhao N, Wei W, et al. A review of research progress on CO_2 capture, storage, and utilization in Chinese Academy of Sciences. In: Fuel. Elsevier; 2013. p. 112–30.

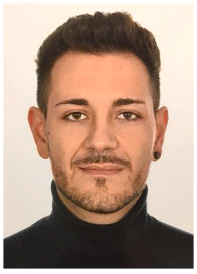

Diego Zapater graduated as a chemical engineer in 2017 after completing his bachelor's and master's degrees at the University of Zaragoza. In 2018 he started a PhD in chemical engineering in the catalysis and reactor engineering group (CREG) at the Aragon Institute for Engineering Research (I3A). His thesis was supported by three main areas: catalysis, reactor engineering, and process intensification, all three applied to the methanol-to-olefins process. Diego graduated *cum laude* in 2021 and moved to the King Abdullah University of Science and Technology (KAUST), in Saudi Arabia, for a two-year postdoc position in the Multiscale Reaction Engineering (MuRE) group, in the KAUST Catalysis Center (KCC), until early 2024. He currently works in TECNALIA, Basque Research and Technology Allience (BRTA), in San Sebastian (Spain). Dr. Zapater's main research interests are catalytic reactors, reactor electrification, hydrogen production, and process intensification.

Shekhar Kulkarni is a chemical engineer by education and profession, holding a master's degree from IIT Madras, India, earned in 2014, and a PhD from Ghent University, Belgium, completed in 2019. Following his doctoral studies, he was a postdoctoral fellow at the KAUST Catalysis Center (KCC) within the King Abdullah University of Science and Technology (KAUST, Saudi Arabia) until March 2023. Currently, he continues his work as a Research Scientist at KAUST. Dr. Kulkarni's expertise encompasses many areas, including multifunctional advanced fluidized bed reactors, computational fluid dynamics (CFD) simulations of multiphase systems, ammonia-to-hydrogen economy, and microkinetic modeling of chemical processes. More information can be found at https://mure.kaust.edu.sa/people/detail/shekhar-kulkarni

Florian Wéry is a PhD candidate at Ghent University focused on Computational Fluid Dynamics. His research extends the application of CFD-DEM towards reactive applications in intensified fluidized bed geometries with a specific focus on the oxidative coupling of methane and the gas-solid vortex reactor.

Mengmeng Cui completed her bachelor's and doctoral's degrees in petroleum and natural gas engineering from Southwest Petroleum University (China) in 2011 and 2016, respectively. She served as an assistant research fellow at the same university after graduation until 2021. During this period, she joined Prof. Pedro Castaño's research group (MuRE) in the KAUST Catalysis Center (KCC) in 2020 and is currently a research scientist since 2022. Dr. Cui's interests focus on computational (particle) fluid dynamic simulations with particle image velocimetry experiments to design, model, optimize, and scale up and down catalytic reactors.

Javier Herguido is full Professor of Chemical Engineering at the University of Zaragoza (Spain) since 2007, and serves as director of its Chemical and Environmental Engineering Department. He is a member of the Aragon Institute for Engineering Research (I3A), where he co-leads the Catalysis and Reactor Engineering Research Group (CREG). He earned his PhD in Science in 1991 working on the development of a double-bed multi-solid circulating system for catalytic gasification of biomass. Holder of the "Chaire Hélioparc" at the Hélioparc Pau-Pyrénées technology center (France) in 1993, and visiting professor at several research centers and universities. He has participated in 45 research projects, largely as principal investigator. His scientific production includes over 125 papers and 380 scientific meetings, 3 patents, and 14 supervised PhD. He has the Extraordinary Doctorate Award and the 3M-Foundation Prize for Innovation - 2004 (environment category). Secretary of the Spanish Catalysis Society (SECAT) governing board and reviewer for several international organizations and journals. Prof. Herguido's work focuses on the area of Chemical Reactor Engineering and current research topics include fluidized bed reactors with separated zones, hydrogen production/purification from diverse sources, Power-to-Gas and Power-to-Liquid processes (*e.g.*, CO_2 methanation, and methanol production), and processes intensification, including the use of membrane reactors.

Miguel Menéndez made the PhD in 1985 at the University of Zaragoza on FCC catalyst deactivation. He has been Graduate Student Assistant (Ayudante), Associate Profesor (Titular) and is now full professor (Catedratico) at the University of Zaragoza. His further research has been mostly about fluidized bed reactors, membrane reactors, and inorganic membranes. In the field of fluidized bed reactors, he introduced the concept of a two-zone fluidized bed reactor, which has been tested successfully in several laboratories. In the field of membrane reactors, he published the first article showing the use of a membrane as a gas distributor in catalytic oxidation, a concept that has been widely studied worldwide. He has also made pioneering work in the use of zeolite membranes, mostly as part of catalytic membrane reactors.

Geraldine J Heynderickx obtained her master's in chemical engineering in 1989, and she received her doctoral degree in 1993, both at UGent. She became junior professor at Laboratory for Chemical Technology (LCT) of UGent in 1994, and senior professor in 2006. Introducing new research at the LCT is the guiding principle in all her research. In 1996, she introduced the use of Computational Fluid Dynamics in chemical engineering research at LCT. In 1999, she added research on polymers to the agenda of LCT. In 2006, she was the first worldwide to study the convection section of a thermal cracker. In 2010, Process Intensification studies became the major lead in her research, with attention to reactor engineering, optimization, and design. Prof. Heynderickx designed and built a pilot prototype of a new reactor technology: a static gas-solid vortex reactor. The optimization of the reactor is ongoing, and 4 new pilots have been built since. The design and construction of 2 gas-liquid vortex reactors prototypes is ongoing. Only recently, she started a study on the magnetization of fluidized beds.

Kevin Van Geem is full professor in the Faculty of Engineering and Architecture at Ghent University (UGent). He is director of the Center of Sustainable Chemistry and director of the board of the Laboratory for Chemical Technology of Ghent University. He is CTO of CAPTURE, an inter-university platform grouping 100 faculty members of different universities with ambition to accelerate radical technological innovations in the field of sustainable resource recovery. His main research interest is reaction engineering in general, with a focus in particular the transition from fossil to alternative resources such as biomass, CO/CO_2 and plastic waste. He is a former Fulbright Research Scholar of MIT and visiting professor at Stanford. He oversees the pilot plants for chemical recycling, oxidative coupling of methane, steam cracking, biomass pyrolysis and super dry reforming. He is the author of more than 300 scientific publications, has 3 patents, and is the managing director of his own spin-off company on modeling steam cracking. He is involved in electrification, process intensification, machine learning & data mining, drug design, scale-up and process modelling

Jorge Gascon was born in Huesca (Spain) in 1977. Jorge received his MSc. in Chemistry in 2002 and his PhD *cum laude* in Chemical Engineering in 2006, both at the University of Zaragoza (Spain). He was post-doc (2006–2009), Assistant Professor (2010–2012), Associate Professor (2012–2014) and Antoni van Leeuwenhoek Professor (2014–2017) of Catalysis Engineering at TUDelft (NL). Since 2017 he is Professor and Director at the KAUST Catalysis Center. He has co-authored over 400 scientific articles and 20 patents. He has been a Clarivate Analytics highly cited researcher for the last 5 years

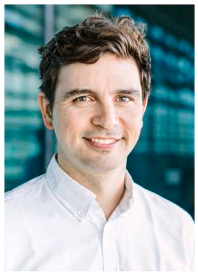

Pedro Castano is an Associate Professor of Chemical Engineering at the King Abdullah University of Science and Technology (KAUST), Physical Science and Engineering (PSE) division and KAUST Catalysis Center (KCC), where he leads the Multiscale Reaction Engineering (MuRE) group. He completed his PhD in Chemical Engineering in 2006 from the University of the Basque Country (UPV/EHU). His research interests are catalytic reaction engineering for waste valorization, sustainable production of chemicals and hydrogen, catalyst deactivation, and multiscale modeling. More information can be found at https://mure.kaust.edu.sa